SHALLOW-WATER SOUND PROPAGATION
BY COHERENT RAY THEORY

by

A.J.A. Kamenyitzky B.Sc

Thesis submitted for the Degree of Master of Science

University of New South Wales
January, 1968

ABSTRACT

Using a ray theory model, the energy transmission loss for sound propagating in shallow isovelocity water was calculated. The exact amplitudes and phases of all rays at the receiver were computed; these amplitudes were then summed coherently and the intensity obtained by squaring the total amplitude. The energy transmission loss was found to increase with:

(i) increasing range

(ii) increasing bottom loss

(iii) decreasing frequency

(iv) decreasing height of receiver off the bottom.

When the bottom loss is small the energy loss with range follows a cylindrical spreading law. As the bottom loss increases the rate of energy loss with range increases approaching a modified Lloyd's mirror type of propagation.

To ascertain the effect on the received energy of a slowly varying bottom depth, a type of perturbation theory was used. From the bottom depth distribution function, the distribution of the phase distortion caused to each ray by the variation in depth was obtained. By adopting a Monte-Carlo procedure and hence computing the transmission loss at one range many times by selecting phase distortions for each ray randomly from the phase distortion distribution, an expected fluctuation in intensity was determined.

The rms fluctuation in intensity due to a variation in the bottom depth was found to increase with:

(i) increasing range

(ii) increasing frequency

(iii) decreasing bottom loss

(iv) increasing bottom depth variation.

To verify Tolstoy's (1,12) comparison between ray and mode theory the arrival times of the first four modes as a function of frequency was computed by ray theory.

CONTENTS

INTRODUCTION

Historical

Lamb (1,1) in a classic paper, first considered the propagation of a disturbance generated in a semi-infinite medium by an impulsive point or line source at the surface. He also derived the formal solutions for internal sources as integrals.

Pekeris (1,2) 1941, developed the normal mode theory of propagation of sound in layered media. In 1948 Pekeris (1,3) extended this theory to cover the case of explosive sound ,and the predictions of the theory about the shape and variation of amplitude in the received pressure pulse were verified by comparison with experimental data. As well as solving the two layered liquid half-space problem, Pekeris obtained the curves of the group and phase velocities for a three layered liquid half-space where the velocities of successive layers increased.

The case where the intermediate layer has a lower sound velocity than the water layer was investigated by Press and Ewing (1,4). They were interested in the fact that in some areas the 'water wave' consisted of a brief burst of high frequency sound which did not show the dispersion and Airy phase normally found. They found from the phase and group velocity curves that a three layered liquid half-space with a low speed intermediate layer could account for this phenomenon. Officer (1,5) has derived the frequency equation and solutions for the three-liquid half space by the use of rays and plane-wave reflection and transmission coefficients.

The models for shallow water sound propagation mentioned so far are idealized. In many circumstances the ideal models are adequate. More often they are not. There are many parameters which influence shallow water sound propagation. Weston and Horrigan 1967 (1,6) have identified ten different mechanisms for the fluctuation of sound propagating over the same path. By observing the amplitude and phase fluctuation of 2kHz sound transmitted continuously over a 74 mile path in the Bristol Channel the periodicity of the fluctuations could be studied. The sound fluctuation was observed to be:

(i) seasonal in amplitude

(ii) seasonal in phase

(iii) diurnal in amplitude due to the changing aggregation of fish

(iv) various due to the depth-dependence of the tidal streaming velocity

(v) various due to the tidal changes in water depth

(vi) phase effects due to changes in the mean tidal streaming velocity

(vii) storm effects

(viii) surface duct effects

(ix) fluctuations of a few minutes period due to fish, daytime only

(x) fluctions of several minutes period due to internal waves, near slack water only.

We see then that sea states, currents, temperature gradients and especially the presence of fish cause large fluctuations in the transmitted sound intensity. In particular, Weston and Horrigan report a 15dB attenuation due to the breaking up of fish shoals at dusk.

We shall, in this paper, not be considering the fluctuation of the just-discussed phenomena, we shall consider the effect on sound propagation of:

(i) a sound absorbing bottom

(ii) variation in the bottom depth.

In 1955 Kornhauser and Raney (1,7) derived the attenuation coefficient for each mode from the attenuation in the lower medium. They found the attenuation coefficient, which is frequency dependent, increases repidly with increasing mode order.

Williams and Lewis (1,8) following on from this work used the modal attenuation coefficients derived by Kornhauser and Raney and allowed for a slowly varying bottom depth to derive average intensity decay curves.

Two criticisms of Williams and Lewis' report are:-

(i) It assumes an unreal dependence of attenuation on frequency.

(ii) It does not allow for modal interference.

Field Work done by the RAN

The RAN has conducted an acoustic trial in shallow water. In keeping with current geophysical practice explosive charges were used as sources. Hydrophones were laid on the bottom in about 200 ft. of water and the trials ship sailed away setting off charges at predetermined ranges. Several radial runs were executed in this fashion as well as one circular run. The acoustic signals received at the hydrophone were tape recorded. These tapes were subsequently analysed and the propagation loss curves, that is the curves of transmission loss in dB re 1 ft. vs range, for the various frequencies were obtained. Sonagrams were made of many shots.

Figs 16 and 30 show typical propagation loss curves and selected sonagrams of shots. A summary of the results obtained is:-

(i) The slope of the propagation loss curves indicate an energy transmission law of $r^{-3.5} \rightarrow r^{-4.5}$ where r is the distance from the source. This slope is frequency dependent, the higher frequencies being attenuated less rapidly.

(ii) The energy loss at a fixed range increases with frequency. Owing to (i) this increase becomes smaller with increasing range.

(iii) Intensities along the constant range runs vary by as much as 15dB. The average water depth remains constant. This variation of intensity is a function of bearing and not a random fluctuation. This can be seen because the energies received from the shots set off on the radial runs correlate well with the energies received from the shots set off on the circular runs at the points where the radial and circular runs cross. Since these independent runs were made at different times of day, the dominant factor influencing the propagation losses is seen to be the bottom.

Discussion of Experimental Results

In order to determine whether the Pekeris model of water overlying a fluid sediment was satisfactory, sonagrams of many shots were studied. If normal-modes were propagating, then the sonagrams of the shot arrivals would show mode structure due to the dispersive propagation. Denham and Kibblewhite (1,9) in their analysis of long range propagation of sound off the New Zealand coast give examples of sonagrams of shots where mode propagation is apparent. The sonagrams of the RAN shots however, showed no distinct mode structure. Nor was dispersion apparent, the shot duration was essentially independent of range. The assumptions needed to incorporate the Pekeris model therefore were not feasible and hence ray theory was used to calculate the acoustic intensity as a function of range.

In previous literature (1,10)(1,11) ray theory had been used assuming incoherence or partial coherence only of the signals from the separate ray arrivals. However to say that in shallow water the separate ray arrivals are randomly distributed in phase is not generally correct. Most authors dismiss this point lightly with very little justification. Two situations which show strong coherence between the ray arrivals are:-

(i) Pekeris' Normal Mode Propagation

Tolstoy (1,12) shows the correspondence between ray theory and mode theory. In ray theory the total set of multiply-reflected ray paths from an infinite set of images displaced along a vertical line through the source as shown in Fig.1. When a shot is fired each of these images simultaneously transmits a shot impulse. These impulses from the various images travel towards the receiver via the shortest route. At discrete points along this path the phase and amplitude of the pulses change abruptly corresponding to surface or bottom reflections. Because the higher order images are further from the receiver than the lower order images, the shot is heard at the receiving point for a much longer time than the duration of the shot itself. In addition to this, the received shot intensity level varies with time. It is this variation with time that indicates the separate rays arrive coherently.

Let us label the images according to the number of surface and bottom reflections a ray, from it to the receiver, undergoes. The group of images for which the total number of reflections en route is approximately the same will arrive at the receiver almost simultaneously. Depending on the distribution of phases within this group, the rays will reinforce or cancel. Since the duration of the shot is small compared to the total received shot duration and successive image sets are further from the receiver these reinforcements and cancellations of the successive image sets manifest themselves as separate modes of propagation arriving at different times at the receiver. If all the rays arrived incoherently, no such mode structure would exist and the received intensity would vary only slowly.

(ii) The Propagation Loss Curves obtained by the RAN

Using ray theory, we calculate the propagation loss curves for isovelocity water as a function of range. If we assume the separate ray arrivals are incoherent, then the slope of the loss curve is between 3 and 6dB per range doubled, Fig 18. This slope increases with increasing bottom loss. A slope of 3dB per range doubled corresponds to lossless reflection from the bottom and hence normal modes propagate. A slope of 6dB per range doubled corresponds to a perfectly absorbing bottom and hence we have only the direct and surface reflected arrival undergoing spherical spreading. 6dB per range doubled is the maximum slope obtainable, assuming the rays add incoherently.

The fact that the propagation loss curves in the area considered exhibit a slope of 10-15dB per range doubled indicates that phase annihilation has occurred and hence the rays arrive coherently at the source.

SYNOPSIS OF THIS PAPER

The present paper analyses shallow water propagation allowing for phase coherence between the separate rays. An IBM 360/50 computer was programmed to calculate the amplitude and phase of each ray at the receiver. The amplitude and phase change of each bottom reflection was computed at each step from the bottom loss and phase change vs grazing angle data fed into the computer. These separate rays were then summed coherently to obtain the total intensity at the receiver.

The propagation loss curves were then plotted on a function of:-

(i) frequency

(ii) bottom loss

(iii) depth of receiver

In the area considered the bottom depth changes by a factor of two several times in the length of a run. Because these depth changes occur over large distances, the bottom is essentially flat with a maximum slope of one in fifty.

To ascertain the effect of this variation in depth a type of perturbation theory was used. To the calculated exact phase of each ray a phase correction was added. This correction was selected randomly from a distribution of phase correction factors. The distribution of phase correction factors was calculated from the change in path length of the ray from source to receiver due to the statistical variation of the bottom depth about the mean. By running this program repetitively with different sets of random numbers an expected variation of the signal intensity at the receiver was determined.

The theoretical 'sonagram' of the shots was calculated using the bottom loss parameters produced in the first section of the paper. These sonagrams show the shot duration over a lossy bottom is small compared to the shot duration which would occur if the bottom were lossless and normal modes were propagating. To verify Tolstoy's(1,12) comparison between ray and mode theory, the arrival times for the first four modes as a function of frequency were computed. The bottom was assumed to be lossless and the range was the same as the range used to calculate the theoretical 'sonagrams' of the shots.

REFERENCES

(1,1) LAMB, H. (1904) "On the Propagation of Tremors over the Surface of an Elastic Solid" Phil. Tr. Roy. Soc.A, 203, 1.

(1,2) PEKERIS, C.L. (1941) "The Propagation of an SH Pulse in a Layered Medium". Am. Geophys. Union, pt 1, p 392.

(1,3) PEKERIS, C.L. (1948) "The Propagation of Explosive Sound in Shallow Water." Geol. Soc. Am. Memoir 27.

(1,4) PRESS, F. and EWING M.(1948) "Low-Speed Layer in Water Covered Areas." Geophysics, Vol.13, pp 404-420.

(1,5) OFFICER, C.B., Jr.(1951) "Normal Mode Propagation in Three-layered Liquid Half Space by Ray Theory." Geophysics, Vol.16,pp 207-212.

(1,6) WESTON, D.E. and HORRIGAN, A.A. (1967) "On Shallow-Water Sound Fluctuations with some Speculations upon an April Evening." Admiralty Research Laboratory, ARL/L/N162.

(1,7) KORNHAUSER, E.I. and RANEY W.P. (1955) "Attenuation in Shallow-water Propagation due to an Absorbing Bottom." J.Acoust. Sec. Am.27, 689

(1,8) WILLIAMS, A.D., Jr. and LEWIS, M.N. "Approximate Normal-Mode Methods of Calculation for Sound Propagation in Shallow Water." Brown University Technical Report 56-1 (Project NR 385-204).

(1,9) DENHAM, R.N. and KIBBLEWHITE A.C. (1966) "Experiment on Sound Propagation in Shallow Water under Isovelocity Conditions." J. Acoust. Soc. Am.40, 1337.

(1,10) MACKENZIE, K.V. (1961) "Long-Range Shallow-Water Transmission". J. Acoust. Soc. Am. 33, 1505.

(1,11) McLEROY, E.G. (1961) "Complex Image Theory of Low-Frequency Sound Propagation in Shallow Water". J.Acoust. Soc. Am.33, 1120.

(1,12) TOLSTOY, I (1959) "Modes, Rays and Travel Times". J. Geophys. Res. 64 pp.815-21.

2. CALCULATION OF PROPAGATION LOSS CURVES USING COHERENT RAY THEORY

In this section we set about calculating the transmitted energy loss as a function of range. We will make no assumptions about the randomness or pseudo-randomness of the phases of the ray arrivals at the receiver as has been done in the past by other authors. We will compute the exact phase of each ray at the receiver in order to find the dependence of transmission loss on:-

(i) Range

(ii) Bottom Loss

(iii) Frequency

(iv) Depth of receiver.

Since we wish to obtain theoretical curves of transmission loss to match the experimental curves obtained by the RAN our model must allow for the important environmental features in the area where the RAN trial was held.

Relevant Geophysical, Oceanographic and Experimental Data

(i) Bathythermograms taken at various stations indicate the water to be essentially isovelocity in nature.

(ii) The bottom consists of a clayey silt to a fine sand.

(iii) The bottom is essentially flat with an average depth of 200 ft.

(iv) The explosive sources were set so they exploded at about 40 ft.

(v) The receiving hydrophones were laid on the bottom in 200 ft. of water.

(vi) Travel time curves (Fig.2) for shots on one run show the bottom to have a layered structure.

(vii) The shot duration is essentially independent of range (Fig.30).

(viii) There was good experimental correlation between the total energy in the shot and the intensity at peak pressure.

Discussion of these results

The Bottom

Since the bottom is muddy or silty, we can attribute to it a density of 1.5 to 2.0 times the density of water (Hamilton(2,1)). Further, we can attribute a sound velocity of .97 to 1.2 times the velocity in water to the sediment. Hampton 1967(2,2) has conducted experiments to determine the attenuation and velocity in water-saturated sediments for a large range of sediment concentrations and several sediment types. He showed that where the sediment was in suspension, the local sound velocity was lower than the sound velocity in water and this velocity increased to the unconsolidated sediment velocity as the concentration of sediment increased. The mechanism that causes the velocity of sound in the suspension to be lower than that in the water is easy to see. We have:-

$$c = \sqrt{\frac{K}{\rho}}$$

where c is the local sound velocity and K and ρ are the compressibility and density of the water-saturated sediment. When we have sediment particles in suspension and hence not intimately in contact, the compressibility K of the water is not modified significantly for low sediment concentrations. The density of the water-saturated sediment increases however and so we see that the sound velocity c is reduced. Hence we see that the sound velocity in water-saturated sediments decreases with increasing sediment concentration until the suspension density becomes so great that the compressibility increases due to adjacent particles constantly touching and hence transmitting stress. Under these circumstances the sound velocity rapidly increases to the normal sediment velocity. Not all sediments will form a suspension : clay and silt will and so we can expect that when the sea floor consists of silty clay, and there is a current, there will be always a layer of sediment in suspension. We see then that under these circumstances, which are frequently encountered, the sound velocity in the sediment will increase from a value below the water sound velocity (at the water/sediment interface), to the normal sediment velocity at some depth in the sediment.

The travel time curves of Fig.2 indicate that the normal sediment velocity is 1.11 times the velocity of sound in water. Whether the sediment arrivals are refracted rays travelling horizontally in the sediment or are rays travelling through the sediment and reflected from a deep high speed layer is of no consequence. Officer (2,3) shows that for large ranges, the slope of the travel time curve of reflected arrivals is asymtotic to the slope of the travel time curve of refracted arrivals. That a low speed layer exists is seen because:-

(a) The high propagation losses encountered in the RAN trial indicate the bottom loss is high even at grazing incidence. A low speed layer will give high losses at low grazing angles since rays will be refracted towards the normal on passing through the water/low speed layer interface. Using Fig.9 we see there are two mechanisms which give large attenuations in the intensity of the sound following path (ii):

(i) Attenuation due to propagation in layer 2.

(ii) Attenuation due to imperfect reflection from the low speed sediment/high speed sediment interface. Figs 6 and 7 give curves of reflection coefficient and energy loss of a plane wave travelling in a low speed layer being reflected from an interface with a high speed layer. The reflection coefficient and energy loss are plotted against angle of incidence for several wave attenuations in the high speed layer.

Both of the mechanisms (i) and (ii) give an energy loss which increases rapidly with frequency. Hence a low speed layer will give a high bottom loss which increases with frequency at low and zero grazing angles.

(b) The thin low speed layer acts as a 'high pass' filter and allows only the higher frequencies to pass from the sediment to the water. Sonagrams (Fig.23) show that the two arrivals before the water wave arrival have a central frequency of 600Hz. A low speed layer 5-10 ft. deep effectively filters out all low frequency components from a sound wave passing through it.

The Nature of the Received Shot

That the received shot duration is independent of range can be seen from Fig.30. If normal modes were propagating over a lossless bottom, the shot duration would be proportional to range (Officer(2,4)). Lack of dispersion in the water wave can be explained in terms of ray theory.

When the bottom loss is high, the signal intensity from the higher order images (Fig.1) becomes rapidly smaller with increasing image order. Dispersion in the received signal however, is due to the late-arriving signals from the higher order images. Hence where bottom loss is high, the received shot duration is essentially independent of range. Since only the rays which have low grazing incidence at the bottom carry significant energy and there is negligible separation in the time of arrival of these rays, the peak intensity at the receiver due to a shot will be the same as the peak intensity due to a continuous source. The peak intensity within a shot is proportional to the total energy when the shot duration is constant. Hence the energy transmission loss curves for a continuous source will be approximately the same as the energy transmission loss curves for an explosive source when

(i) Shot duration is short

(ii) Shot duration is constant with range.

The Model Adopted

The model is that of Fig.1, consisting of a two layer model of isovelocity water overlying a sediment base. The water depth is taken as 200 ft. The source is a continuous point source situated 40 ft. below the surface. The bottom is assumed to be lossy and the bottom reflection and phase change on reflection curves of the form given in Fig.3.

A full account of the derivation of the reflection coefficient of Fig.3 is given in Appendix 1.

Formulation of the Problem

Considering Fig.1 now, we see that at any instant of time the source and all of the images will be in phase, transmitting omnidirectionally a uniform intensity signal. The time independent amplitude potential at the receiver for the Ray$_\alpha$(I,J) is given by:- (Officer)

$$X_\alpha\ (I,J) = \frac{X_o\, \mu_\alpha^I\ (I,J)}{R_\alpha\ (I,J)}\ e^{-j\{kR_\alpha(I,J) + \Psi_\alpha(I,J)\}} \qquad (2.1)$$

or $$X_\alpha = \frac{X_o}{R}\ \mu^I\ e^{-j(kR + \Psi)} \qquad (2.2)$$

where:-

X_o is the amplitude at unit distance

α = T or B representing the upper or lower image sets respectively as shown in Fig.1

X = X_α (I,J) is the amplitude at the receiver of the Ray_α (I,J)

μ = μ_α (I,J) is the bottom reflection coefficient

I is the number of bottom reflections undergone by Ray_α (I,J)

J is the number of surface reflections undergone by Ray_α (I,J)

R = R_α (I,J) is the path length of the Ray_α (I,J) from source to receiver.

k is the wave number.

Ψ = Ψ_α (I,J) is the total phase change en route due to surface and bottom reflections.

Referring again to Fig.1.

$$\begin{aligned} W_T(I,J) &= Z-D + 2DJ + 2(H-D)\ I \\ W_B(I,J) &= D-Z + 2DJ + 2(H-D)\ I \end{aligned} \qquad (2.3)$$

and so

$$R = \sqrt{(W^2 + T^2)} \qquad (2.4)$$

The angle of incidence A of the Ray_α (I,J) is given by:-

$$A = \tan^{-1}(T/W) \qquad (2.5)$$

The critical angle of incidence C is given by

$$C = \sin^{-1}(C1/C2) \qquad (2.6)$$

From Fig.3 we see that when A <C, the bottom reflection coefficient is very low and rays which have an angle of incidence greater than critical will be rapidly attenuated.

In the summation of X_B and X_T over I and J, we see (Fig.1) that since we will be summing successively higher order images, it is useful to redefine X_B and X_T.

Let

$$\left.\begin{aligned} X_B\,(2K-1) &= X_B(K,\ K-1) \\ X_B\,(2K) &= X_B(K,\ K) \\ \text{and}\quad X_T\,(2L-1) &= X_T(L-1,\ L) \\ X_T\,(2L) &= X_T(L,\ L) \end{aligned}\right\} \qquad (2.7)$$

The total amplitude at the receiver will be given by

$$X = X(o) + \sum_{K=1}^{M},\ \sum_{L=1}^{N} (X_B(K) + X_T(L)) \qquad (2.8)$$

We are summing successive orders of images and hence W is an increasing function of K and L. This means A is an increasing function of K and L.

Using the changed notation of equation 7., we define M and N

$$\begin{aligned} A_B(M) > C > A_B(M+1) \\ A_T(N) > C > A_T(N+1) \end{aligned} \qquad (2.9)$$

M and N are then the values of the dummy parameters K and L which give the highest order images below cutoff.

From equation 2.2, the total change in amplitude and phase due to all of the bottom and surface reflections from source to receiver is given by:-

$$\mathrm{Ref} = \mu^{I} e^{j\Psi} \qquad (2.10)$$

The reflection from the surface is assumed lossless with a phase change of II. Associated with each bottom reflection, there is an amplitude change of μ and a phase change of ϵ . μ and ϵ are selected from the family of μ and ϵ vs A given in Fig.3.

The total reflection coefficient from source to receiver for the Ray $_{\alpha}$ (I,J) is given by:-

$$\mathrm{Ref} = \mu^{I}{}_{\alpha}(I,J)\ e^{j[(\Pi J + \epsilon_{\alpha}(I,J)I]} = \mu^{I}{}_{\alpha}(I,J)\ e^{j\Psi_{\alpha}(I,J)} \qquad (2.11)$$

$$\text{Hence}\quad \Psi_{\alpha}(I,J) = \Pi J + \epsilon I \qquad (2.12)$$

Computation

Using the form of reflection coefficient and phase change given in Fig.3, we now evaluate the series(2.8) by a computer program (Appendix 2). The propagation loss as a function of range, frequency, receiver depth and bottom loss can be obtained by varying each of these parameters separately while keeping the others constant. Figs 10-15 plot the theoretical propagation loss curves as a function of range, frequency bottom loss and receiver depth.

These graphs show:-

(a) The slope of the propagation loss curve increases with:-

(i) decreasing frequency Fig.10(b)
unless bottom is lossless Fig.10(a)

(ii) increasing bottom loss Fig.11

(iii) increasing range Figs.10-15

(b) The propagation loss (dB re 1 ft) decreases with

(i) decreasing bottom loss Fig.11

(ii) Increasing height off bottom Fig.14
unless bottom lossless Fig.12

(iii) decreasing distance from sound source Figs.10-15.

(c) The difference between hydrophone response on the bottom and 40 ft. off the bottom increases with

(i) increasing frequency Fig.15

(ii) increasing bottom loss Fig.13

(iii) increasing range for low frequencies
decreasing size for higher frequencies } Fig.13

3. INTERPRETATION AND DISCUSSION OF THE RESULTS

(a) That the slope of the propagation loss curves increase with increasing range we expect. Indeed all of the curves are found to have envelopes of the form:

$$I = r^{-1} e^{-\mu r} \qquad (2.12)$$

and we immediately see the 1-1 correspondence between this decay law and the one obtained when we use normal mode propagation.

$$I = \sum_{i=1}^{N} r^{-1} e^{-\mu_i r} \qquad (2.13)$$

In the latter case μ_i is the attenuation coefficient of the i^{th} mode.

Where the bottom is lossless, so many rays are tramsmitted from the source to the receiver without loss that the phases of these are arbitrary and so from geometrical considerations alone the spreading law is r^{-1} irrespective of the propagating frequency. Where there is a bottom loss, only the rays with small grazing angles at the bottom and hence few bottom bounces from source to receiver, carry significant energy. Each low grazing incidence ray has an approximately antiphase surface reflected pair, the degree of out-of-antiphase increasing with increasing grazing angle of the ray. The degree of out-of-antiphase, being due to path length differences between the ray and its surface reflected pair, increases with increasing wave number and hence frequency.

We expect that phase cancellation will be more complete as the frequency decreases and the bottom loss increases and so the rate of energy loss with range will be correspondingly higher. In equation 2.12 μ can now be seen to increase with bottom loss and decrease with frequency. Bottom loss is a function of frequency and so μ can be expressed as a function of frequency only.

(b) Where the bottom loss is non-zero, there is an improvement of the order of 10dB in the receiver response by raising the receiver off the bottom. Very close to the bottom each ray has a bottom reflected pair that has traversed almost exactly the same path length but has undergone a phase change of approximately Π radians at the bottom reflection. Thus the sound intensity in the near vicinity of the bottom is considerably reduced. However, while there is strong phase cancellation close to the bottom, the phase coherence, and hence cancellation, several wavelengths above the bottom is not nearly so strong, and so the receiver response is greater off than on the bottom.

If the bottom is lossless, a ray with large grazing angle will not be antiphase with its bottom reflected pair. The phase change at a bottom reflection is dependent on the grazing angle of the ray : the phase change decreasing from Π radians at zero grazing incidence to zero at critical grazing incidence. Thus the effect of the lossless bottom is to allow the rays with high grazing angles, large numbers of surface and bottom reflections, and hence effectively random phases, to propagate with the result that the receiver response is not depth dependent.

When we compare the family of theoretical curves with the experimental curves of Fig.16 we find bottom reflection parameters can be found to make the theoretical curves 'fit' the experimental curves. The theoretical curves thus found are given in Fig.17 and the predicted bottom reflection curves are given in Fig.4. It is useful to note that the bottom reflection parameters used to make the theoretical curves fit the experimental curves are very frequency dependent. This is in accordance with the experimental results of Marsh (2,5) and is in fact generally accepted to be the case. The high bottom loss at grazing incidence is explained using the model of Fig.2 in Appendix 1.

It is interesting to note the theoretical curves obtained, using the bottom reflection parameters found above, for the case where no coherence of rays is allowed. These curves Fig.18 exhibit:

(i) No frequency dependence

(ii) A max slope of 6dB per octave doubled

(iii) No depth dependence of receiver response.

4. CONCLUSIONS

We see that to account for the high rate ($r^{-3.5} \rightarrow r^{-4.5}$) of transmitted energy loss in shallow isovelocity water and the dependence of receiver response on receiver depth, we must allow for the phase coherence of the rays. It is maintained that it is only in exceptional circumstances that the phases of the propagating rays can be considered random.

In chapter 3 we will be considering the effect on transmission loss of a perturbation in the bottom depth. The results of chapter 3 show that the propagation loss curves obtained in this chapter are stable under a small perturbation of the parameters and hence these propagation loss curves are not singularities in a mathematical solution but are physically realizable.

REFERENCES

2,1 Hamilton, E.L. et al(1956) "Acoustic and other physical properties of shallow water sediments off San Diego". J. Acoust. Soc.Am.28.1

2,2 Hampton, L.D.(1967) "Acoustic properties of sediments". J. Acoust. Soc. An. 42.4

2,3 Officer, C.B.(1958) " Introduction to the theory of sound transmission". McGraw-Hill Book Co., p.9 242.

2,4 Officer, C.B.(1958) "Introduction to the theory of sound transmission" McGraw-Hill Book Co., p.7.39

2,5 Marsh, H.W. and Horton,C.W.(1965) "Reflection and scattering of sound by the sea bottom". Auco Marine Electronics Office.

3. THE VARIATION IN SIGNAL INTENSITY DUE TO THE ROUGH BOTTOM

Recent Work in the Field

Tolstoy and Clay (3,1) discuss the variation in intensity due to inhomogenities in the medium. They treat :

(a) The Reflection of acoustic signals at a rough boundary.

(b) The reflection from a slightly irregular stratified medium.

(c) Propagation in a waveguide with slightly irregular interfaces.

In the treatment of (c), Tolstoy and Clay assume :

(i) The eigenvalues of the characteristic equation correspond to the local stratification.

(ii) The stratification varies slowly from one local region to another.

(iii) There is no reflection or appreciable scattering of energy from one mode to another in the transition regions.

The model assumed then,is one of normal mode propagation, assuming the modes 'accommodate' themselves to a slowly changing bottom depth with no interaction between the separate modes.

Since normal modes consist of wave packets of 'stationary phase' propagating down the waveguide, we see that the largest single cause of intensity fluctuation is mode interference. A small change in the phase of each mode can result in a large change in the received intensity. These small phase fluctuations can be caused by inhomogeneties in the propagating medium or by irregularities in the waveguide interface. Tolstoy and Clay evaluate the effect of the irregular waveguide on mode propagation by considering the phase perturbations of each mode introduced by a small variation in the bottom depth. Their line of argument is as follows:-

Consider the wave equation,

$$\nabla^2\phi + \frac{\omega^2}{c^2}\phi = 0$$

put $\phi = R(r).\,\phi(z)$

then $\nabla_r^2 R(r) + k^2 R(r) = 0$

$$\frac{\delta^2}{\delta z^2}(\phi(z)) + \gamma^2\phi(z) = 0$$

where $k^2 + \gamma^2 = \frac{\omega^2}{c^2}$

Now the solution $\phi(z)$ can be expanded into normal modes $\phi(m,z)$ and these functions are discrete for trapped modes.

The acoustic pressure at depth z and range r can be expressed as : (Tolstoy & Clay)

$$p(t) = -\frac{i\rho}{\sqrt{r}} \sum_{m=1}^{M} P_m e^{-i(\bar{k}_m r - \omega t - \Pi/4) - \delta_m r}.$$

where P_m is a factor taking into account the effect of transmitter depth, receiver depth, source strength and the horizontal component of the wave number on the received pressure due to the m^{th} mode. ρ is the density of the propagating medium and δ_m is the attenuation coefficient of the m^{th} mode.

If now there is a perturbation in the bottom depth, the pressure at the receiver will be given by:-

$$p(t) = -\frac{i\rho}{\sqrt{r}} \sum_{m=1}^{M} \bar{P}_m e^{-i(\bar{k}_m r - \omega t - \Pi/4 + \Delta S_m) - \delta_m r}$$

where $\bar{P}_m$ is $\sqrt{P_m(\text{source}).\ P_m(\text{receiver})}$

and $\bar{k}_m = \langle k_m(r) \rangle_r$

and ΔS_m is the total phase change of the m^{th} mode over the distance r due to a perturbation in the wave number k_m of $\epsilon_m(r)$

$$\text{i.e.} \quad k_m(r) = \bar{k}_m + \epsilon_m(r)$$

and so
$$\Delta S_m = \int_o^r \epsilon_m dr$$

Hence Tolstoy and Clay derive the formulae for the intensity fluctuation to be expected in waveguide propagation due to mode interference. To be useable we must know the distribution ϵ_m and hence the distribution of ΔS_m.

The above analysis of Tolstoy and Clay is limited in its application because

(i) All the rays comprising the 'stationary phase' of a mode do not travel identical paths. If they did the intercept time of each mode would be very short. That the intercept time is not short can be seen from typical sonagrams of shallow water propagation. (Tolstoy and Clay pg.111). Hence the several paths which constitute one mode will have phase correction factors which can differ markedly.

Consider Fig.1. The rays undergoing approximately the same total number of reflections will strike the bottom at points which can be large distances apart. If these rays in the unperturbed case constituted the coherent wave packet of a mode, we could hardly say all these rays in the perturbed case had their path lengths altered by the same amount due to a varying bottom depth. Consider, for example, the two rays having a total number of surface and bottom reflections of 10; unless the source and receiver are both near one of the interfaces we can expect the positions of bottom bounce of these two rays to be separated by up to 2,000 feet where the source/ receiver separation is 10,000 ft.

We see then that ϵ_m and hence ΔS_m can vary substantially depending on which ray we are considering and hence

$$\Delta S_m = \int_o^r \epsilon_m(r) \, dr$$

is a good approximation to the phase correction to be applied to each mode only for the higher order modes which interact strongly with the bottom.

(ii) No account is taken of the variation in the slope of the bottom.

(iii) No scattering of sound 'out' of a mode is allowed.

(iv) Since mode interference is assumed to cause the fluctuations in intensity the analysis is only applicable to a C.W. source. When we have an explosive source of short duration the separate modes have different arrival times and no mode interference can occur. The fluctuation in received intensity does occur however and so the analysis of Tolstoy and Clay is not applicable to the case where the source is an impulsive one.

<u>Procedure Followed in this Paper</u>

In order to evaluate the rms fluctuation in the received intensity of transmission and hence in the transmission loss, caused by the variation in the bottom depth, we must allow for the phase distortion caused by the path lengths of the several rays, which in the unperturbed case constituted a mode, being altered by varying amounts. Once again we use the model of Fig.1 and make the assumption that, since the bottom loss is high, only those rays with low grazing incidence contribute significant amounts of energy. This assumption is verified in the next chapter where we plot the intensity within the received shot as a function of time.

The amplitude of sound at the receiver due to the K^{th} image on the α (top or bottom) side is given by (2.2) (2.7)

$$X_\alpha(K) = \frac{X_o}{R} u^I e^{j(kR + \Psi)} \tag{3.1}$$

where $\Psi = I.B + J.\Pi$

The bottom depth varies about some mean value H and so the ray path lengths from source to receiver will vary about some mean value also

Put $$R = \bar{R} + \Delta R \tag{3.2}$$

where $$\bar{R} = \sqrt{W^2 + T^2} \tag{2.4}$$

Hence $$X_\alpha(K) = \frac{X_o}{R} u^I e^{j(k\bar{R} + \Psi + \delta)} \tag{3.3}$$

where $$\delta = k.\Delta R \tag{3.4}$$

and so when $\Delta R \ll R$

$$X_\alpha(K) \doteq \frac{X_o}{\bar{R}} u^I e^{j(k\bar{R} + \Psi + \delta)} \tag{3.5}$$

$$= \bar{X}_\alpha(K)\, e^{j\delta} \tag{3.6}$$

where $$\bar{X}_\alpha(K) = \frac{X_o}{\bar{R}} u^I e^{j(k\bar{R} + \Psi)} \tag{3.7}$$

Thus, when $\Delta R \ll \overline{R}$, the effect of a small increase in path length is to alter the phase of the received image by δ.

The total intensity at the receiver will be given by:-

$$X = X(0) + \sum_{K=1}^{M} \sum_{L=1}^{N} \left(\overline{X}_B(K)e^{i\delta(K)} + \overline{X}_T(L)e^{i\delta(L)} \right) \qquad (3.8)$$

In order to evaluate (3.8) we must know all the δ's. We see that the phase distortion δ for a particular ray will be described by a distribution the standard deviation of which increases with:-

(i) T he magnitude of the fluctuation in bottom depth.

(ii) The grazing incidence of the ray upon striking the bottom.

(iii) The total number of bottom bounces from source to receiver.

<u>The Perturbation of Phase δ.</u>

Typical bottom profiles for several runs in the area where the RAN acoustic trial was held are shown in Fig.19. From these and more detailed records of echo soundings we see that the bottom depth, although varying by a factor of two, does so in such a large distance that the bottom in any small area can be considered flat and horizontal. Depth/frequency curves for all of these runs were drawn Fig 20 (a $\rightarrow$ e) and a representative depth distribution curve was determined Fig.20f. We can assume then that when the bottom depth fluctuates about a mean depth, the depth/distribution curve has the bimodal form of Fig.20f. We shall use Fig.20f, with a change of origin, as the depth distribution function $W(\Delta h)$ about the mean.

Referring to Fig. 24, we see that the increase in path length per bounce due to a perturbation in the depth of Δh is

$$\Delta r = -2 \times \Delta h \times \cos(\phi) \text{ to the first order} \tag{3.9}$$

If the surface of the water is smooth, the total variation in path length due to the bottom depth variation for a ray undergoing I bottom bounces is given by:-

$$\Delta R(I) = \sum_{i=1}^{I} \Delta r_i \tag{3.10}$$

$$= -2 \cos\phi \sum_{i=1}^{I} \Delta h_i \tag{3.11}$$

where the Δh_i are selected from the distribution $W(\Delta h)$. For the convenience of computation, we define a variable $\Delta H(I)$

$$\Delta H(I) = \sum_{i=1}^{I} \Delta h_i \tag{3.12}$$

where the Δh_i are selected from $W(\Delta h)$.

Then $\Delta R(I) = -2 \cos\phi \, \Delta H(I)$ (3.13)

where $H(I)$ is selected from $W(\Delta H(I))$, the distribution of $\Delta H(I)$.

Since $W(\Delta h)$ is a symmetrical finite distribution, $W(\Delta H(I))$ is a normal distribution (for sufficiently large I) with standard deviation given by

$$\sigma = \sigma_0 \sqrt{I} \tag{3.14}$$

where σ_0 is the standard deviation of $W(\Delta h)$.

To confirm that (3.14) is a good approximation to σ a Monte Carlo procedure was adopted where the distribution and standard deviation of $W(\Delta H(I))$ was obtained by summing sets of I variables selected from $W(\Delta h)$ randomly. This was done for several values of I and hence the distribution curve and standard deviation as a function of I could be graphed as in Fig.23a. From the distribution curves we see that $W(\Delta H(I))$ is approximately a normal distribution even for I as small as twenty and we also see that $\sigma = 22\sqrt{I}$ is a good fit to the points of σ vs I shown in Fig.23b σ_o was taken as 22 for the purposes of computation and so equation 3.14 was verified.

To obtain a random variable $\Delta_o H(I)$ from approximately the distribution $W(\Delta H(I))$, we first generate a normal random variable $\Delta_o H(1)$ with mean zero and standard deviation σ_o, and then we multiply the variable so obtained by $\sqrt{I}$. We now have a normal random variable with an approximate distribution of $W(\Delta H(I))$.

To evaluate equation (4.8) we obtain all of the $\delta(K)$ by noting:-

$$\delta(K) = \delta_\alpha(I.J) \quad \text{using (E 1.7)} \tag{3.15}$$

$$= -2k\cos\phi\,\Delta H(I) \tag{3.16}$$

$$\doteq -2k\cos\phi\sqrt{I}\;\Delta_o H(1) \tag{3.17}$$

Thus by generating at each step a normal variable with mean o and standard deviation σ_o we can compute using (3.17) a pseudo -random phase correction for each ray.

The fact that for small I, say I <5 the distribution of $W(\Delta H(I))$ is not normal concerns us very little since:-

(i) The grazing angle for the lowest order rays is so low that the change in path length due to a perturbation in bottom depth is very small.

(ii) The very lowest order rays arrive at the receiver antiphase and hence there is very little contribution to the received intensity from the rays with very few bottom bounces.

Evaluation of the Sound Intensity Variation.

The series (Equation 4.8) was evaluated by the same computer program as that given in Appendix 2 using the reflection parameters of Fig.4 except that to the arrival phase of each ray a pseudo-random phase δ was added. $W(\delta)$, the distribution of δ, as we can see from above is a function of the angle of incidence of the ray, the no. of bottom bounces the ray undergoes and the bottom roughness. The details of the subroutine which computes a pseudo-random phase δ for each ray are given in Appendix 3. By repeating this entire process over and over, we generate by a Monte-Carlo technique the distribution function of the received intensity X.

We wish to find the behaviour of:-

(i) The rms fluctuation of received intensity.

(ii) The mean received intensity

as we vary:-

(i) the frequency

(ii) the magnitude of the bottom perturbation

(iii) the range.

Summary of results obtained

Figs 24-28 show that

(a) the rms fluctuation in received intensity:-

(i) Increases with frequency

(ii) Increases with range

(iii) Increases with increasing bottom roughness.

In each of the above cases the rms fluctuation increases to a <u>maximum</u> finite value for some value of the frequency, range and bottom roughness.

(b) The mean signal intensity increases with increasing bottom roughness.

(c) The intensity fluctuation is a slowly varying function of frequency.

<u>Discussion and Interpretation of Results</u>

The bottom loss parameters assumed are those of Fig.4 and the mean bottom depth is 200 ft. By using the exact depth distribution curve of Fig.20F having a standard deviation of bottom depth variation of 22 ft. about the mean, we ought to be able to predict the variability of the received intensity, of sound propagating in the shallow water area of the RAN trial. The propagation loss curves of Fig.17 then, are those obtained where the bottom depth is constant at 200 ft. If the bottom is not flat but fluctuating in depth, we can expect that the propagation loss over a given distance in any one area will vary by as much as 10dB. This variation arises because the bottom depth variation causes the several propagating rays to undergo phase distortion and so the total coherent intensity also varies. The present theory gives that successive transmissions over the <u>same</u> path will undergo the same transmission loss. However, a small change in transmission path by means of a change in position or bearing will cause the transmission loss to vary. This is because the bottom profile varies extensively for changes in position and bearing and hence is best described statistically.

The intensity of the received energy fluctuates to an extent which increases with increasing bottom roughness. This intensity fluctuation does not increase indefinitely but assumes a maximum value when the bottom is rougher than a given value. The way in which the standard deviation of the intensity fluctuation increases with increasing bottom roughness for 100Hz is shown in Fig.24. Notice that Fig.25 shows that the rms fluctuation increases with range for fairly smooth bottoms. When the bottom is sufficiently rough we can no longer consider the received energy to be a perturbation of the energy received when the bottom is smooth. The phase distortions caused by the extra path lengths travelled by the several propagating rays become very large and so the rays can be considered to arrive with totally random phases. It is more appropriate in these circumstances to add the intensities of the several ray arrivals to obtain the total received intensity. When the bottom becomes so rough that this happens the fluctuation in received intensity will be a function of the number of rays which contribute to the total intensity.

Notice here that when we say the bottom is 'rough' we mean 'rough enough to cause an appreciable phase difference to a low grazing incidence ray'. We specify low grazing incidence because for a high loss bottom only these rays carry enough energy to be of significance. Hence 'roughness' increases with frequency and range. For high frequencies even a small perturbation in bottom depth can cause large phase fluctuations at the receiver and the phase fluctuation increases with increasing range.

Bottom loss also affects the apparent 'roughness' of the bottom. In an area where the bottom loss is high, the only rays which carry significant energies are those which have very low grazing incidences. Since the phase variation for any one ray is proportional to the number of bottom bounces and the grazing angle as well as the standard deviation of variation in the bottom depth, we see that rays with few bottom bounces and hence low grazing angles will not have their phases greatly modified. Where bottom loss is low however, rays which undergo a large number of bounces contribute significantly to the received signal intensity. Because these rays interact with the bottom so frequently, their phases become random in very short ranges and so the total received intensity is best obtained by summing the intensity of the several received ray intensities. Notice that any mode structure, expecially for the higher modes would be destroyed although the spreading law would be a cylindrical spreading law. This is because the rays add in intensity which gives r^{-2} spreading, but in addition to this the total received shot duration is proportional to r and hence the overall spreading law is

$$I \propto r^{-1}$$

We expect then that:-

(i) For small bottom 'roughness' the extent of received intensity fluctuation increases with increasing range.

(ii) 'Roughness' increases with:-

(a) increasing frequency

(b) increasing range

(c) decreasing bottom loss.

From the previous discussion we expect that as the roughness of the bottom increases, the phases of the rays carrying significant energy at the receiver will become more random. The energy loss rate of $r^{-3.5} \rightarrow r^{-4.5}$ we obtained in Fig.17 is due to the fact that each arriving ray which undergoes 'x' bottom reflections has a corresponding pair which has undergone 'x' bottom reflections also and has traversed the same distance from source to receiver. This latter ray has undergone one more surface reflection and so the received amplitudes due to these two rays are approximately antiphase because there is a phase change of 180° associated with each surface reflection. Hence by causing the phases of the separate rays to fluctuate, the signals from an image and its surface reflected pair will not be exactly antiphase.

As the phase distortion increases, so the rays will tend to become more and more incoherent, and more and more will the propagation loss approximate that obtained by adding the intensities only of the separate ray arrivals (Fig.18). A plot of the mean of the received intensity fluctuation vs standard deviation of bottom roughness (Fig.24) for 100Hz shows that for a standard deviation of bottom roughness greater than 50 ft. the separate ray signals can be thought to be incoherent while for a bottom variation of less than five feet, there is little change in the level of received signal intensity due to phase distortion.

We include Table 1, a typical table giving tabulated results of ten values of intensity for ranges 100,000 ft. and 200,000 ft. and frequencies 100, 500 and 1000.

TABLE 1

Variability in the Intensity(dB re 1 ft)

σ = 10 ft.

Range 100,000 ft.

Frequency	100	500	1000
Samples	- 94.17	- 99.65	-109.71
	- 93.38	-106.00	-107.42
	- 98.25	-102.19	-109.76
	- 100.85	-100.62	-121.01
	- 97.86	-100.18	- 99.54
	- 100.31	-100.00	-101.93
	- 106.83	-101.19	- 98.63
	- 103.34	-100.52	- 99.64
	- 95.27	-101.38	-100.42
	- 95.27	-104.78	-111.04
Mean	- 98.55	-101.65	-105.91
Standard Dev^{n} of Sample	4.1	2.1	6.8

Range 200,000 ft.

Frequency	100	500	1000
Samples	- 112.43	-110.25	-114.65
	- 111.07	-111.72	-120.65
	-107 .37	-109.93	-118.49
	- 117.44	-107.59	-110.92
	- 119.05	-108.10	-116.27
	- 114.10	-104.04	-114.55
	- 99.13	-107.42	-122.55
	- 105.56	-106.03	-114.30
	- 108.13	-108.41	-114.13
	- 125.71	-111.37	-112.92
Mean	- 112.00	-108.49	-115.92
Standard Dev^{n} of Sample	7.5	2.3	3.6

The standard deviation of bottom depth variation is assumed to be 10 ft. Notice that while at 100HZ the intensity fluctuation increases with range, it is difficult to make such a prediction at 500 or 1000 Hz.

So far, we have considered the intensity fluctuation of a single frequency sound. The question arises. If we have a discrete bandwidth of sound, how well does the intensity at one frequency correlate with the intensity at another frequency, over the <u>same</u> propagation path? (viz the same bottom profile). If the variation of intensity is rapid with frequency, then the total intensity from a finite bandwidth of sound will fluctuate very little.

To ascertain the affect of altering the propagating frequency slightly, equation 3.8 was evaluated for the central frequencies 100, 500, 1000Hz and also for six equally spaced frequencies about the central frequency <u>using the same set of random numbers in each case</u>. This corresponded to finding the received intensity for several closely spaced frequencies for sound propagating over the same bottom. The intensity variations with frequency are shown in Fig. 26 for many different ranges. Since the intensities at different ranges are calculated using different sets of random numbers, we see that Fig. 26 gives us a good idea of how the intensity fluctuates with frequency.

The normalized autocovariance functions of the intensity variation with frequency are given for several cases Fig. 27. The intensity variations are taken compared to the mean intensity at that range as determined from Fig. 8. We see from the autocovariance functions that the intensity varies only slowly with frequency. In addition to this we see that the rate of variation is proportional to the frequency.

That the intensity is a slowly varying function of frequency can be seen since

(i) The mean propagation loss at any one range varies very little indeed for a small change in frequency if all other parameters stay constant.

(ii) The phase changes caused by perturbations in the bottom depth differ only slightly when the frequency changes. In fact, the phase change differs at a rate which is proportional to the rate of change of frequency.

Consider a perturbation in path length of ΔR. The associated phase change due to this perturbation is:-

$$\epsilon = \frac{\Delta R}{X} . 2 \Pi \qquad (3.16)$$

$$= \frac{\Delta R \,.\, f.\, 2\Pi}{C}$$

$$\frac{d\epsilon}{\epsilon} = \frac{df}{f} \qquad (3.17)$$

and so the phase changes by the same fractional amount as the frequency. Where $df \ll f$ then $d\,\epsilon \ll \epsilon$ and hence a small frequency perturbation results in only a small variation in the phase perturbation. Equation 4.17 also tells us that the intensity varies slowly with respect to small <u>fractional</u> changes in the frequency of propagation.

Hence the fact that the intensity at 1000Hz varies slowly compared with changes in frequency of 10Hz while the intensity at 100Hz varies slowly when we change the frequency by 1Hz is expected.

From Fig.26 we can say now that if we are considering the intensity fluctuation as received from a broadband signal, the expected variation in intensity for a 6% filtered signal is only 1 or 2dB less than the expected variation when we filter out a single frequency. The intensity fluctuation we can expect is still of the order of 6dB when we use a 6% filter. Notice also that this fluctuation is constant for a 6% filter for frequencies in the range 100-1000Hz.

When we look at Fig.24 we see that the average transmission loss where the standard deviation of bottom depth variation is 22 ft (Fig.20F) is significantly lower than that when the bottom is flat. This would make the slope of the propagation loss curve much less than that required to simulate the experimental results obtained by the RAN except for one important oversight on our part. We have chosen variables from $W(\Delta H(I))$ randomly. Strictly speaking we ought not do so since the bottom depth does not vary in a <u>rapid</u> random fashion. The bottom depth is a slowly varying function even when we take into account the long propagation path. Since it is the relative changes in phase which the rays undergo due to the bottom depth variations that are significant and not the absolute magnitudes of the phase changes, we can adequately allow for the good auto-correlation with distance of the bottom depth by suitably reducing the magnitude of fluctuation by a factor μ.

To assess the magnitude of μ, we need the joint probability distribution of $\Delta R(I)$ and $\Delta R(I+J)$ as well as the autocorrelation function of the depth variation about the mean. Without performing the extensive calculation we see that μ will be in the range $.1 \rightarrow .99$. Taking $\mu = .45$, the series(4.8) was evaluated for twenty different ranges and three frequencies. In each case the series was evaluated four times using different sets of random phases. The energy losses as a function of range obtained thus are shown in Fig.21. Not enough points have been plotted to make a quantitative analysis of the results,but we see from a qualitative viewpoint the extent of fluctuation of the signal intensity.

Conclusions:

Where the bottom depth in one particular area varies statistically about a mean depth, we see that sound travelling equal distances over different paths will be attenuated by different amounts. The magnitude of the rms fluctuation in intensity is several dB.

As the bottom becomes rougher, the rms fluctuation increases from zero to a maximum value; the mean energy loss decreases from the value obtained for the case where the bottom is perfectly flat and the intensities of the rays are added coherently, to the value obtained when we add the intensities of the rays incoherently.

The rms fluctuation of intensity increases slightly with increasing range (10 to 20 miles) for low frequencies when the bottom is reasonably smooth. Otherwise the rms fluctuations are dependent upon bottom loss primarily, increasing bottom loss causing increasing rms fluctuation of the received signal intensity.

The autocorrelation function of the intensity fluctuation with respect to frequency indicates the intensity fluctuation is a slowly varying function of frequency. Thus the expected variation in the signal intensity for a 6% bandwidth signal is only one or twodB less than the expected variation in the signal intensity for a single frequency signal.

Suggestions for Future Work

As can be seen from this chapter the Monte Carlo technique of calculating expected variations in intensity lends itself immediately to the solution of the problem when we use a high speed digital computer. We use the same simulation technique to assess the affect on sound propagation of

(i) Internal waves

(ii) Perturbations of the velocity/depth profile about a mean value

(iii) Inhomogenities in the propagating medium : local variations in temperature salinity; fish

(iv) The changing bottom; change of sediment; rocky outcrops

where we can assign a statistical probability for any of the aforementioned events occurring. We must, of course, know the effect on propagation of these perturbations quantitatively in order to proceed with the simulation.

References

(3,1) Tolstoy & Clay : "Ocean Acoustics" McGraw-Hill Book Co.

4. CALCULATION OF THE RECEIVED WAVEFORM

A feature of the sonagrams of the shots of Fig.23 is that the propagation is essentially non-dispersive. Consider a ray with grazing angle ϕ striking a flat bottom

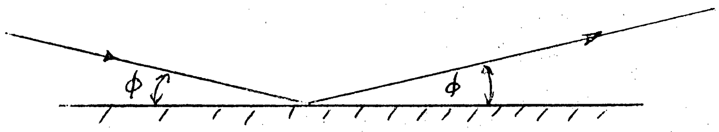

Referring to Fig.1, we see that

$$\tan\phi \doteqdot \sin\phi \doteqdot \frac{2HN}{R} \tag{4.1}$$

where H is the depth of water

N is the no. of bottom bounces from source to receiver

R is the total path length of the ray from source to receiver.

The extra path length travelled by this ray from the source to receiver compared to the path length of the direct ray is approximately:-

$$\Delta R \doteqdot R(\sec\phi - 1)$$

$$= \tfrac{1}{2}R\sin^2\phi \tag{4.2}$$

$$= 2\,\frac{H^2N^2}{R} \tag{4.3}$$

Now the received shot duration τ is proportional to R and hence:

$$\tau \propto \frac{N^2}{R} \tag{4.4}$$

Hence the received shot duration in water of uniform depth is proportional to the square of the maximum number of bottom bounces. The maximum number of bottom bounces is determined by our criterion of how much energy a ray must carry before it is considered to contribute significantly to the received signal intensity. We may arbitrarily choose -20dB as the threshold energy to be carried by a ray before it is considered to contribute to the total intensity. The maximum number of bottom bounces per ray allowed will be determined by the loss per bounce and the threshold intensity we choose.

The maximum number of bottom bounces will be a function of bottom loss. Since bottom loss increases with increasing grazing incidence, the maximum number of bottom bounces is not constant, but rather a function of grazing angle and hence range.

Consider these examples:-

(a) Normal-Mode Propagation

Here all rays with grazing incidence less than critical are reflected from the bottom without energy loss

Hence $N \alpha R$

and so $\tau \alpha R$ (4.5)

and the received shot duration increases linealy with range.

(b) Bottom Loss Independent of Angle of Incidence

N is constant.

Hence $\tau \alpha \frac{1}{R}$ (4.6)

and the received shot duration is inversely proportional to range.

(c) Bottom Loss dependent on Grazing Angle

$N = N(\phi, R)$

Let bottom loss be given by

$B = f(\phi)$

Then the total bottom loss from source to receiver for a ray undergoing N reflections is given by

$$BN = Nf(\phi)$$

Let the criterion for the contribution of a ray to be considered sufficient be:-

$$BN \leqslant A$$

where A is the threshold value.

If $N \leqslant A/f(\phi)$ the contribution of this ray will be considered. The received shot duration will be defined by

$$N = A/f(\phi)$$

Now $\quad \tau \;\alpha\; N \sin\phi$

i.e. $$\tau \;\alpha\; \frac{\sin\phi}{f(\phi)} \tag{4.7}$$

and for small ϕ, $\sin\phi \doteqdot \phi$

i.e. if τ is constant

$$f(\phi) \;\alpha\; \phi \tag{4.8}$$

and so for a constant pulse duration, the bottom loss must be proportional to grazing angle. The constant of proportionality will determine the pulse duration : the larger the constant; the shorter the received shot duration.

Hence for the assumed bottom loss profiles of Fig.3, we expect the received shot duration will be constant with range if ST = 1.0 and S $\neq$ 0 and that the received shot duration will decrease with range if ST <1.0.

It is to be noticed that where S is small, the shot duration will be proportional to range at short ranges since all rays up to the critical ray will contribute to the total received intensity. This proportionality with range will persist until the criterion:-

$$Nf(\phi) \leq A \text{ can be} \tag{4.9}$$

satisfied by $\phi < \phi_c$ where ϕ_c is the critical angle.

Tolstoy (II) points out that: "Travel times and intercept measurements of refracted waves cannot be connected directly to the concept of group velocity until the complete wave problem for the actual situation is solved. However, for very long ranges, such that the spherical wave fronts due to a point source, have become essentially plane, the group-velocity curves may permit us to estimate the velocity of the corresponding wave pockets. Note that for sufficiently long ranges the effects of a finite intercept will correspond to a very small relative error in the total travel time and that, in this sense, the group valocity concept also gives an asymptotically correct answer for travel time. But it cannot provide an accurate value for intercept time, since the latter is the literal calculation of travel time along a certain refracted ray path. A proper theoretical prediction for the intercept by normal mode methods can only be obtained from an exact solution of the receiver-plus-transient-source problem."

Pekeris, of course, has solved the receiver-plus-transient-source problem for normal mode sound propagation in shallow water. We shall in this section compute the intercept time for the case where the source is a square pulse of monochromatic sound.

We will calculate the contribution at the receiver due to <u>all</u> rays which have grazing incidence less than critical. Where bottom loss is non-zero, the highest order rays will make negligible contributions to the total received intensity. We will not discriminate against these rays. In this case the total received shot duration will be:

$$\tau = \tfrac{1}{2} R \sin^2\phi_c \qquad (4.2)$$

We wish to compute the received shot intensity at 100 discrete uniformly spaced times during τ

Consider a shot fired at t=o

If $t = t_o$ is the time of arrival of the direct ray, then

$t = t_o + \tau$ is the time of arrival of the ray from the highest order image such that its grazing angle is less than critical. We wish to calculate the received shot intansity at time:

$t = t_o + \Delta t \qquad o \leq \Delta t \leq \tau$

Assume the duration of the step pulse is γ .

The transmitted pulse has the form

$$\left.\begin{array}{ll} I = o & t \leq o,\ t > \gamma \\ I = I_o \sin wt & o < t \leq \gamma \end{array}\right\} \qquad (4.10)$$

The images which will contribute to the shot intensity at time $t = t_o + \Delta t$ are those images which satisfy the condition:

$$R_{t_o} + \Delta t - \gamma < R \leq R_{t_o} + \Delta t \qquad (4.11)$$

Where R is the total ray path for the ray which takes $t_o + \Delta t - \gamma$ seconds to travel from source to receiver.

Equation (4.11) can be restated

$$c.(to + t - \gamma) < R \leq c(to + \Delta t) \qquad (4.12)$$

By allowing Δt to assume all values from o to τ then, we obtain the shot intensity at all times during the received shot duration.

Full details of the program used to evaluate the intensity variation within the duration of the shot are given in Appendix 4.

We wish to obtain some idea of the mode structure within the received shot where the source is an explosion. The shape of an explosive pulse is the form:

$$I = o, \quad t < o \qquad (4.13)$$

$$I = I_o \, e^{-\lambda t}, \; t \geq o$$

After several surface and bottom reflections however, this pulse shape becomes broader and flatter so that the assumption of a square tone pulse will give the correct qualitative information about the mode structure and intensity within the shot although it will not give the exact shape of the received pulse. γ, the pulse length at the transmission point, at the receiver is a measure of how much temporal integration will occur between the several rays arriving within a short time at the receiver.

The received shot waveform was computed for frequencies of 100, 500, 1000Hz using the bottom loss parameters of Fig.14. The received shot waveform is shown in Fig.29. It is interesting to note that when the frequency within the γ sec long burst is 100Hz, two modes are present, the second being 20dB weaker than the first. For the higher frequencies, where the bottom loss is considerable, the shot duration is approximately γ.

This indicates that only a very few of the lowest order rays are being transmitted with significant energy. The high slope of the propagation loss curves of Fig.16 can then be expected since a modified Lloyd's mirror type of propagation has occurred. Inherent in the assumptions of para.2 was the assumption that γ is comparable to the total shot duration. From the above we see that this is in fact the case and so:

(i) The energy transmitted from high order images can be neglected.

(ii) There is little dispersion and the shot duration is short and roughly constant.

The verification of these assumptions in terms of the results of the theoretical sonagrams of Fig.29 and the experimental sonagrams of Fig.30, validates our former claim that the peak energy received from a CW source is proportional to the peak energy from a transient source and that the constant of proportionality is approximately constant over the range interval considered.

To show the correspondence between ray theory and mode theory, the theoretical 'sonagram' for a square impulsive source was computed. As bottom loss was assumed to be zero for all grazing angles less than critical, the intensity over the entire shot duration was significant with a total variation of 30dB. The peak intensities within the received shot waveform, corresponding to modes of propagation were at the same level $\pm$ 5dB.

There is a trend for the peak intensity of the second mode to be higher than the peak intensity of the first mode. This trend is due to the fact that a large number of rays contribute to the signal of the first mode and the rays which are antiphase are not separated in arrival time sufficiently. Hence due to the finite integration time of γ, many antiphase rays also contribute to the total intensity of the first mode. We could take a smaller value of γ to obtain finer discrimination, but this is not physically valid since the separate pulses due to different rays are fairly broad. For any finite γ for a sufficiently high frequency, γ will be larger than the separation in arrival times of successive modes. For high frequencies then, mode structure will not be as distinctive as for the lower frequencies and in the limit as $f \to \infty$, no modes are apparent. Then the intensity of the received shot varies only slowly with time.

In order to find the number of possible modes of propagation of sound at a given frequency, we consider the cutoff frequency for a particular mode.

$$f_n = \frac{(2n-1)V}{4H} \left(\frac{V^2}{c_1^2} -1 \right)^{-\frac{1}{2}}$$

The number of possible modes of propagation for a frequency f will be given by N where f_N is the largest value of f_n

such that $f > f_N$

A theoretical sonagram of the received shot waveform for a lossless bottom is shown in Fig.29. The arrival times of the first four modes is shown as a function of frequency. The results of Fig.29 demonstrate the 1-1 correspondence between ray and mode theory and verify Tolstoy's (4,1) ascertion that the rays comprising the n^{th} mode in normal mode propagation can be thought of as coming from the image sets which have grazing angles of approximately ϕ_n

REFERENCES

4,1 TOLSTOY, I.(1959) "Modes, Rays and Travel Times".
J. Geophysics Res. Vol 64 No 7.

APPENDIX I

THE BOTTOM REFLECTION COEFFICIENT

The reflection of a sound wave from an attenuating bottom which varies from 'slow' at the water interface, to 'fast' at some depth, is complex. With no detailed knowledge of the velocity profile or the attenuation in the sediment no exact model for bottom reflection can be proposed. We can, however, use a simple model which gives the overall effect of the complex situation.

To obtain a qualitative idea of what the reflection from the bottom will be like we investigate the reflection from:-

(i) A perfect bottom

(ii) A lossy bottom

(iii) A two layer bottom where the top layer is 'slow'.

We follow Brekhovshikh (5,1) closely in this section.

(i) Two-Liquid Model without Attenuation

The reflection coefficient for a plane wave reflected from an interface separating two liquids is:-

$$V = \frac{m \cos \theta - (n^2 - \sin^2 \theta)}{m \cos \theta + (n^2 - \sin^2 \theta)} \qquad 1.$$

where $m = \frac{\rho_2}{\rho_1}$, $n = \frac{c_1}{c_2}$ 2.

and θ is the angle of incidence.

We see that when $n < \sin\theta$ total internal reflection occurs with an associated phase change of:-

$$\epsilon = -2 \tan^{-1} \left(\frac{(\sin^2\theta - n^2)}{m \cos\theta} \right) \qquad 3.$$

The Rayleigh wave reflection coefficient for the case $\frac{c_2}{c_1} = 1.11$, $\frac{\rho_2}{\rho_1} = 1.5$ is given by the curve corresponding to S=0, ST=1 of Fig.3.

Two Layer Liquid Model with Attenuation in the Lower Layer

If there is absorption in the lower medium, n will be complex:

$$n = n_o (1 + i\alpha) \qquad 4.$$

We consider the case $\alpha \ll 1$, so

$$n^2 = n_o^2 (1 + 2i\alpha) \qquad 5.$$

and use the notation

$$\sin^2\theta - n_o^2 = A, \quad 2n_o^2\alpha = B \qquad 6.$$

Then taking into account that

$$\sqrt{(A - iB)} = M_1 + M_2 \qquad 7.$$

$$M_1 = \frac{1}{\sqrt{2}} \left([\sqrt{(A^2 + B^2)} + A] \right), \; M_2 = -\frac{1}{\sqrt{2}} \left([\sqrt{(A^2 + B^2)} - A] \right) \qquad 8.$$

and using equation 1

$$V = \frac{m \cos\theta + M_2 - iM_1}{m \cos\theta - M_2 + iM_1} \qquad 9.$$

and $\epsilon = \tan^{-1}\left(\frac{-M_1}{m\cos\theta + M_2}\right) - \tan^{-1}\left(\frac{M_1}{m\cos\theta - M_2}\right)$ 10.

The family of V and ϵ vs grazing angle for several values of the attenuation are shown in Figures 6, 7, 8. Note that $\alpha = o$ corresponds to no absorption and gives the Rayleigh Reflection Coefficient.

Where a low speed layer exists (Fig.9), rays travelling in the water and striking the low speed layer at very low grazing angles will be reflected from layer 3 at an angle that is significantly larger than zero. For $\frac{c_2}{c_1} = .97$, the ray travelling parallel to the 1/2 interface will strike the 2/3 interface with a grazing angle of 14° From Fig.7 we see the reflection loss from 2/3 interface can be as high as 4dB for $\alpha = .1$.

It is well known that the absorption coefficient increases with frequency. We see that where a low speed layer exists, the bottom loss at low grazing angles in non-zero and increases with grazing angle and frequency

It is reasonable to adopt a bottom reflection coefficient of the form given in Fig.3 such that:

$$V = ST - S\left(\frac{\theta_1}{\theta_c}\right) \qquad 11.$$

$$\epsilon = \pi\left(.9\left(\frac{\theta_1}{\theta_c}\right) - 1\right) \qquad 12.$$

where θ_1 is the grazing angle of the ray in water

θc is the critical grazing angle.

REFERENCES

(5,1) BREKHOUSKIKH (1960) "Waves in Layered Media" Academic Press

APPENDIX 2

COMPUTATION OF THE RECEIVED INTENSITY

To evaluate the series of equation in Chapter 2, we must use a digital computer. The procedure adopted is as follows:

(i) A range is selected.

(ii) The amplitudes of the signals due to all the lower images are summed observing phase coherence.

(iii) The amplitudes of the signals due to all the upper images are summed observing phase coherence.

(iv) The complex sum of the results of (i) and (ii) is computed and the total intensity at the receiver is found by multiplying this total amplitude by its complex conjugate. The energy loss in dB re 1ft. is obtained by taking 10 $\log_{10}$ of the total intensity.

(v) The process is repeated for a larger range unless the range exceeds 2×10^5 ft. when we proceed to (vi).

(vi) The graph of energy loss in dB on a linear scale is plotted against range on a logarithmic scale by the computer.

THE PROGRAM

(a) The Parameters Used.

A	Angle of Incidence of Ray
AI	Grazing Angle of Ray
ATTEN	Reflection Coefficient at each Bottom Bounce
B	Phase Change at each Bottom Reflection
C	Critical Angle of Incidence
CI	Critical Grazing Angle
D	Source Depth
E	Total Phase Change of Ray due to Bottom and Surface Reflections
FREQ.	Frequency of Sound Propagation
H	Depth of Water
I	No. of Bottom Bounces
J	No. of Surface Bounces
N	Total No. of rays.
P	Wave Number ($2\pi/\lambda$)
PI	3.14159265
R	Total Distance of Ray Path from Source to Receiver
S	Bottom Reflection Parameter
SIGNAL	Total Received Intensity at Receiver
ST	Bottom Reflection Parameter
T	Distance (in feet) from Source to Receiver

<u>Parameters used</u> (cont'd)

U	U = ρ_2/ρ_1, = 1.5
V	V = c_1/c_2 = .89
W	Vertical Distance between Receiver and Image
X	Cumulative Total of Real Part of Signal at Receiver
Y	Cumulative Total of Imaginary Part of Signal at Receiver
Z	Receiver Depth.

(b) COHERENT RAY THEORY FLOW CHART PART. 1.

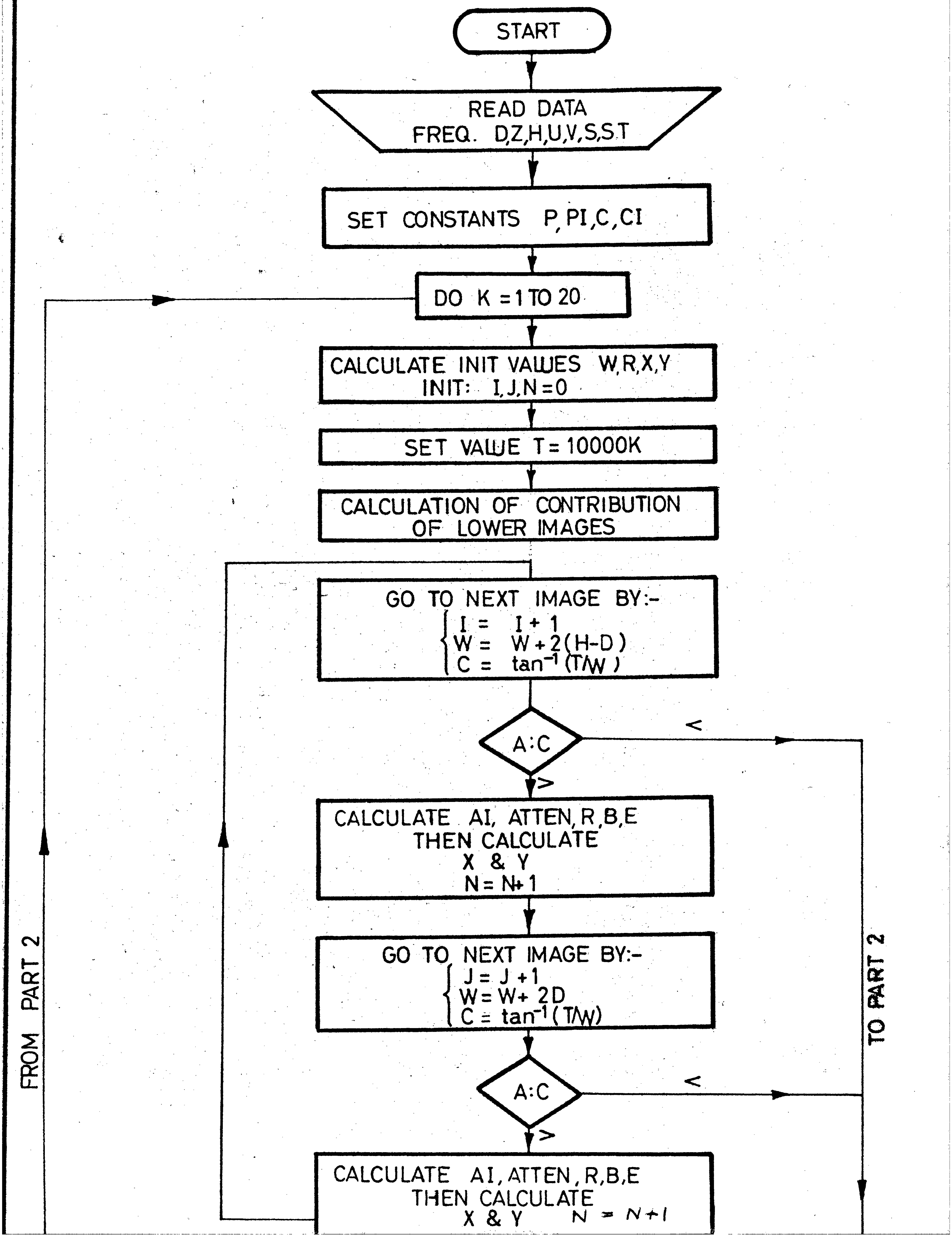

(b) COHERENT RAY THEORY FLOW CHART PART 2.

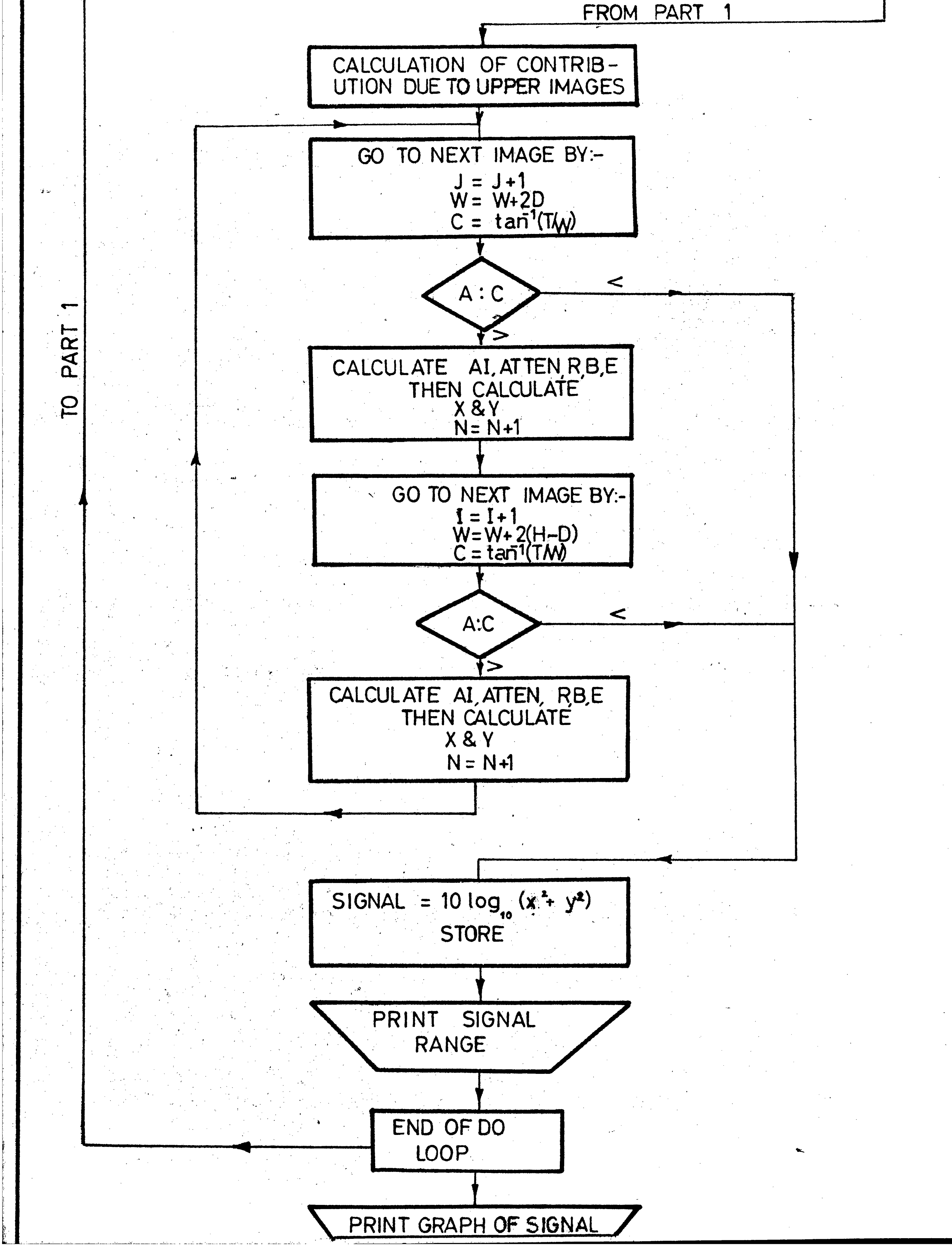

(c) Formulae Used in the Program

	Symbol in Program		Value		Symbol in Chapt.2
(i)	B	=	$\pi\left(.9\left(\frac{AI}{CI}\right)-1\right)$	=	ϵ
(ii)	ATTEN	=	$ST - S \times \frac{AI}{CI}$	=	V
(iii)	E	=	$I \times B + J \times PI$	=	Ψ
(iv)	R	=	$\sqrt{(T^2 + W^2)}$	=	R

APPENDIX 3

THE GENERATION OF PSEUDO-RANDOM PHASE DISTORTIONS

Using the model of Fig(1), we wish to find the rms fluctuation in received signal intensity due to a perturbation in the bottom depth. As indicated in Chapter 3, a pseudo random phase:

$$\delta = 2 \cos(A).k. \sqrt{I} . \Delta_o H(1)$$

where δ is the phase perturbation

A is the angle of incidence of the ray at the bottom

k is the wave number

I is the number of bottom bounces from source to receiver

$\Delta_o H(1)$ is a random normal variable with mean o and standard deviation 22

is added to the phase of each ray arrival. We need then to select a random variable with mean zero and standard deviation 22 ft. We do this by generating a random number in the range $0 \rightarrow 2^{31}$ with Subroutine Randu.

Subroutine Randu produces 2^{29} odd integers evenly distributed in the range $0 \rightarrow 2^{31}$. Each execution of Subroutine Randu uses as input an integer and produces a new pseudo-random integer. This new integer becomes the input for the next execution of Randu; and so we generate up to 2^{28} pseudo-random integers. We need then select only an initial value for the input of Randu.

We include details of Subroutine Randu.

SUBROUTINE RANDU

```
IZ      =  IZ*  65539
YFL     =  IZ
YFL     =  YFL* .4656613 E-9
RETURN
END
```

IZ is given an initial value at an appropriate position in the program.

We can generate conveniently normally distributed random variables using two methods.

(a) RANDU, as well as giving a uniformly distributed integral random number in the range $0 \rightarrow 2^{31}$ also gives YFL, a uniformly distributed real number in the range $0 \rightarrow 1$.

Consider now the distribution of YFL, W(YFL). W(YFL) has mean $\frac{1}{2}$ and a variance of 1/12. If we consider sums of twelve variables selected randomly from W(YFL), the distribution W(YFL12) thus obtained has a mean of 6 and variance of 1. Thus by summing twelve successive values of YFL we obtain a normal random variable with standard deviation 1 and mean 6. Hence to obtain a normal variable Δh with mean zero and standard deviation σ we compute twelve values of YFL, sum them, subtract six and multiply the result by σ

$$\text{i.e.} \quad \Delta h = \sigma \left[\left(\sum_{i=1}^{12} \text{YFL}_i \right) - 6 \right] \tag{7.1}$$

and so the total perturbation in path length ΔR for a ray undergoing I bounces is given by

$$\Delta R = \sigma \sqrt{I} \left[\left(\sum_{i=1}^{12} YFL_i \right) - 6 \right] \tag{7.2}$$

(b) We can also generate normally distributed random variables by selecting randomly from a frequency distribution curve. Indeed, if the distribution from which we wish to select variables is not gaussian, nor simply defined mathematically as in the case of the distribution of Fig. 20F, then we are left with no alternatige but to sample directly from the distribution.

Consider a distribution defined by

$$\left.\begin{array}{lll} W(x) = f(x) & & a \leqslant x < b \\ W(x) = 0 & & x < a \;, \; x > b \end{array}\right\} \tag{7.3}$$

The distribution we consider is finite, since we can only consider a finite distribution if we sample discreetly. Many distributions which are infinite in the range of x can be adequately approximated to by neglecting values of x which have less than a fixed (small) probability of occurrence. If $W(x)$ is a normal distribution, we can define

$$\left.\begin{array}{ll} W(x) = N(x) = \dfrac{1}{\sigma\sqrt{2\pi}} e^{-\frac{x^2}{2\sigma^2}} & -3\sigma \leqslant x \leqslant 3\sigma \\ W(x) = 0 & x < -3\sigma \;, \; x > 3\sigma \end{array}\right\} \tag{7.4}$$

and so here we consider the finite range of a normal distribution between the 3 σ limits.

To select a maximum of n different random variables from the distribution (7.3) we divide the internal ab into n equal segments

Let x_i be the mid-point of the i^{th} segment and so

$$x_i = a + \frac{(2i - 1)}{2n} (b-a) \tag{7.5}$$

and we see that the probability of x lying in the range:

$$x_i - \frac{1}{2n} (b-a) < x \leq x_i + \frac{1}{2n} (b-a) \tag{7.6}$$

that is in the i^{th} segment; is approximately $f(x_i)$.

Suppose now we generate uniformly distributed random numbers y, in the range $c \leq y \leq d$. If we divide the interval cd into n segments so that the length l_i of the i^{th} segment is proportional to $f(x_i)$;

$$\text{i.e.} \qquad l_i = \frac{1}{d-c} f(x_i) \tag{7.7}$$

Then the probability of a random variable x from the distribution W(x) having a value which lies in the range of the i^{th} segment of ab, is equal to the probability of a uniformly distributed random variable having a value y which lies in the range of the i^{th} segment of cd.

So to select one of n different variables from the distribution W(x), we first generate a uniformly distributed variable y. Next we find the segment in cd within the range of which y lies. Then, supposing y lies in the range of the j^{th} segment, the corresponding pseudo-random variable from W(x) is given by x_i.

This latter procedure was the one followed to obtain a normal variable with standard deviation and mean zero. The uniformly distributed random variables were obtained in a range $0 \rightarrow 999$ by computing a new random variable IX in the range:

$$0 \leq IX \leq 999 \tag{7.13}$$

by letting $IX = IZ \text{ MOD } (1000)$ (7.14)

where IZ is the integer calculated by Randu.

IX here then is our previous y.

The ℓ_i were calculated to give a normal distribution between the 3σ limits and the x_i were chosen so that $W(x)$ has a standard deviation of 22 ft and a mean of zero. It is essential to the whole process that IX be uniformly and randomly distributed in the range

$$0 \leq IX < 999$$

The distribution of IX was tested by observing the distribution of twenty classes each of fifty numbers. The distribution was plotted for several sample sizes and the results are shown in Fig. 22a. The auto correlation functions of one set of sixty random values of IX was also determined and shown in Fig. 22b.

We see then that the distribution of IX is quite uniform in the range 0-999 and that the IX are sufficiently random for our purposes.

Having thus computed Δh we obtain

$$\Delta R = 2 \cos(A). \Delta h \sqrt{I}$$

and $$\delta = \Delta R. f. 2\pi / c$$

The flow chart of the sub-routine which is called for at each stage to apply a phase perturbation to the phase of each ray is included in this appendix.

PSEUDO RANDOM PHASE GENERATOR SUBROUTINE RANDU 1

(a) Symbols Used

AB	Normal Random Variable, Mean 0, Standard Deviation 22
IX	Random Integer Selected from Distribution Uniform in the Range 0-999
RA	Random Integer Selected from Distribution Uniform in the Range $0-2^{31}$
DEL 1	Pseudo-random Phase Correction
P	Wave Number ($2\pi/\lambda$)
X	Discreet Samples from Normal Distribution Mean 0 Standard Deviation 22
FACTOR	An Input Variable to alter the Magnitude of the Bottom Depth Variation.

PSEUDO RANDOM PHASE GENERATOR
SUBROUTINE RANDU 1

b) FLOW DIAGRAM.

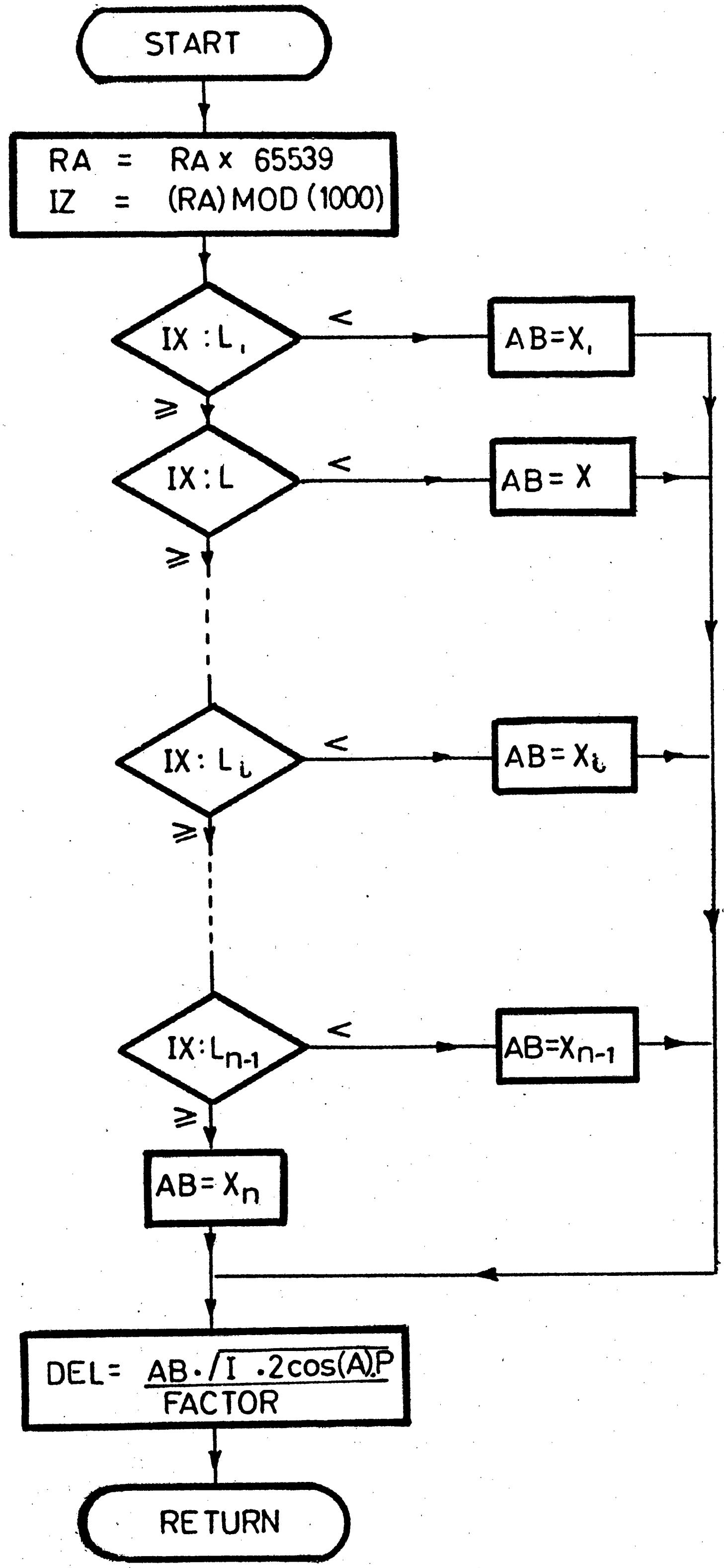

APPENDIX 4

COMPUTATION OF THE RECEIVED WAVEFORM

Using the model of Fig (1), we aim to compute the received waveform when a short burst of sound of one frequency is transmitted from O.

The transmitted wave has the form:-

$$\left.\begin{aligned} I &= o \qquad t \leqslant o,\ t > \gamma \\ I &= I_o \sin wt \qquad 0 < t \leqslant \gamma \end{aligned}\right\} \tag{8.1}$$

where γ is the duration of the burst.

We see that simultaneously all of the images of Fig (1) will transmit coherent 'tone bursts' of equal amplitude. If the arrival time at the receiver of the direct ray is $t = t_o$, then at time $t = t_o + \Delta t$, the images which will contribute to the total received intensity satisfy the condition:-

$$R_{t_o} + \Delta t - \gamma < R_t \leqslant R_{t_o} + \Delta t \tag{8.2}$$

where R_t is the distance travelled by the ray with arrival time of t.

)8.2) can be rewritten

$$c(t_o + \Delta t - \gamma) < R_t \leqslant c(t_o + \Delta t) \tag{8.3}$$

where c is the velocity of sound in water.

To compute the received shot intensity as a function of time, we must compute the amplitude and phase of the arrival signal due to each image as well as compute the path length from each image to the receiver.

We wish to compute the intensity at 100 equally spaced value of Δt where $\Delta t_{max} = \tau$. To do this we notice the rays which contribute to the intensity at time $t + \Delta t$ satisfy (8.2). The signal from all of these contributing rays are added coherently and the resultant intensity of the signal is hence obtained by squaring the total amplitude.

The details of the computer program used to evaluate the intensity of the received wave as a function of time follow.

(a) Parameters Used

A	Angle of Incidence of Ray
AI	Grazing Angle of Ray
ATTEN	Reflection Coefficient at Bottom Reflection
B	Phase Change at each Bottom Reflection
C	Critical Angle of Incidence
CI	Critical Grazing Angle
D	Source Depth
DELTA	Increment in Path Length
E	Total Phase Change of Ray due to Reflections
FREQ	Frequency of Sound within the 'Burst'
H	Depth of Water
I	No. of Bottom Reflections
IX	Duration of Pulse in DELTA's
J	No. of Surface Reflections
K	'Do' Variable used to Compute the Intensity at 100 Discrete Times during the Shot Arrival
N	Cumulative No. of Rays/Subscript for Ray Identification
P	Wave Number ($2\pi / \lambda$)

Parameters Used (cont'd)

PAG	Imaginary part of the Received Amplitude
PI	3.14159265
R(N)	Path Length of Ray(N) from source to Receiver
REL	Real Part of the Received Amplitude
RX) RY)	Upper and Lower Distance Limits for any One K
S	Bottom Reflection Parameter
SIGNAL	Total Intensity Received for a Value of K
ST	Bottom Reflection Parameter
T	Horizontal Distance (ft) from Source to Receiver
U	$U = \rho_2 / \rho_1 = 1.5 = m$
V	$V = \frac{c_1}{c_2} = .89 = n$
W	Vertical Distance between Receiver and Image
X(N)	Real Part of Signal due to Ray$_\alpha$ (N)
Y(N)	Imaginary Part of Signal due to R_α (N)
Z	Receiver Depth

RECEIVED INTENSITY VARIATION WITH TIME FLOW CHART

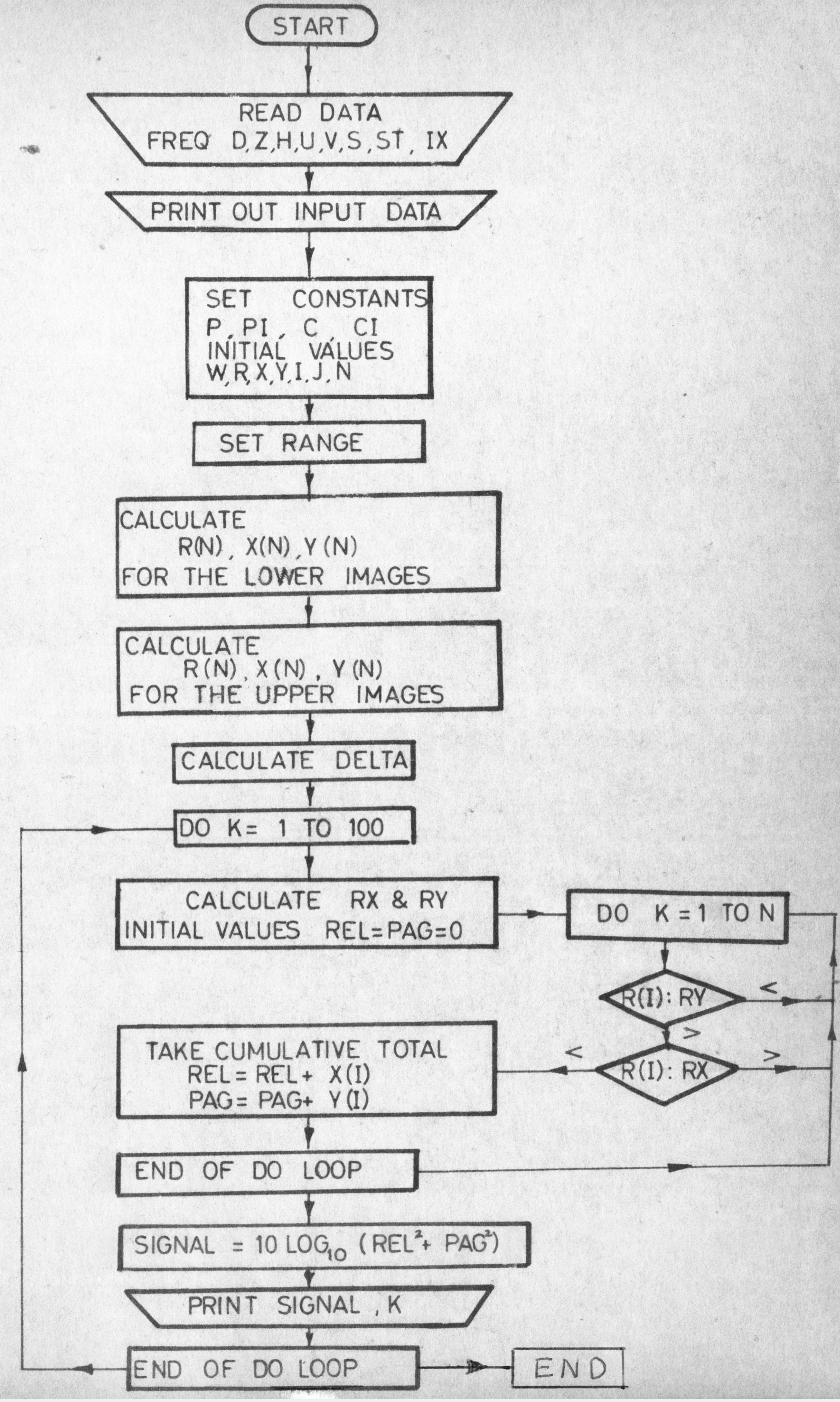

Formulae Used in the Program

(i) $B = PI\ (.9 \times \frac{AI}{CI} - 1)$

(ii) $ATTEN = ST - S \times \frac{AI}{CI}$

(iii) $E = I \times B + J \times PI$

(iv) $R = (T^2 + W^2)$

(v) $RX = R(1) + (K-1) \times DELTA$

$RY = RX - IX \times DELTA$

(vi) $DELTA = (R(N) - R(1))\ /100$

SUMMARY AND COMMENTS

Using the model of coherent ray theory:

(i) The propagation loss curves obtained by the RAN can be simulated.

(ii) The dependence of receiver response on receiver depth is predicted.

(iii) The variation in the received intensity from one transmission to the next, where the acoustic transmission paths are of equal lengths, are in the same geophysical area but are over different sea paths, can be explained.

The theory tells us that, owing to the large variation in the bottom depth, we cannot hope to predict the received intensity to a greater accuracy than "plus or minus several dB".

Further theoretical work is being done and experiments are envisaged to verify:

(i) the existence of the low-speed layer of ooze in shallow water areas. Experiments will shortly be carried out in harbour sediments using detonators as sources.

(ii) (assuming the low-speed layer does exist), that the low-speed layer causes high bottom losses even at small grazing angles and acts as a high-pass filter allowing only the high frequencies to propagate in the sediment. This would then explain the phenomenon illustrated in the sonagrams of Fig.30 that all sediment arrivals were high frequency arrivals centred about a frequency of 600Hz.

FIG.1.

THE RAY MODEL.

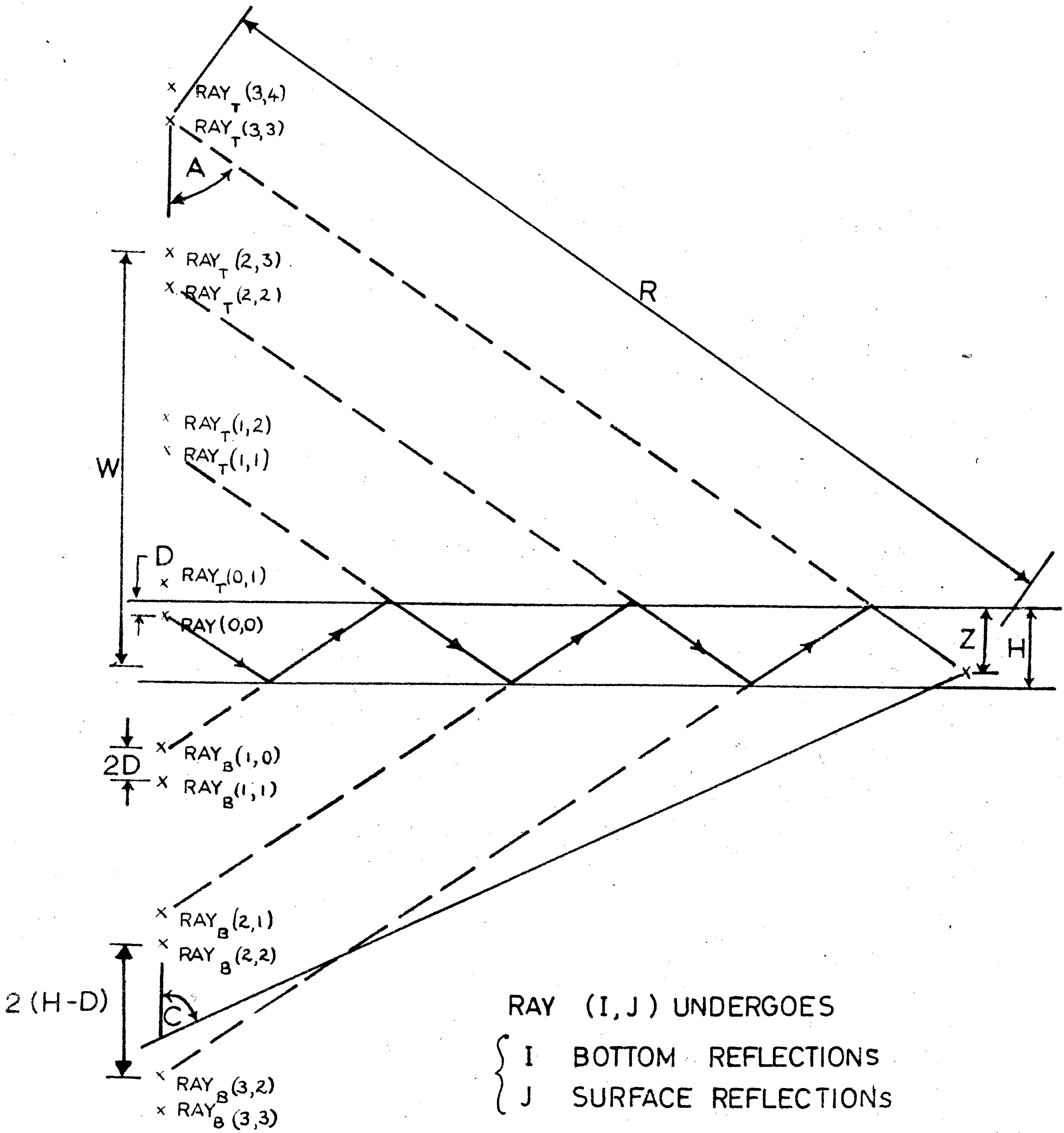

RAY (I, J) UNDERGOES

- I BOTTOM REFLECTIONS
- J SURFACE REFLECTIONS

A ANGLE OF INCIDENCE OF RAY (3,3)

C CRITICAL ANGLE OF INCIDENCE.

FIG. 2

TRAVEL TIME CURVES.

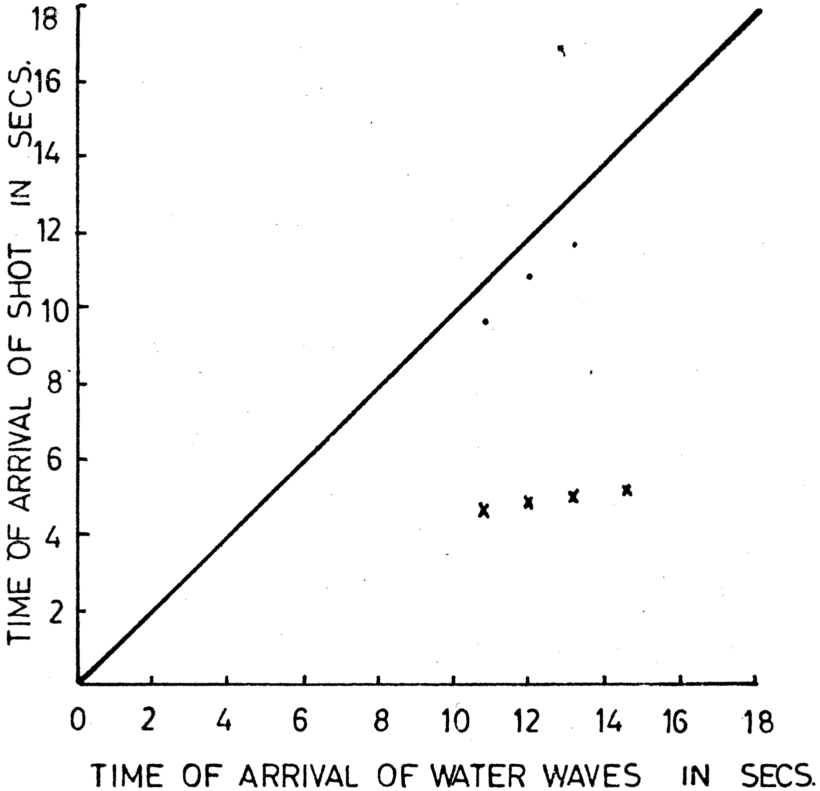

• SEDIMENT ARRIVAL.

x HIGH SPEED ROCK ARRIVAL.

— WATER WAVE ARRIVAL

FIG. 3.

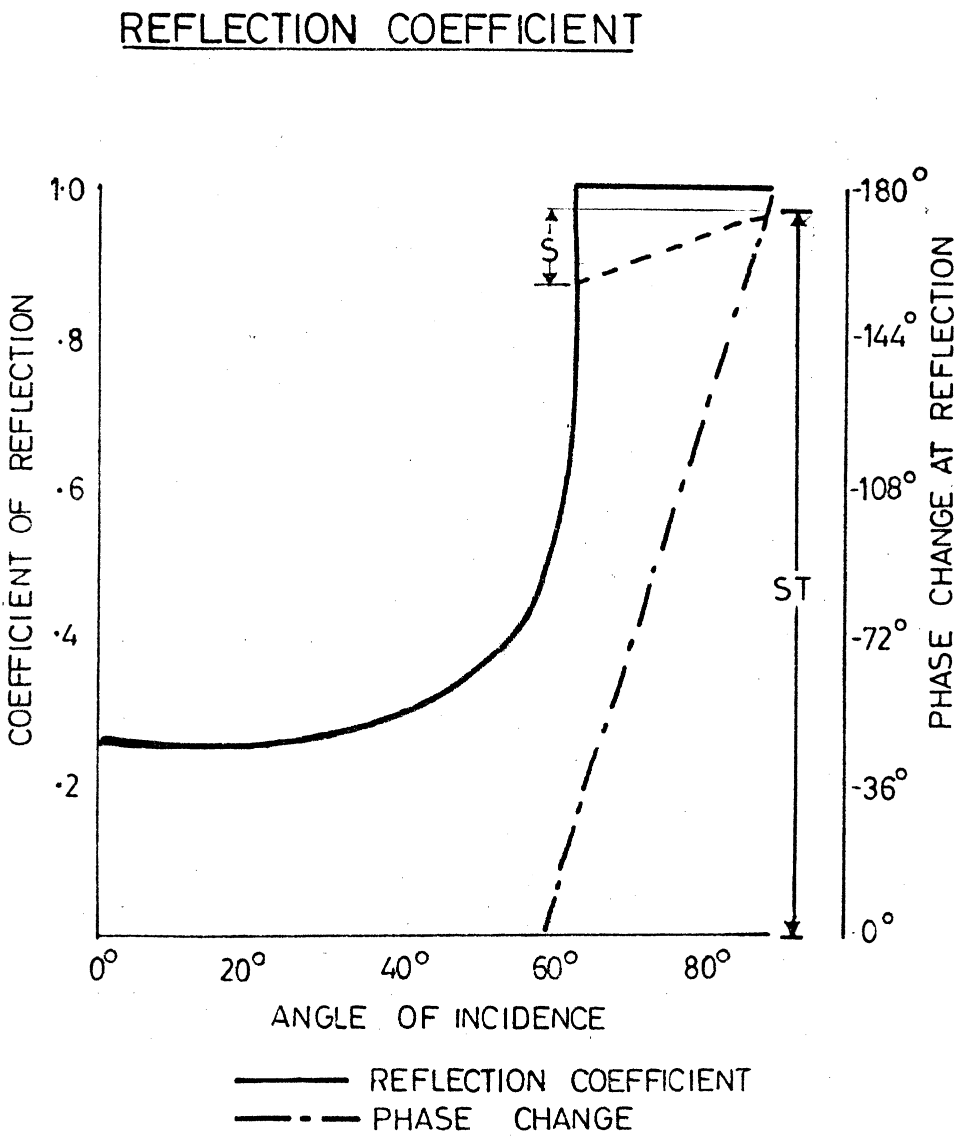

THE BOTTOM REFLECTION PARAMETERS USED IN THE COMPUTER PROGRAM.

FIG. 4.

COMPUTED BOTTOM REFLECTION COEFFICIENT.

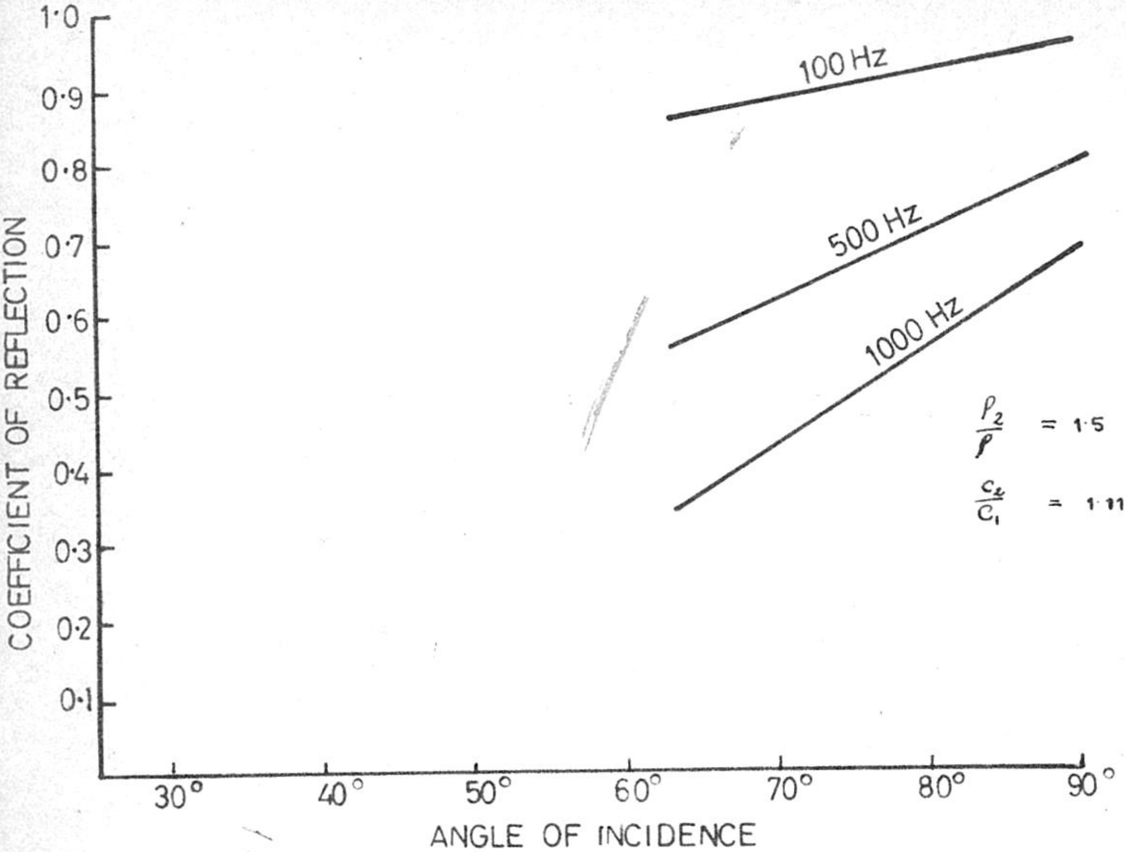

COMPUTED BOTTOM LOSS FIG. 5.

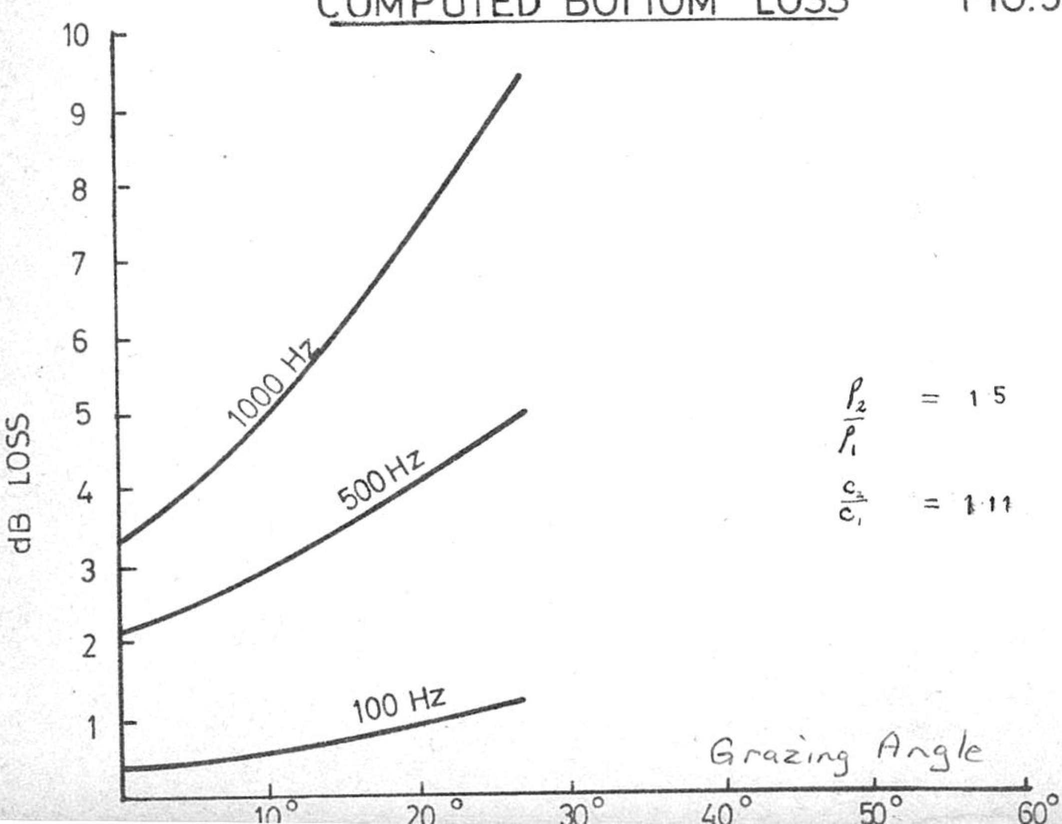

FIG. 6.

REFLECTION COEFFICIENT FOR DIFFERENT WAVE ATTENUATIONS IN SEDIMENT.

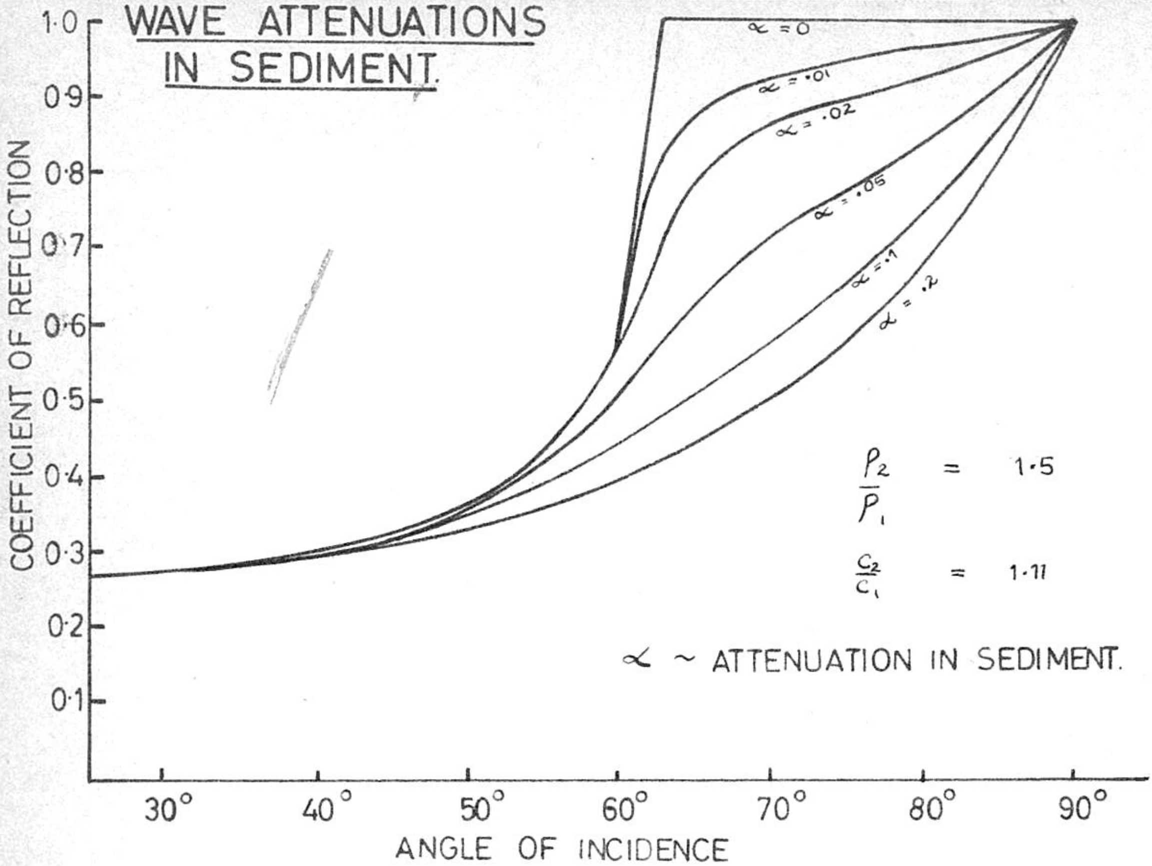

FIG. 7.

BOTTOM LOSS (dB) FOR DIFFERENT WAVE ATTENUATIONS IN SEDIMENT.

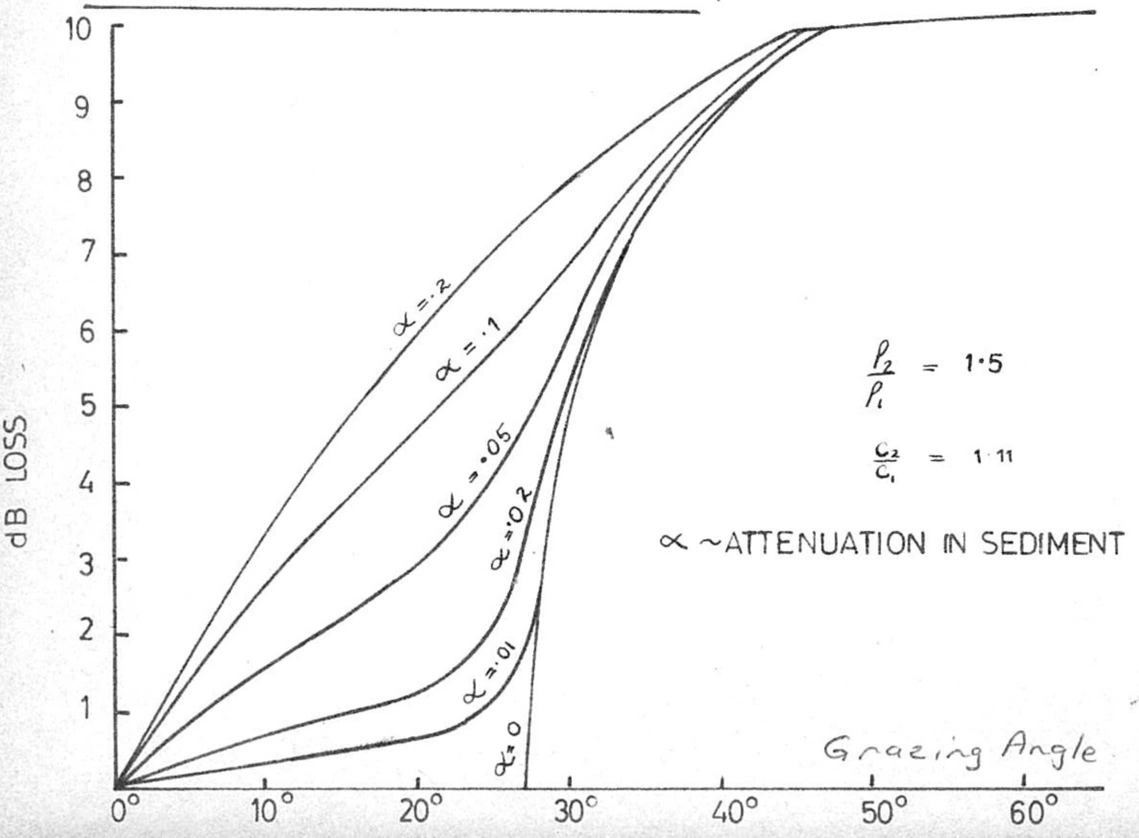

FIG. 8.

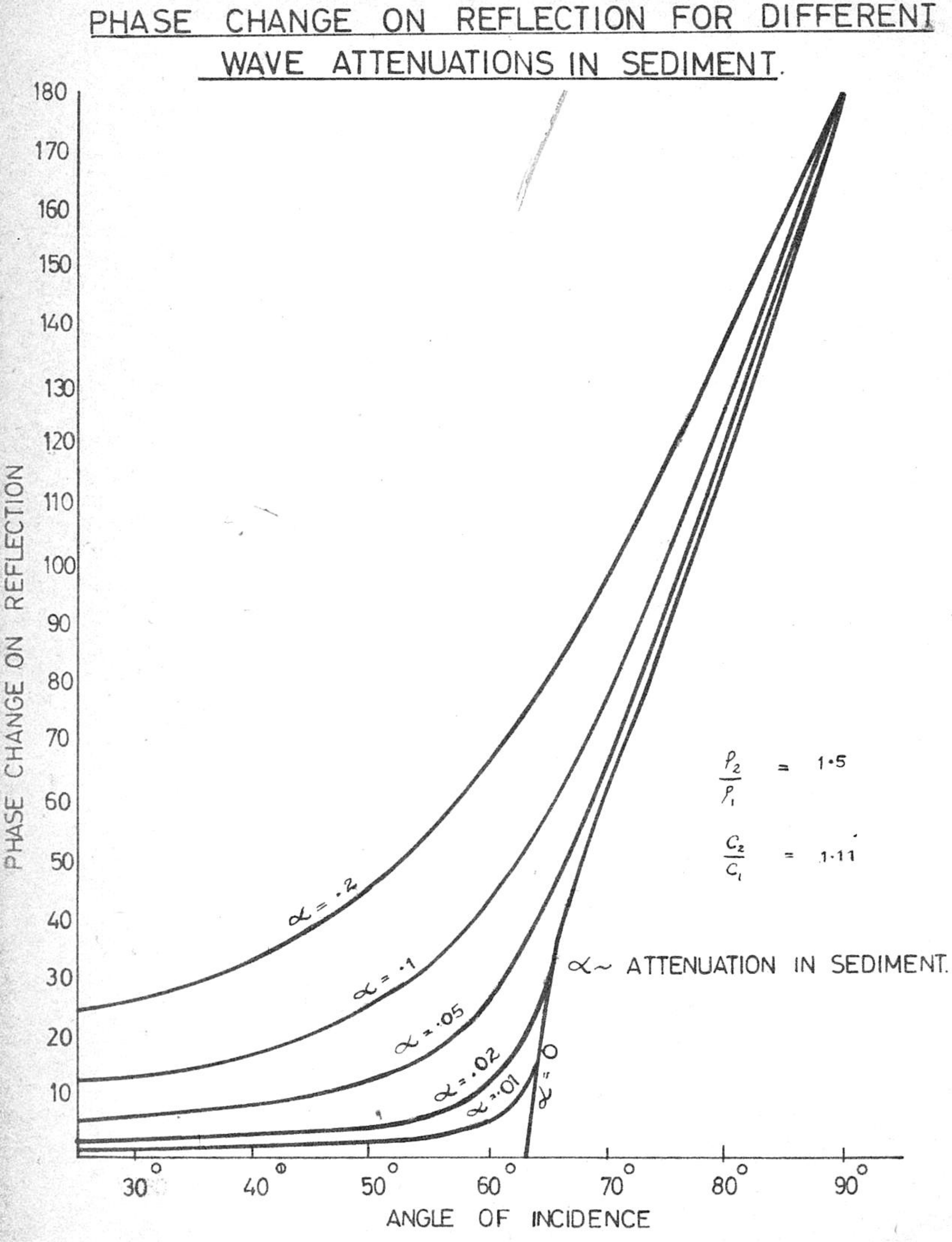
PHASE CHANGE ON REFLECTION FOR DIFFERENT WAVE ATTENUATIONS IN SEDIMENT.
180
170
160
150
140
130
120
110
100
90
80
70
60
50
40
30
20
10
PHASE CHANGE ON REFLECTION
30°
40°
50°
60°
70°
80°
90°
ANGLE OF INCIDENCE
α = ·2
α = ·1
α = ·05
α = ·02
α = ·01
α = 0
ρ2/ρ1 = 1·5
C2/C1 = 1·11
α ~ ATTENUATION IN SEDIMENT.

REFLECTION FROM "FAST" BOTTOM OVERLAIN WITH A THIN "SLOW" LAYER.

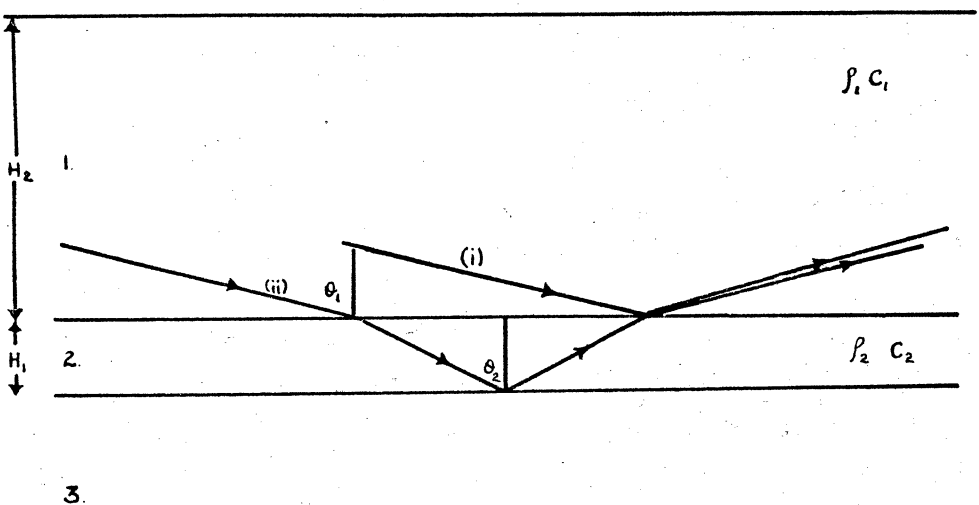

1. Isovelocity Water
2. Mud - Ooze
3. Fine Sand Subspace

$\rho_3 > \rho_2 > \rho_1$

$C_3 > C_1 > C_2$

$\rho_2 C_2 > \rho_1 C_1$

From FIG 2 $\dfrac{C_3}{C_1} = 1{\cdot}11$

From literature $\dfrac{C_2}{C_1} = 0{\cdot}97$

$$\frac{\rho_2}{\rho_1} = 1{\cdot}4$$

$$\frac{\rho_3}{\rho_1} = 1{\cdot}6$$

FIG.10(a)

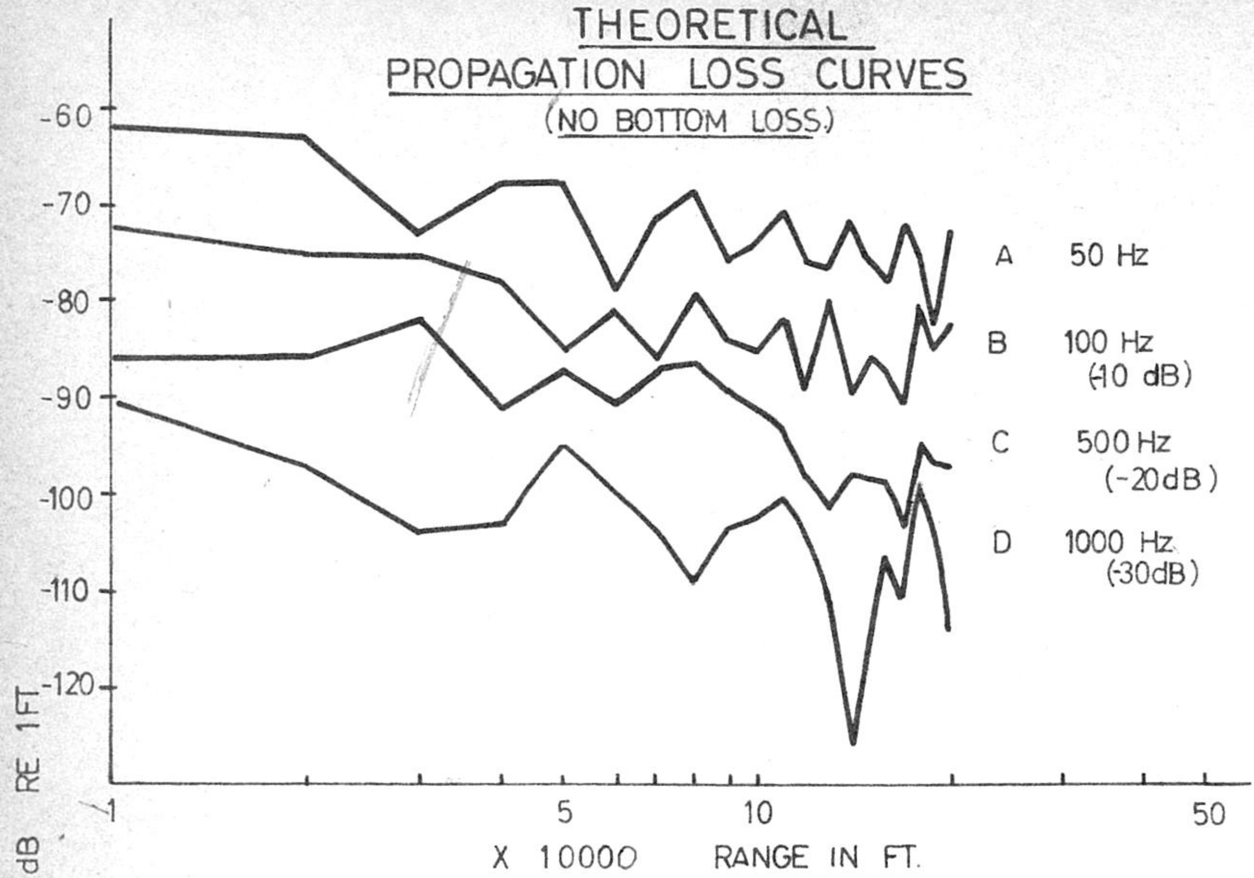

FIG.10(b)

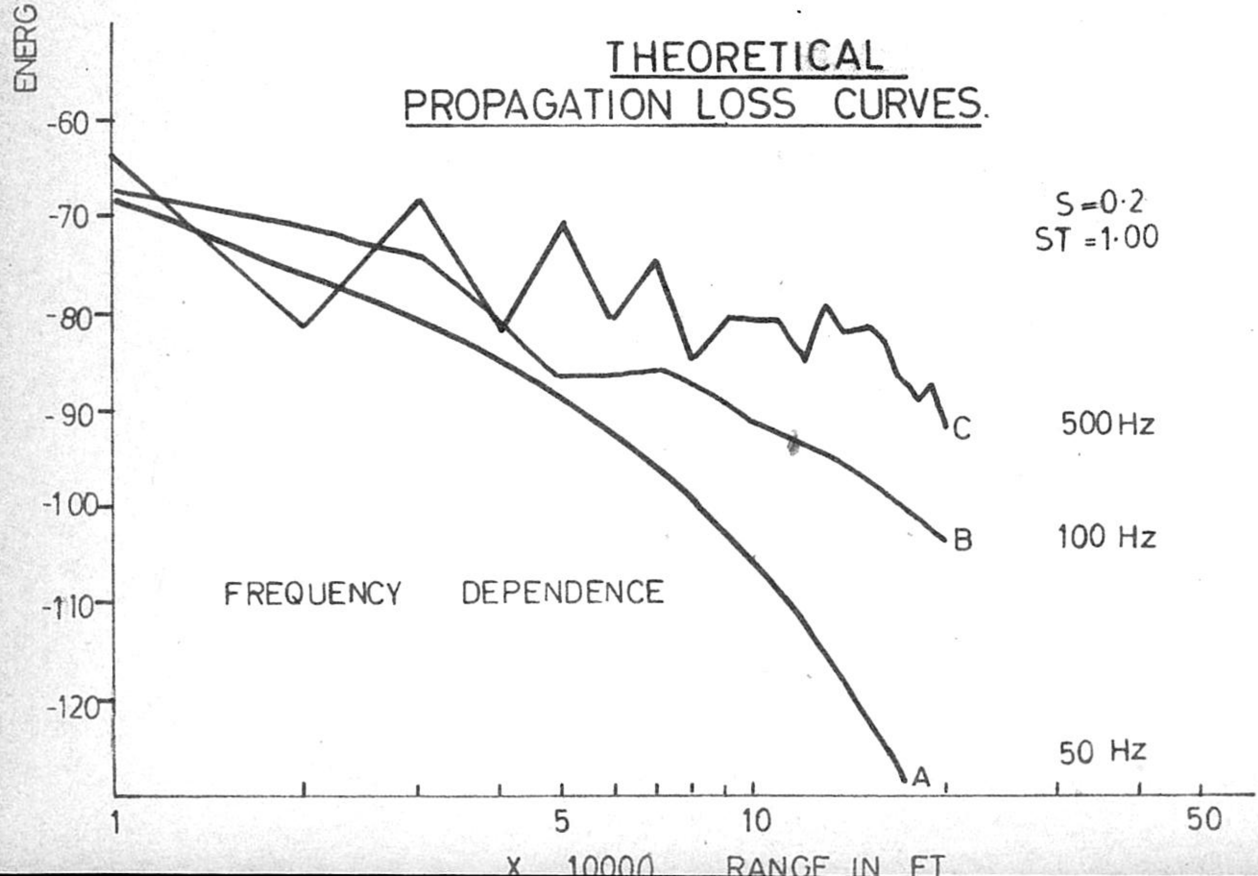

FIG. 11(a).

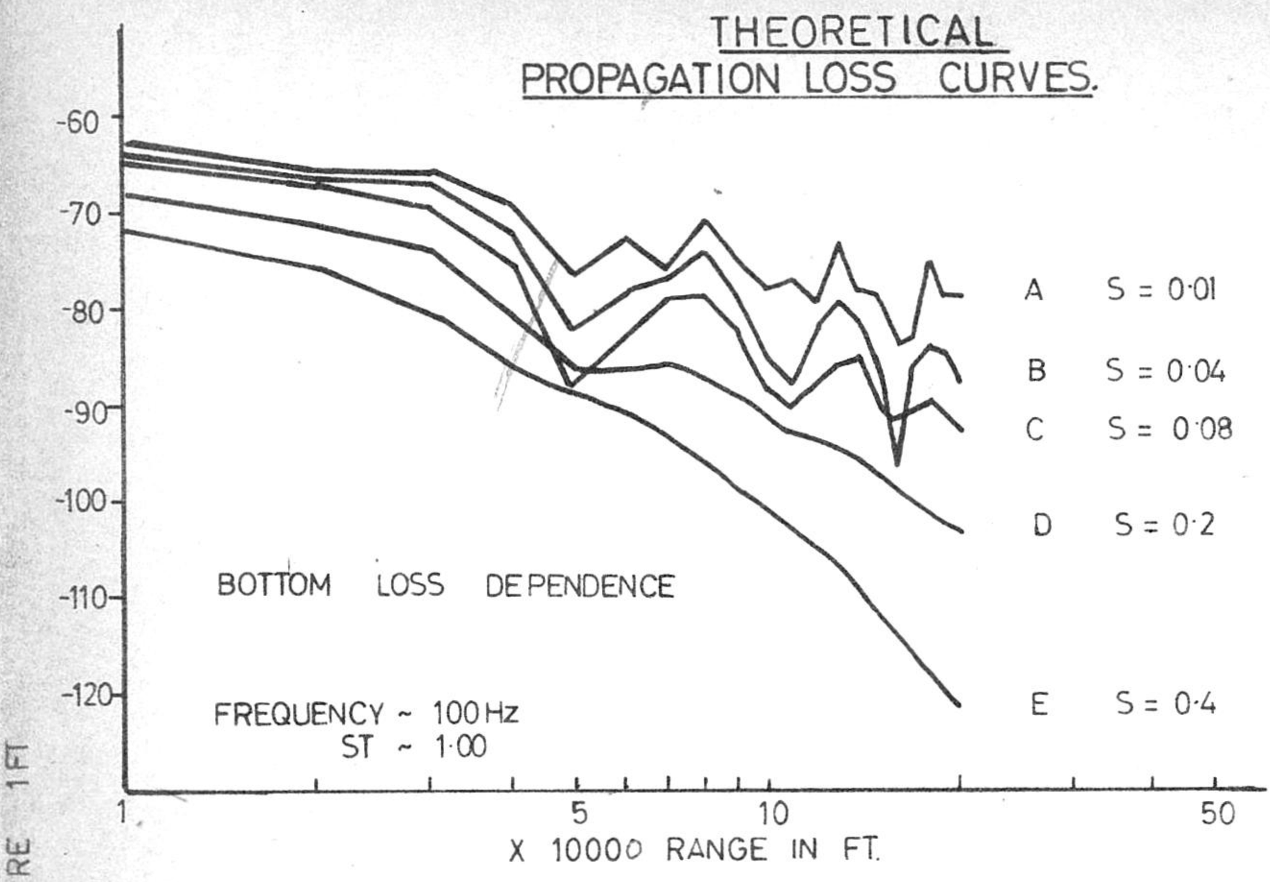

FIG. 11 (b)

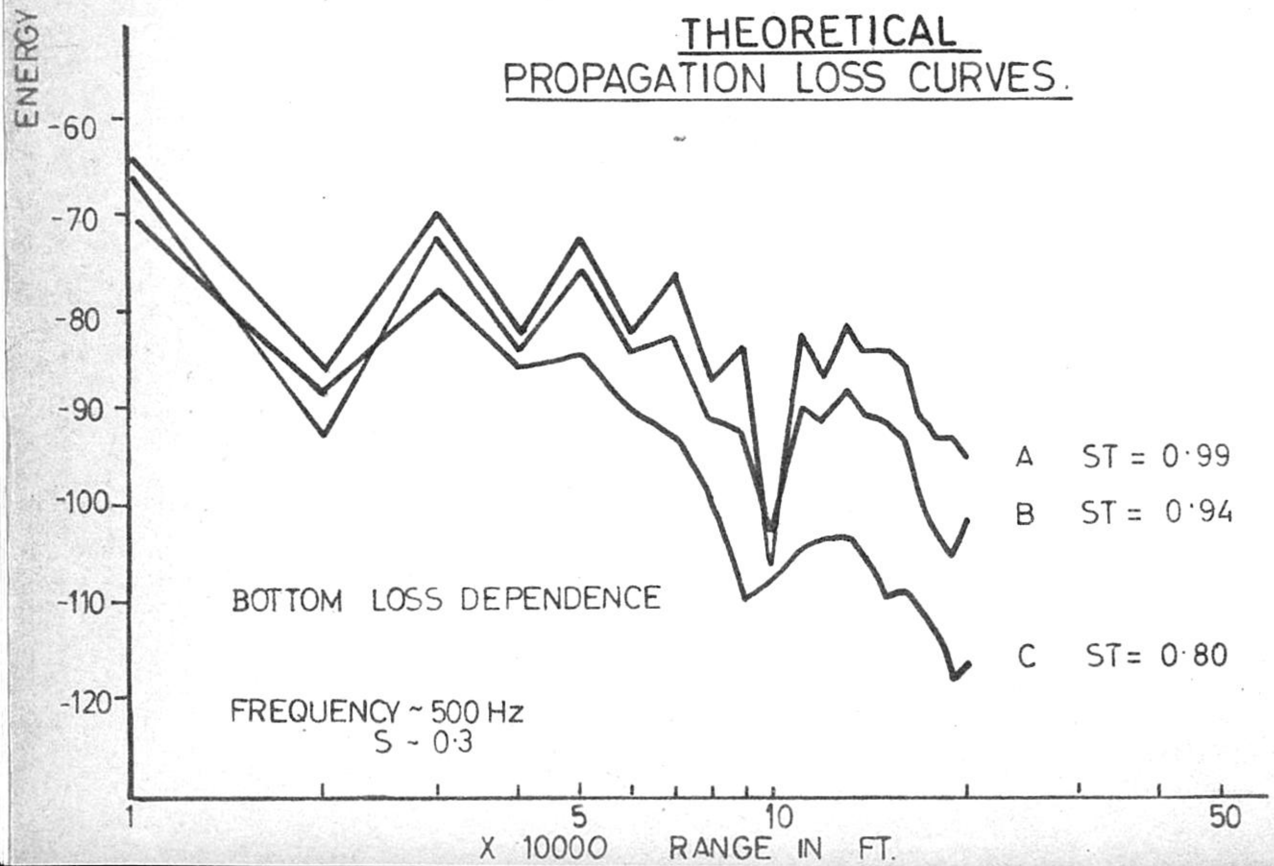

THEORETICAL FIG. 12(a)

RESPONSE OF RECEIVER VERSUS RANGE FOR DIFFERENT RECEIVER DEPTHS.

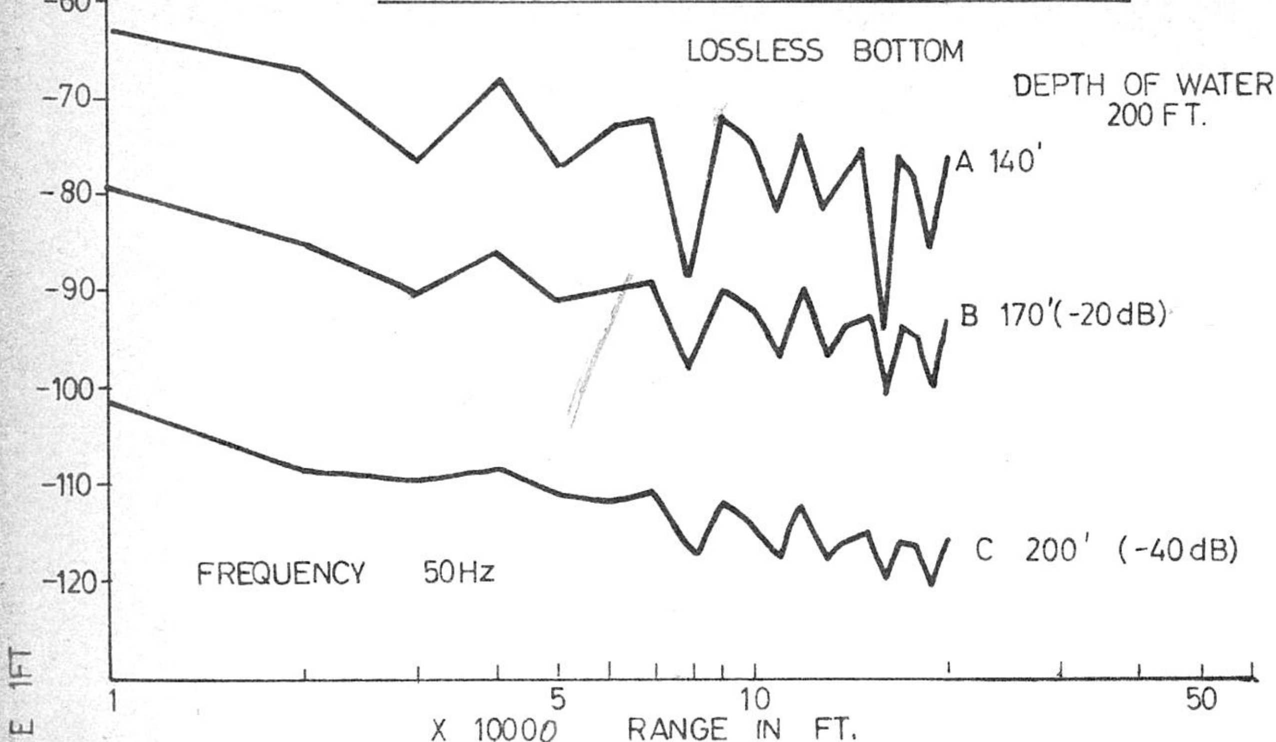

FIG 12(b)

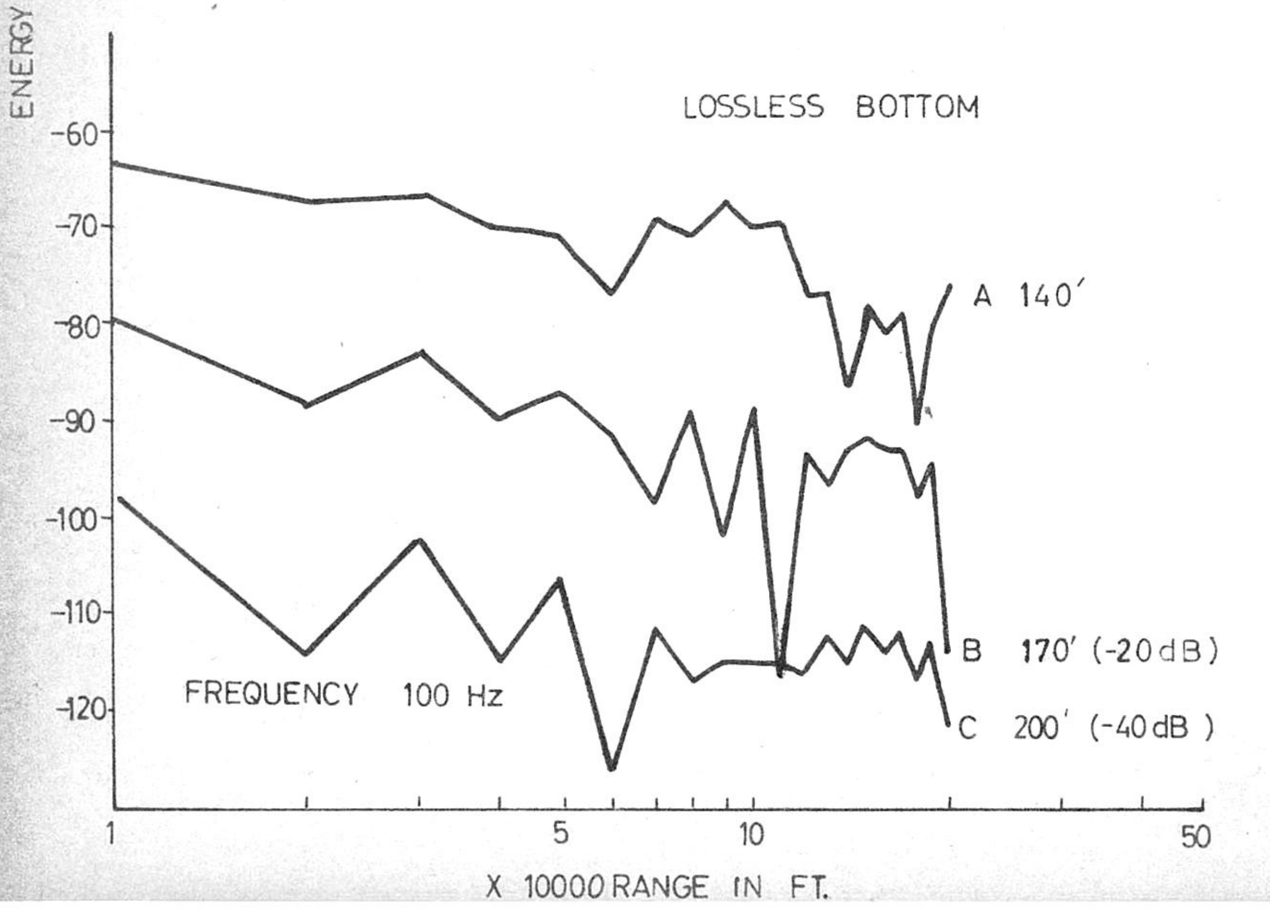

FIG. 12 (c)

THEORETICAL
RESPONSE OF RECEIVER VERSUS RANGE
FOR DIFFERENT RECEIVER DEPTHS.

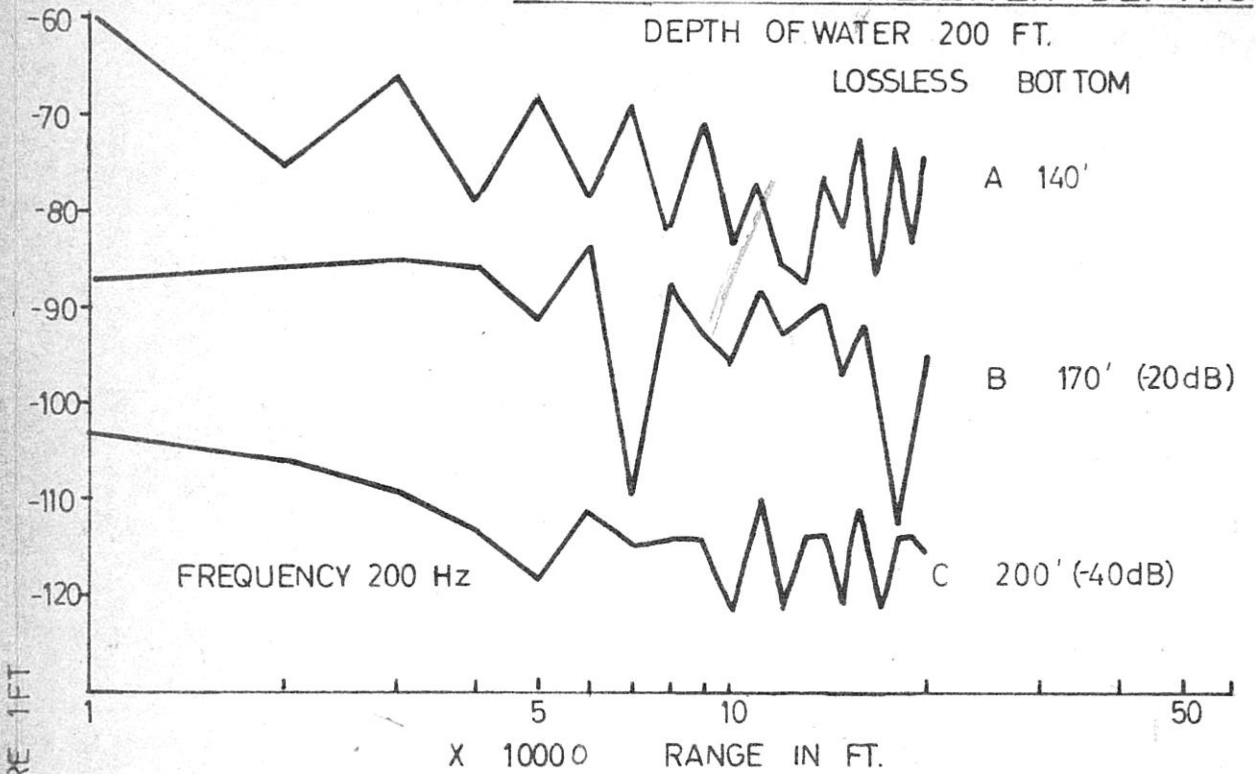

FIG. 12(d)

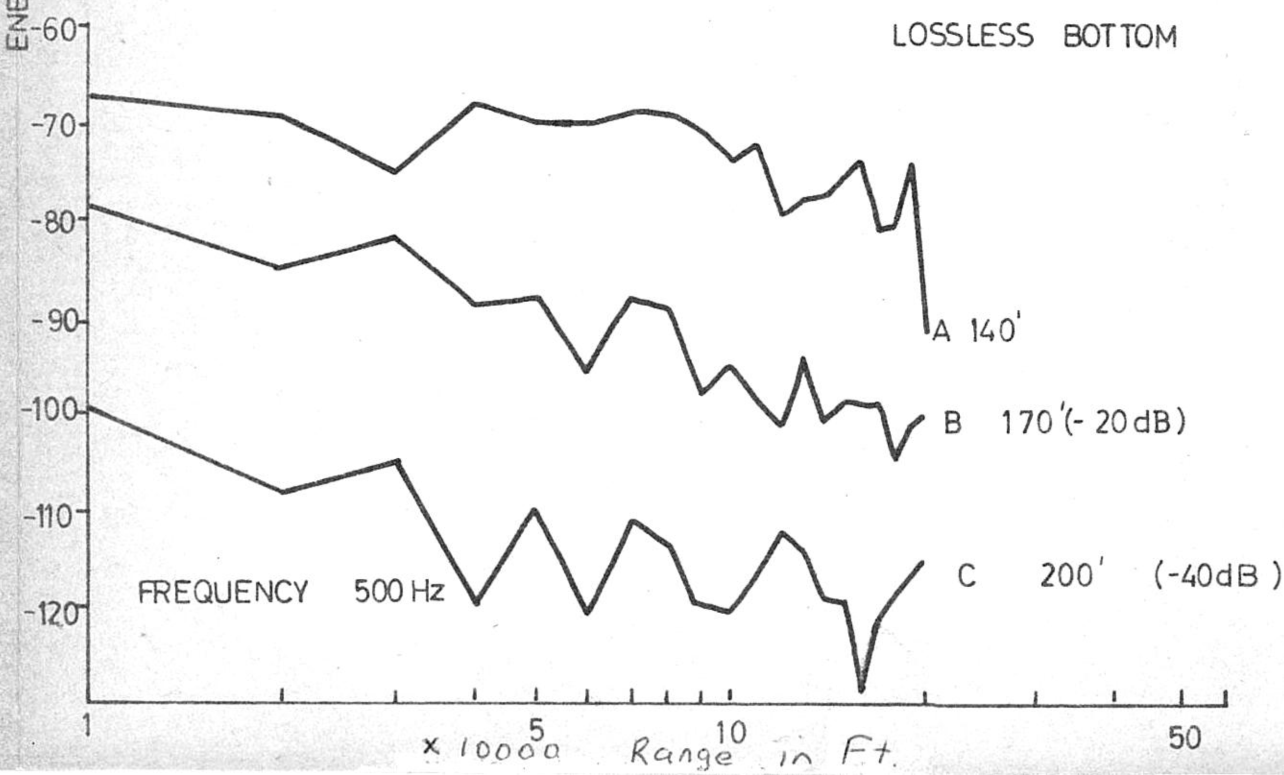

FIG.13

THEORETICAL DIFFERENCE OF ENERGY AT TWO RECEIVERS ONE ON THE BOTTOM, THE OTHER 40′ OFF THE BOTTOM.

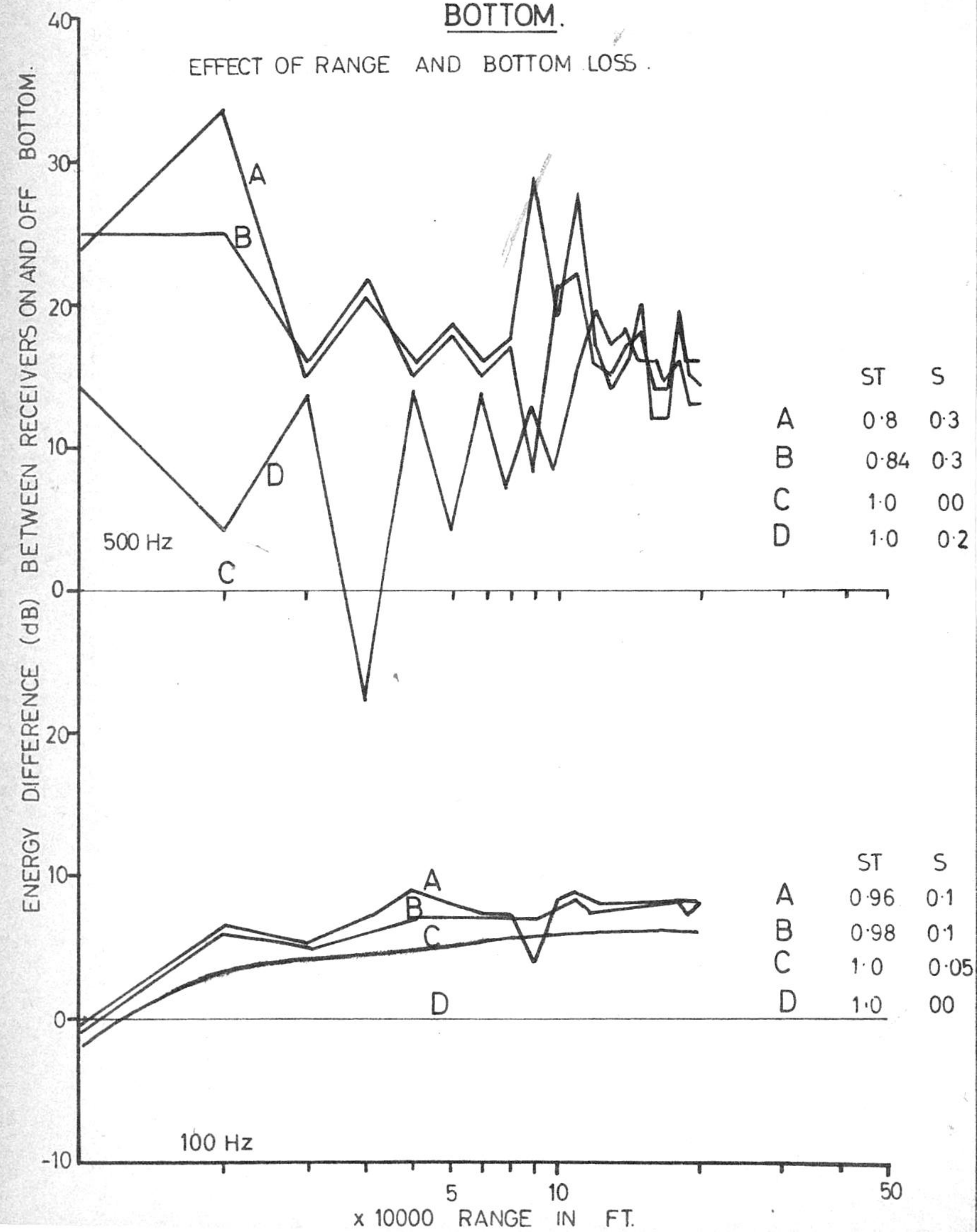

FIG. 14(a)

THEORETICAL
EFFECT OF DEPTH ON RECEIVER RESPONSE

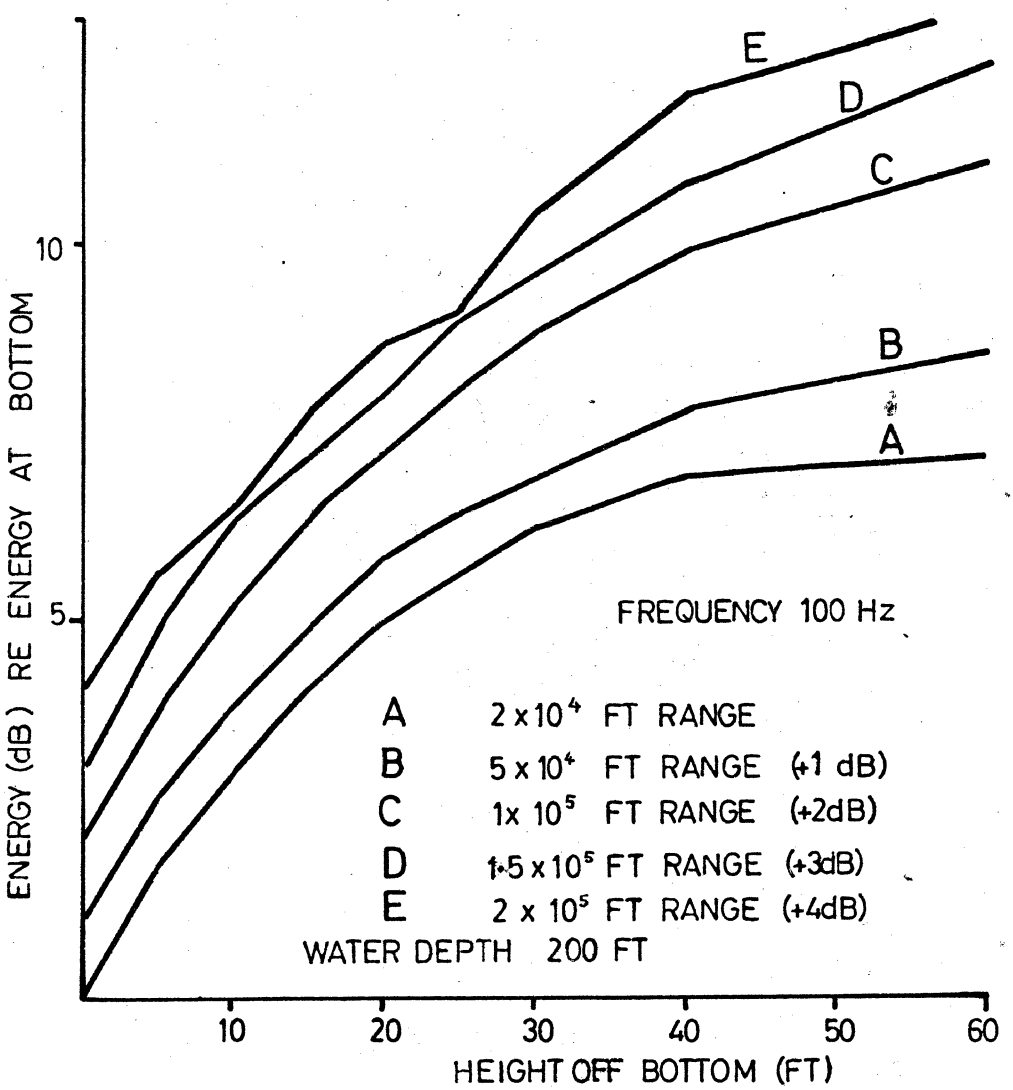

S = 0·1

ST = 0·96

FIG. 14(b)

THEORETRICAL
EFFECT OF DEPTH ON RECEIVER RESPONSE.

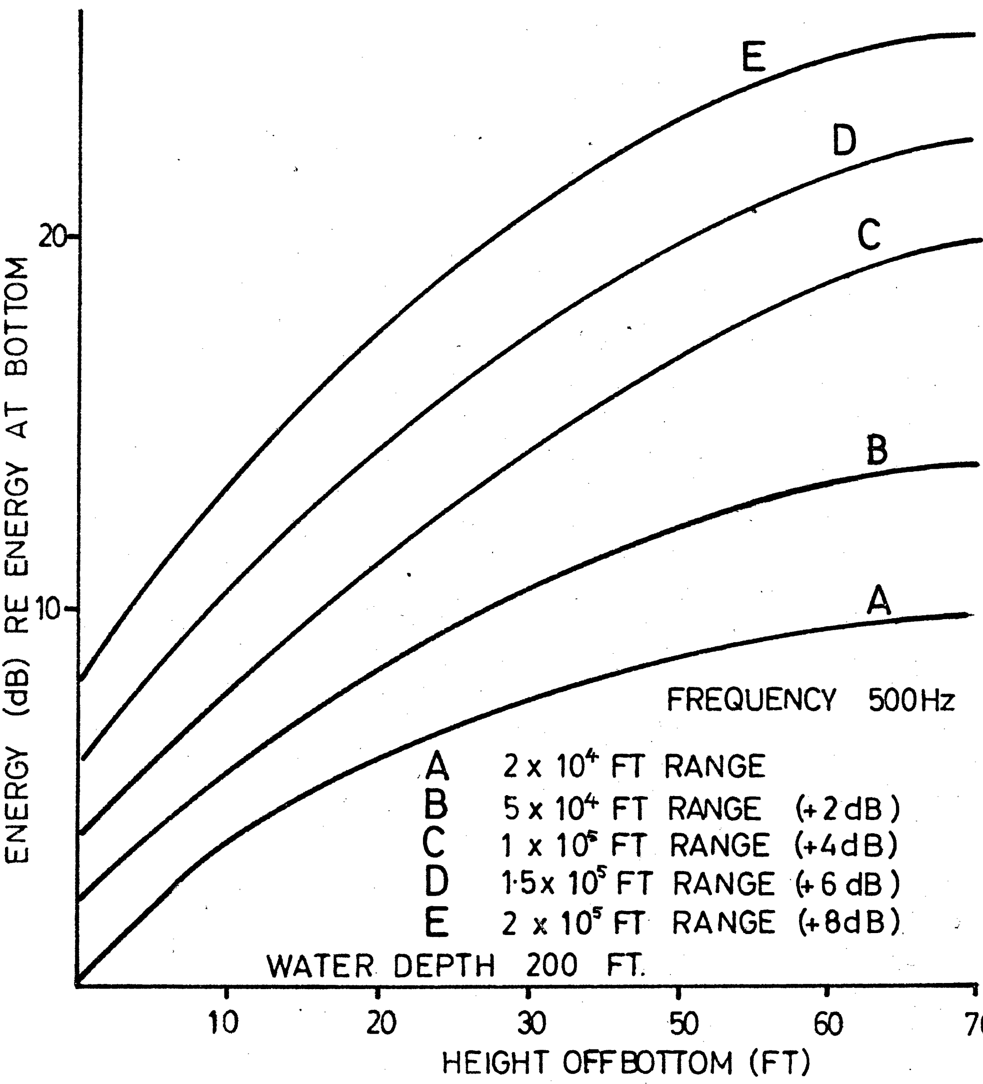

S = 0·3
ST = 0·8

FIG.15

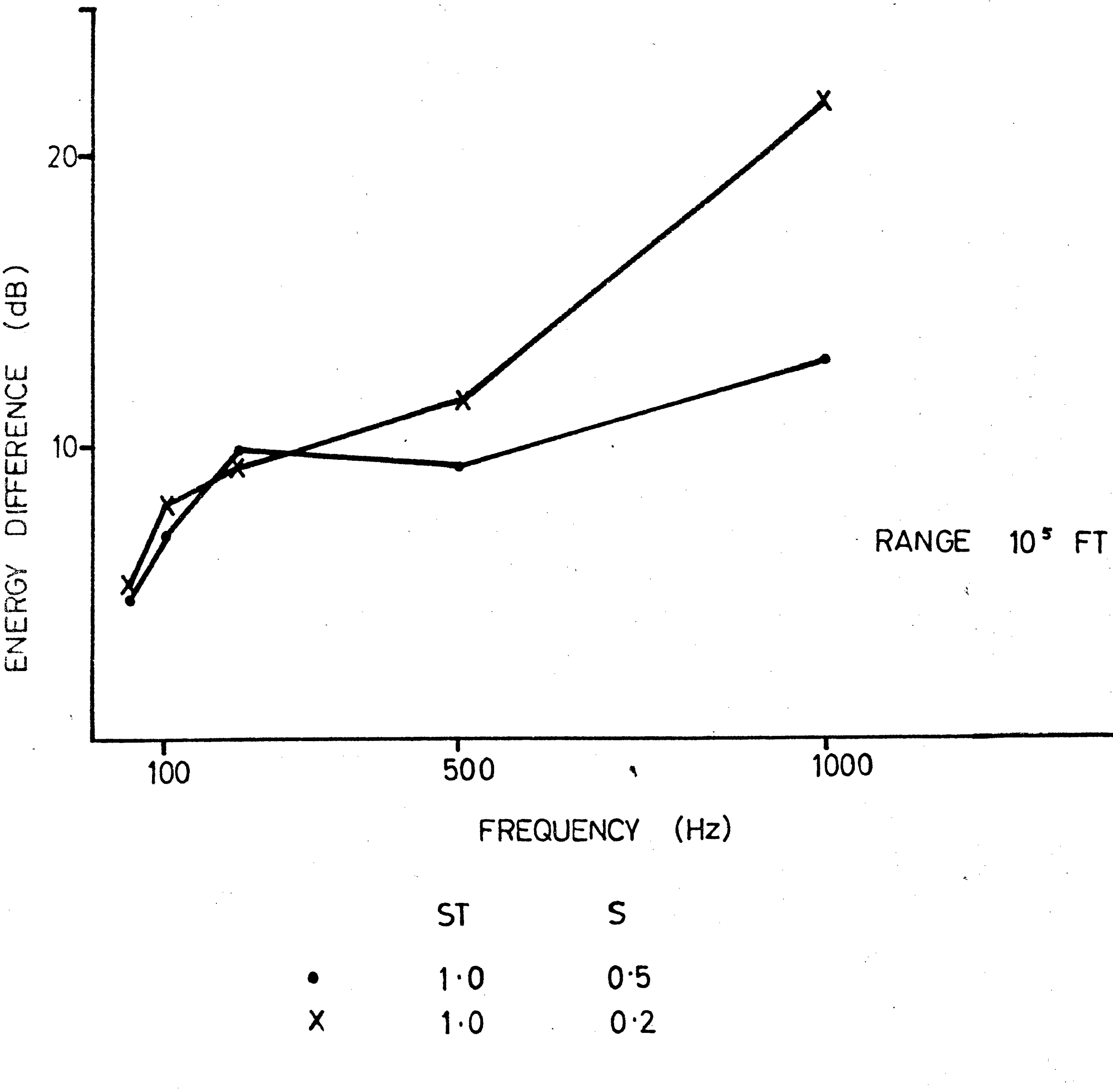

THEORETICAL
DIFFERENCE IN RESPONSE BETWEEN
RECEIVER ON AND 40′ OFF THE BOTTOM AS
A FUNCTION OF FREQUENCY.

FIG. 16(a)

PROPAGATION LOSS CURVES EXPERIMENTAL DATA

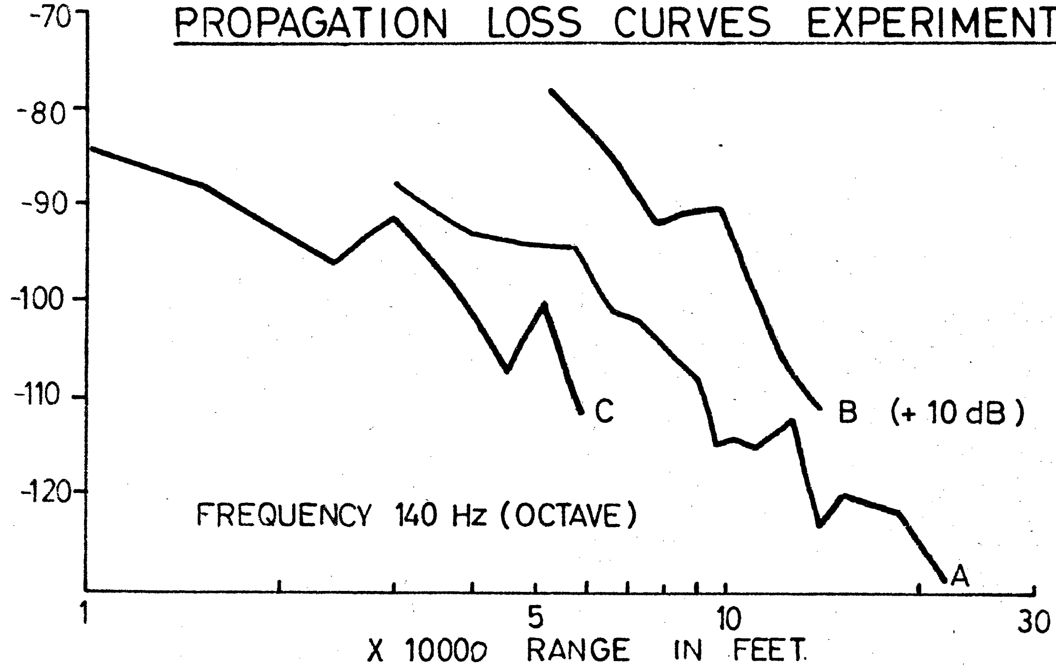

FIG.16(b)

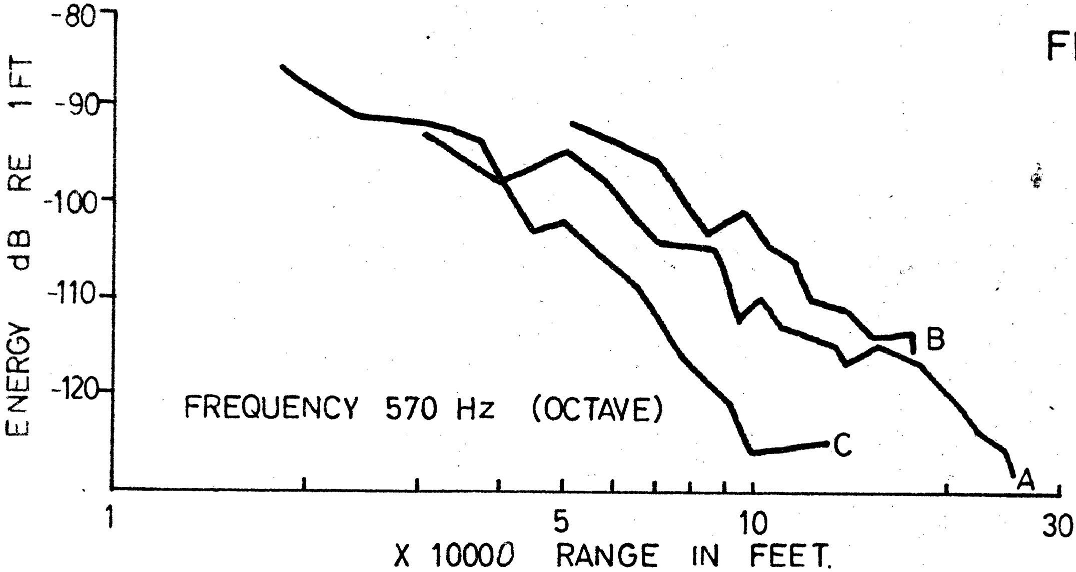

FIG. 16(c)

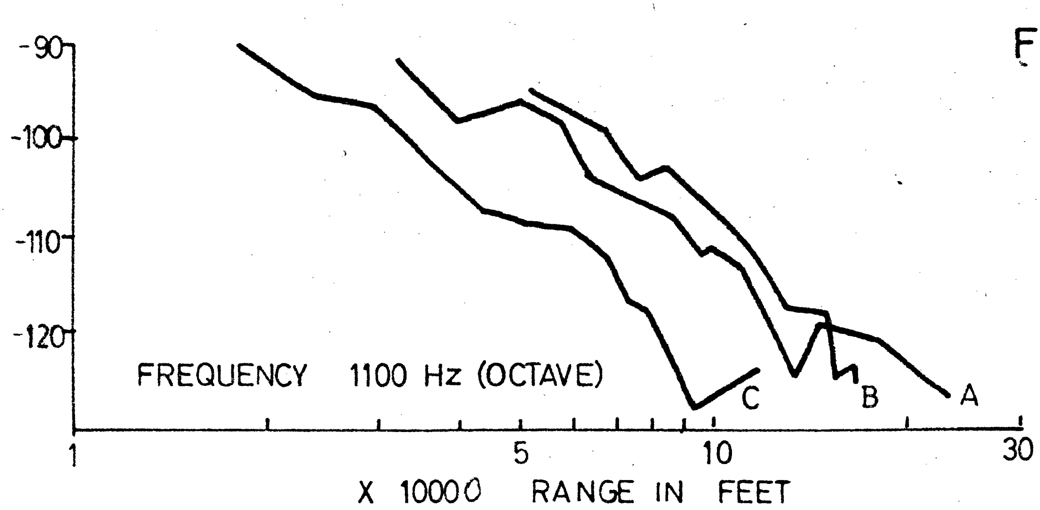

FIG. 17

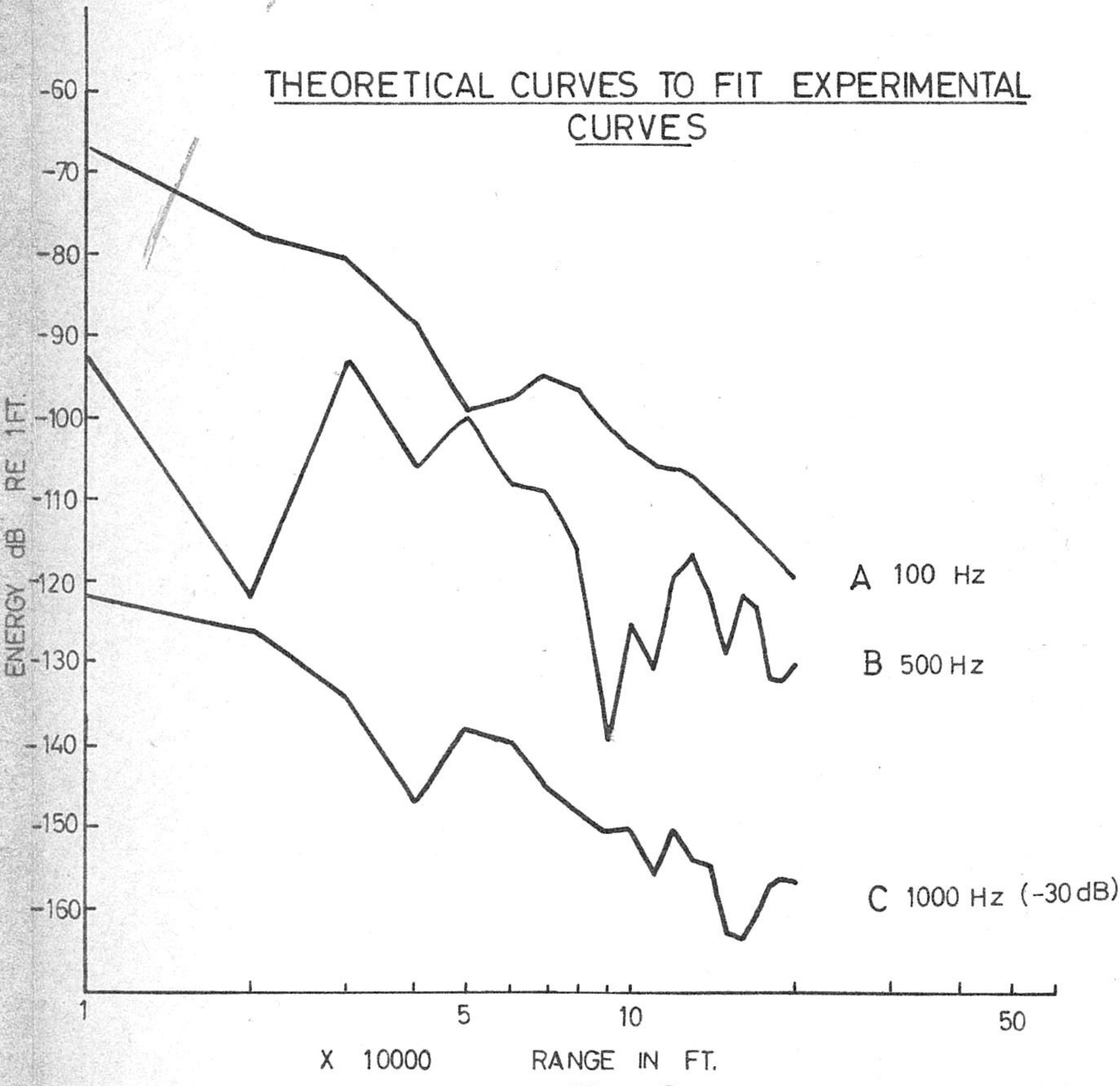

	ST	S
A	0·96	0·1
B	0·80	0·3
C	0·68	0·5

THEORETICAL PROPAGATION LOSS CURVES OBTAINED, ASSUMING RAYS ARRIVE INCOHERENTLY.

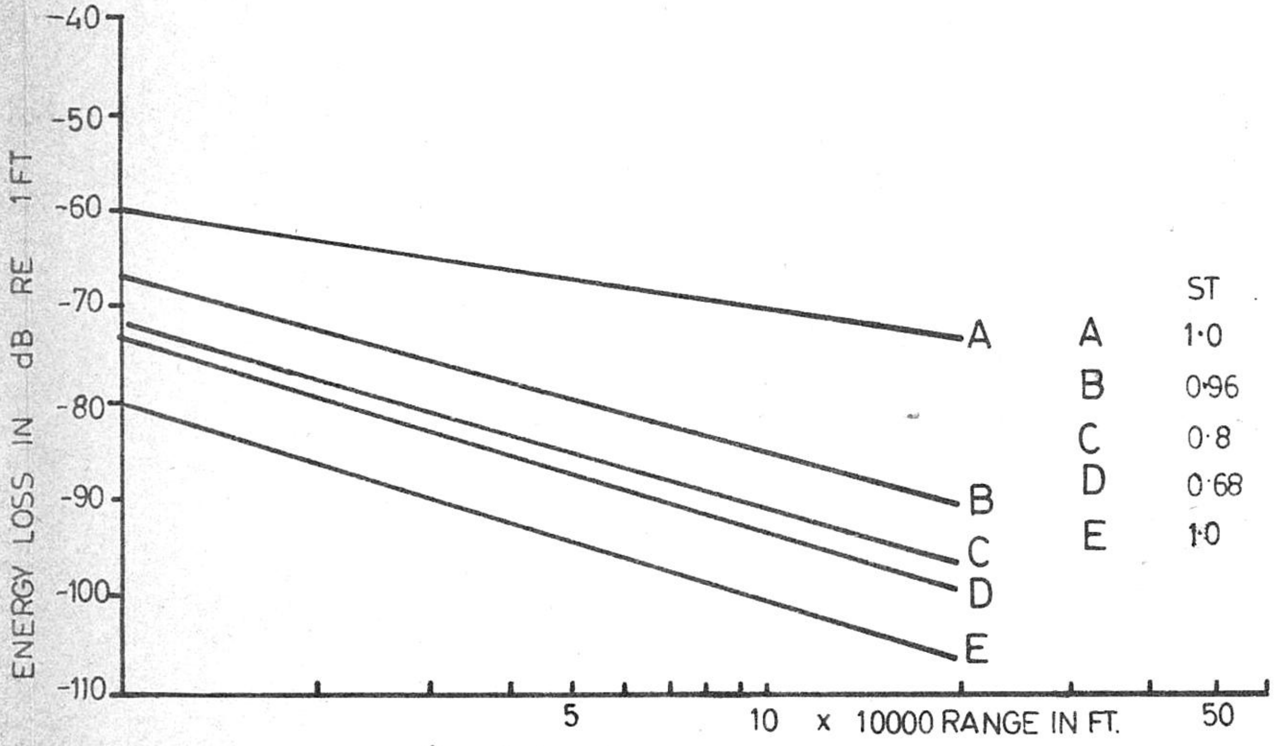

	ST	S
A	1·0	0
B	0·96	0·1
C	0·8	0·3
D	0·68	0·5
E	1·0	0

A CORRESPONDS TO NORMAL MODE PROPAGATION.

B,C,D, ARE THE CURVES OBTAINED USING PREDICTED BOTTOM LOSS PARAMETERS OF FIG. 17.

E CORRESPONDS TO SPHERICAL SPREADING

FIG. 19.

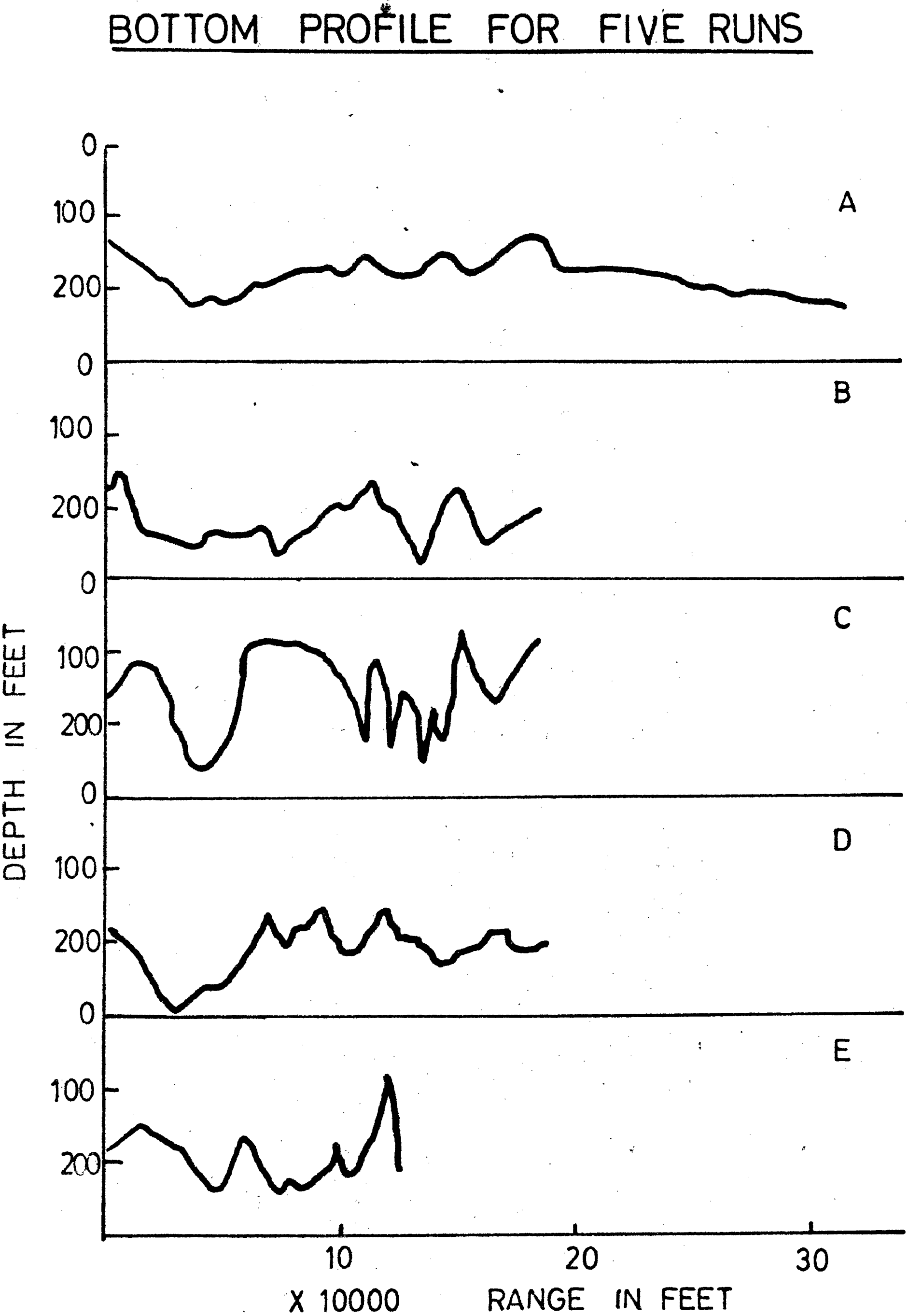
BOTTOM PROFILE FOR FIVE RUNS
A
B
C
D
E
0
100
200
DEPTH IN FEET
10
20
30
X 10000 RANGE IN FEET

FIG. 20

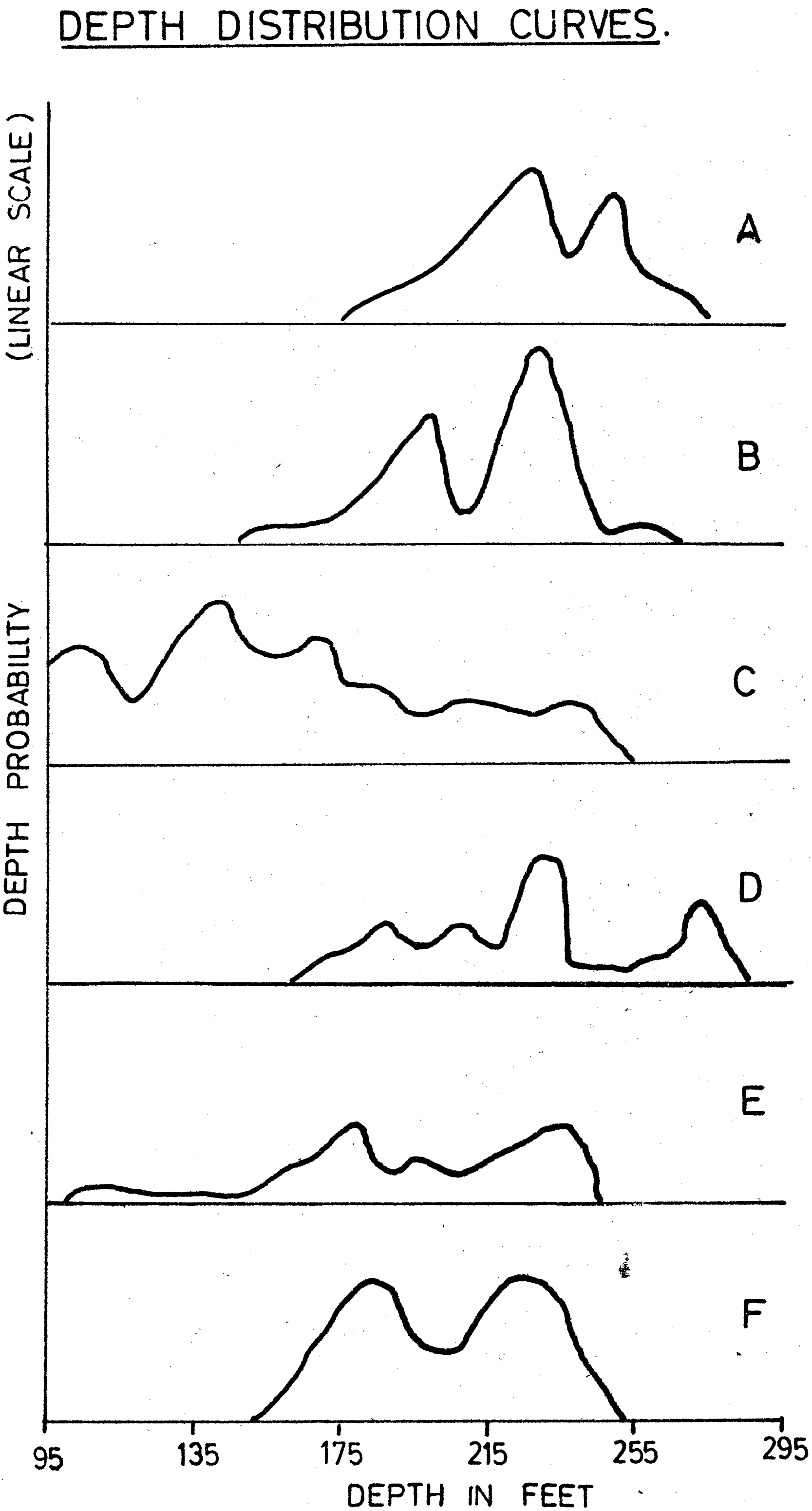

A,B,C,D,E ARE THE DEPTH DISTRIBUTION CURVES CORRESPONDING TO THE PROFILES OF FIG. 19.

F IS THE REPRESENTATIVE DEPTH DISTRIBUTION CURVE USED IN THE COMPUTER PROGRAM.

FIG. 21

EXTRA RAY PATH LENGTH DUE TO A VARIATION IN THE BOTTOM DEPTH.

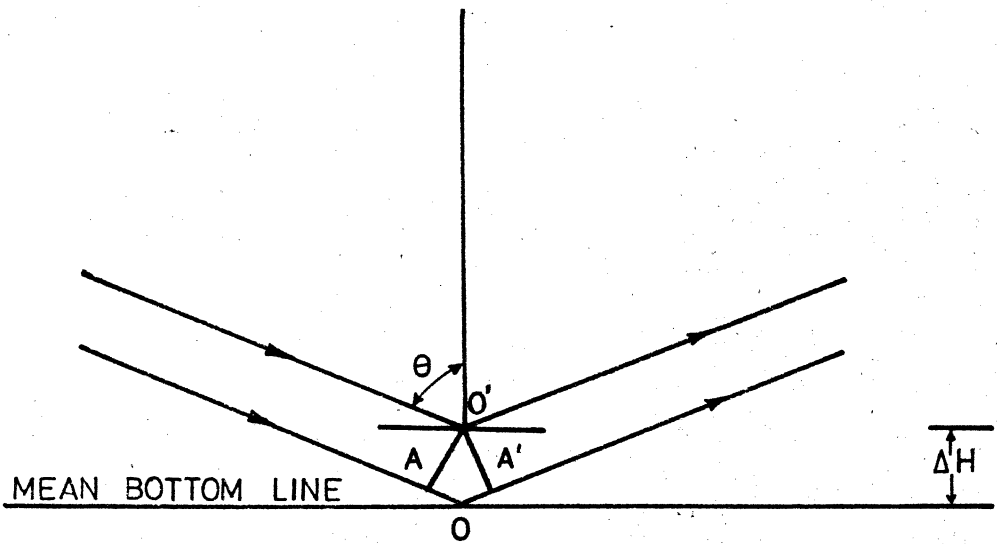

EXTRA PATH LENGTH DUE TO DECREASE IN WATER DEPTH OF ΔH IS

$$L = -(OA + OA')$$
$$= -2.\Delta H. \;\; \cos(\theta)$$

THE RANDOM NUMBERS (0-999) FIG.22.

(a) DISTRIBUTION

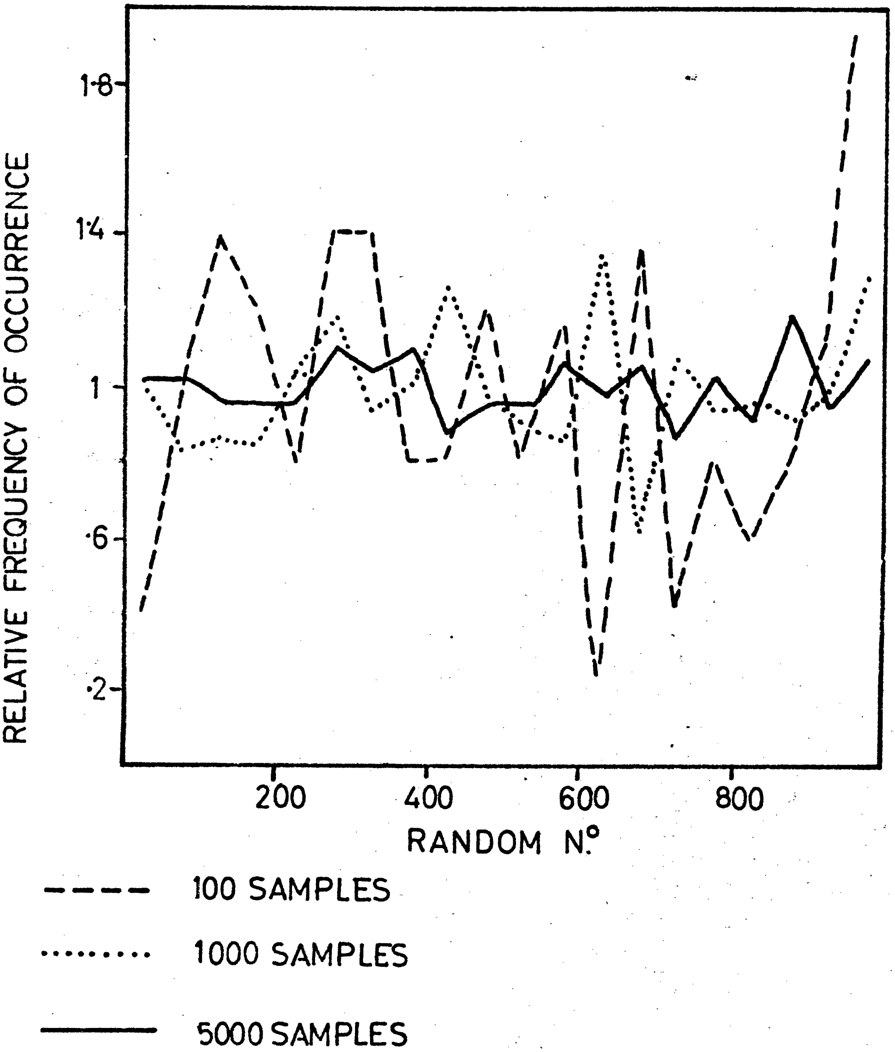

b) NORMALIZED AUTOCOVARIANCE

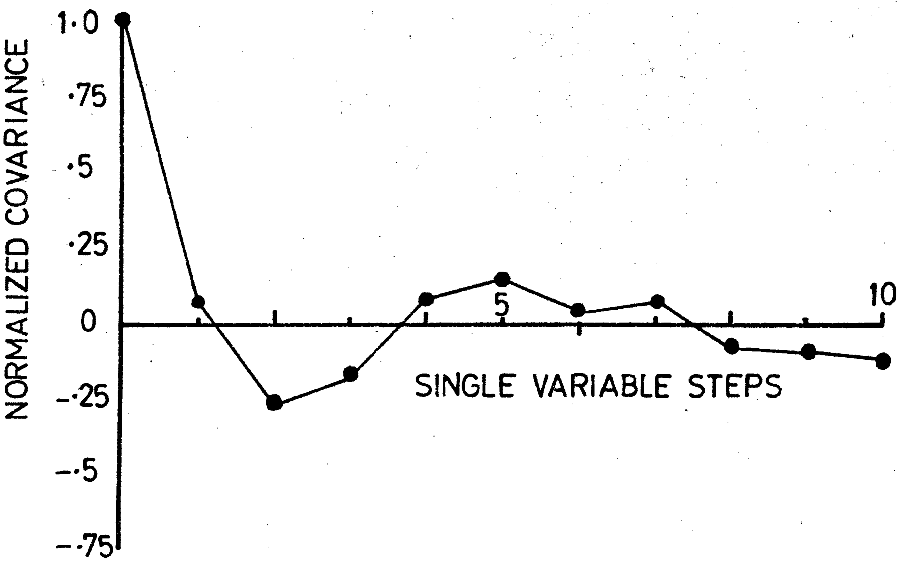

VARIATION IN PATH LENGTH OF RAY FROM SOURCE TO RECEIVER DUE TO A PERTURBATION IN THE BOTTOM DEPTH.

a.

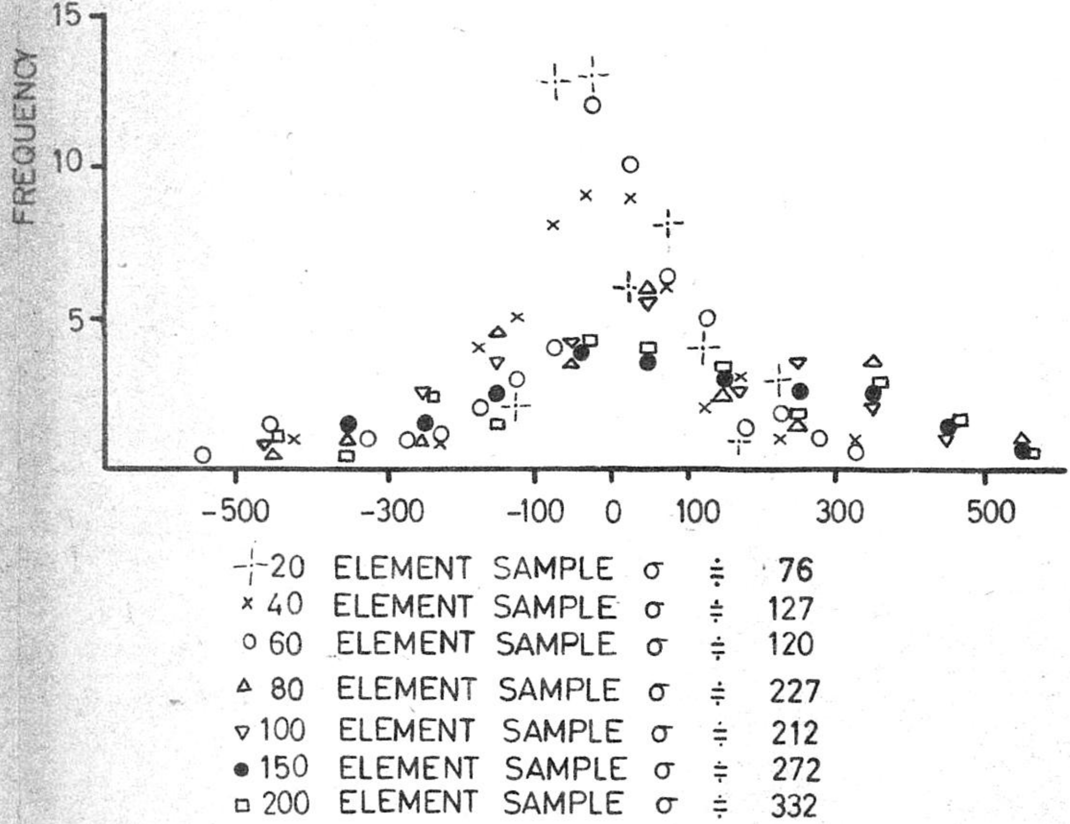

STANDARD DEVIATION OF THE VARIATION IN PATH LENGTH VS NO. OF BOUNCES.

b.

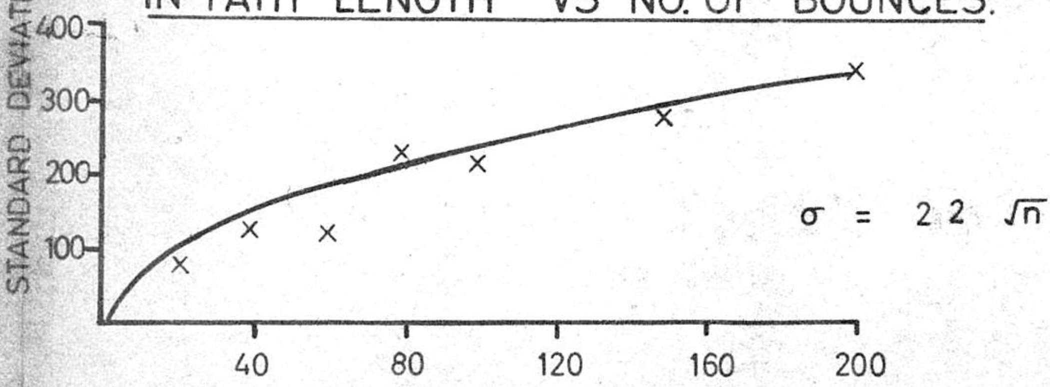

X STANDARD DEVIATION USING DISTRIBUTION OF FIG. a.

THE EFFECT OF THE MAGNITUDE OF BOTTOM ROUGHNESS ON THE MEAN SIGNAL INTENSITY.

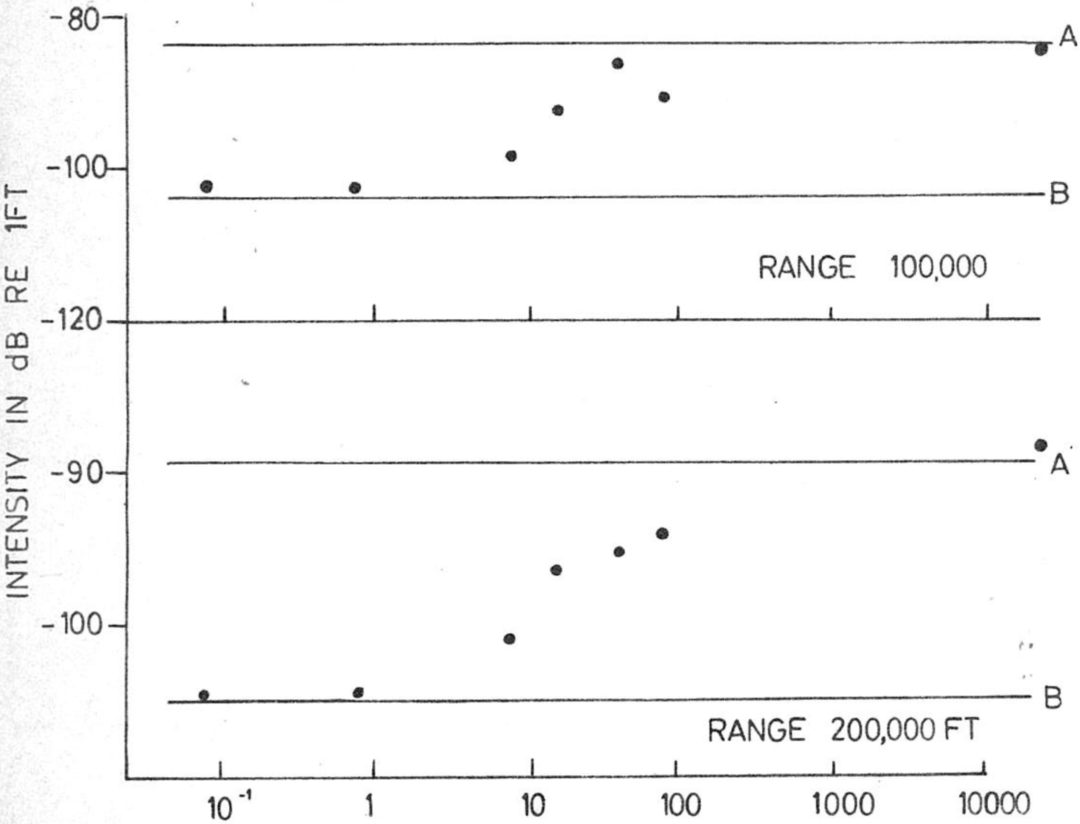

STANDARD DEVIATION σ OF DISTRIBUTION OF BOTTOM DEPTH VARIATION

A SIGNAL LEVEL OBTAINED WHEN RAY CONTRIBUTIONS ARE ADDED INCOHERENTLY.

B SIGNAL LEVEL OBTAINED WHEN RAY CONTRIBUTIONS ARE ADDED COHERENTLY

FIG. 25.

STANDARD DEVIATION OF INTENSITY VARIATION.

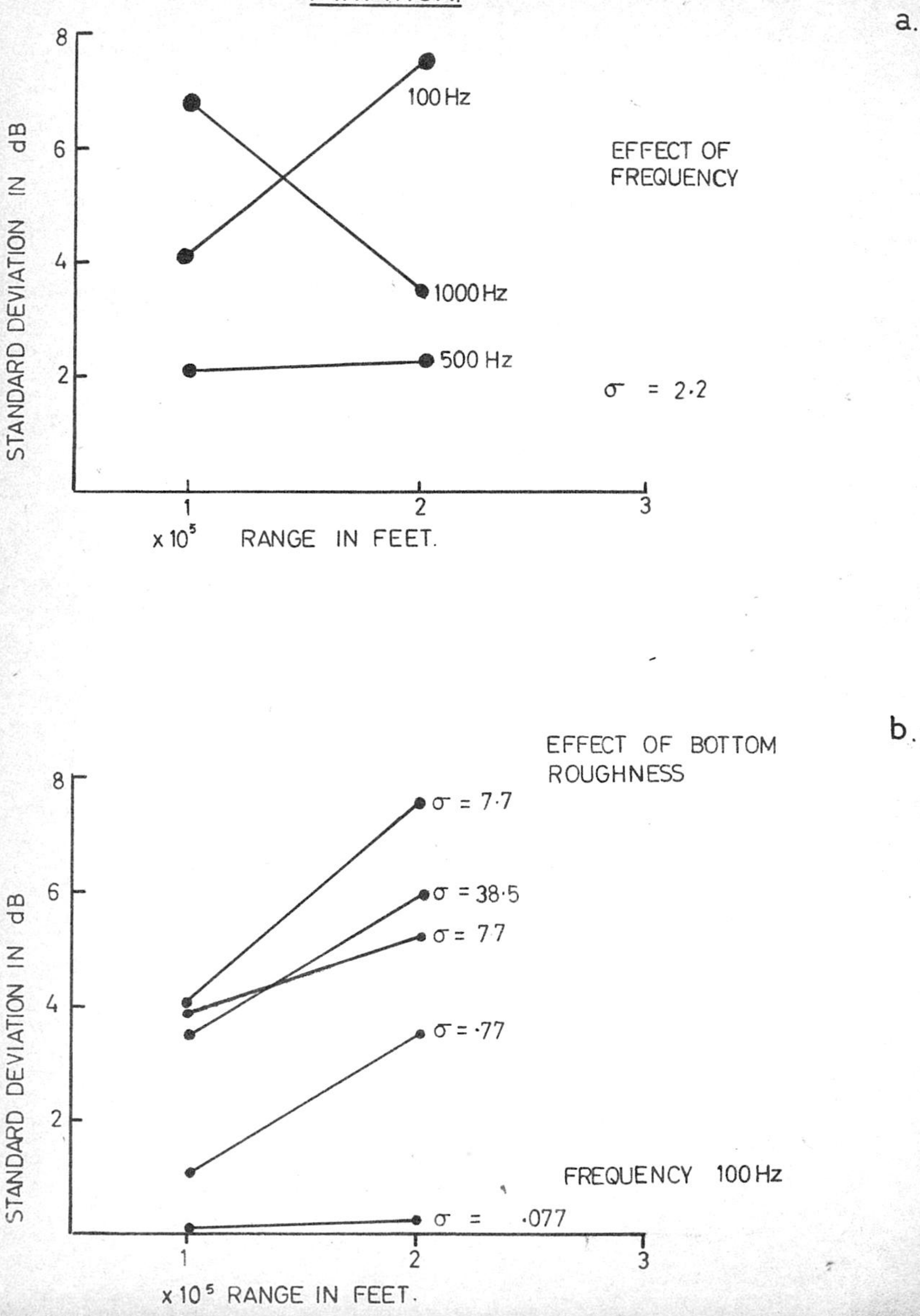

INTENSITY VARIATION FROM MEAN WITH FREQUENCY.

FIG. 26.

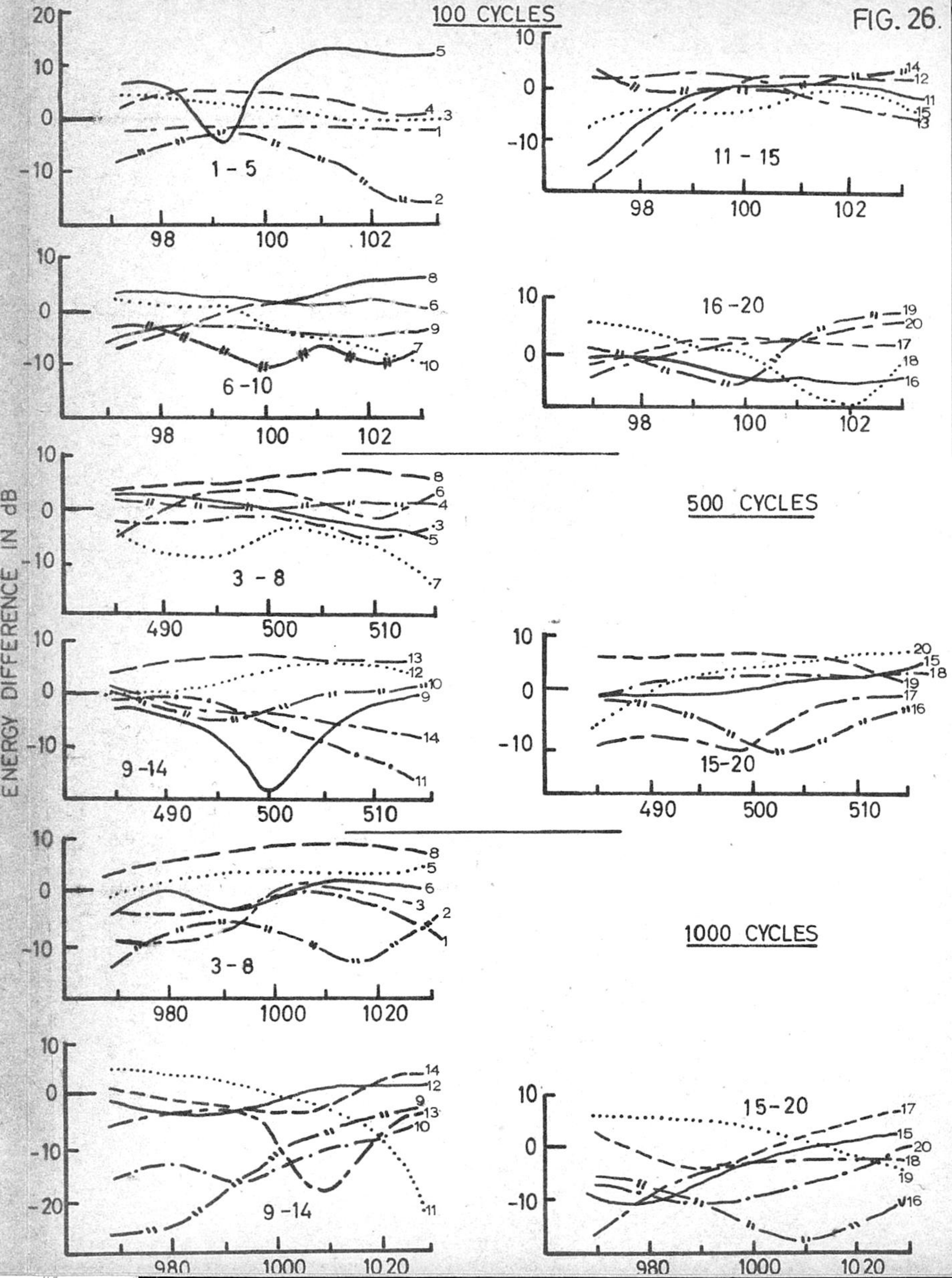

NORMALIZED AUTOCOVARIANCE OF INTENSITY FLUCTUATION WITH FREQUENCY. FIG.27.

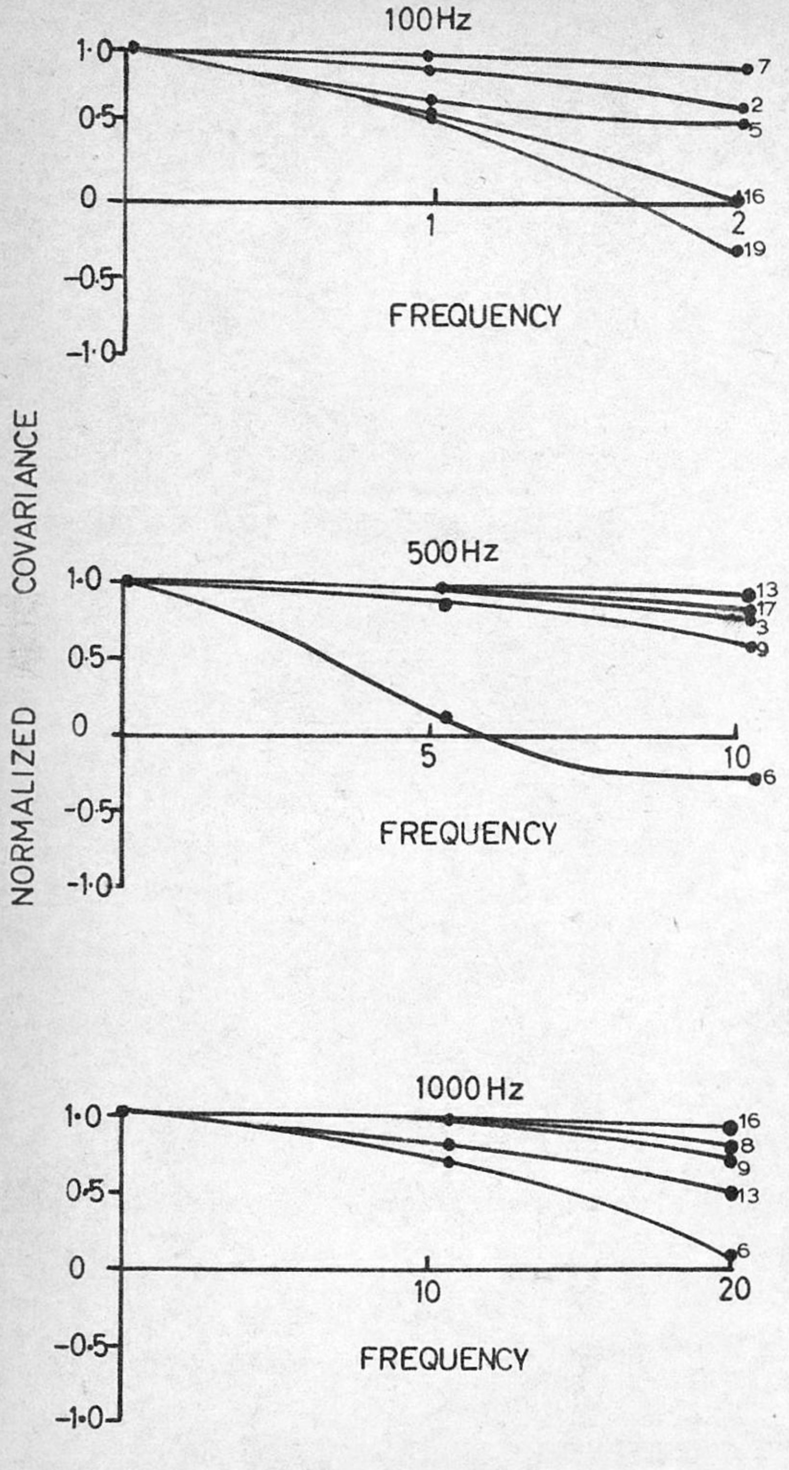

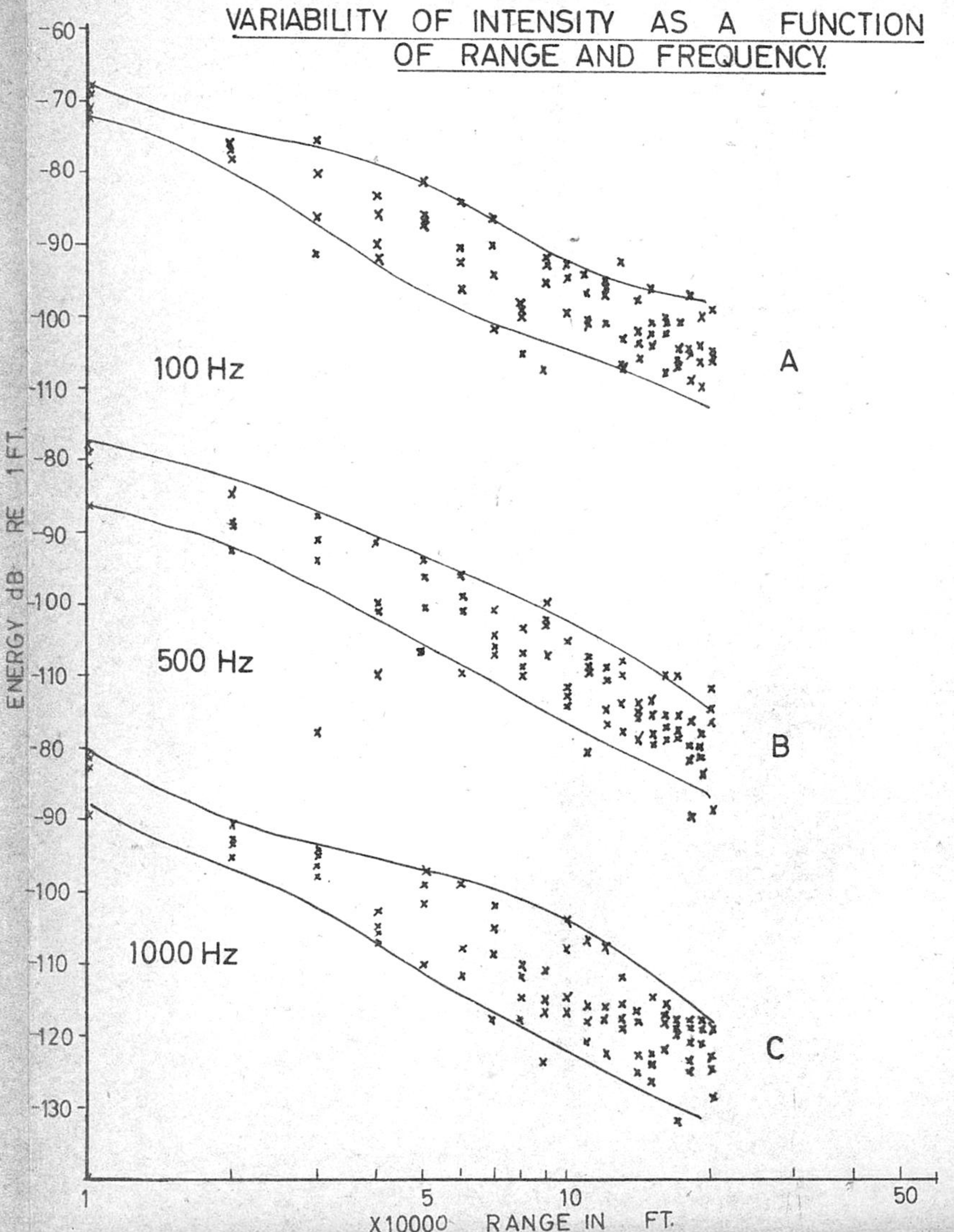
VARIABILITY OF INTENSITY AS A FUNCTION OF RANGE AND FREQUENCY.
ENERGY dB RE 1 FT.
-60
-70
-80
-90
-100
-110
-120
-130
100 Hz
500 Hz
1000 Hz
A
B
C
1
5
10
50
X10000 RANGE IN FT.

FIG. 29(a)

INTENSITY OF SHOT AS A FUNCTION OF TIME.

RANGE 10^5 FT

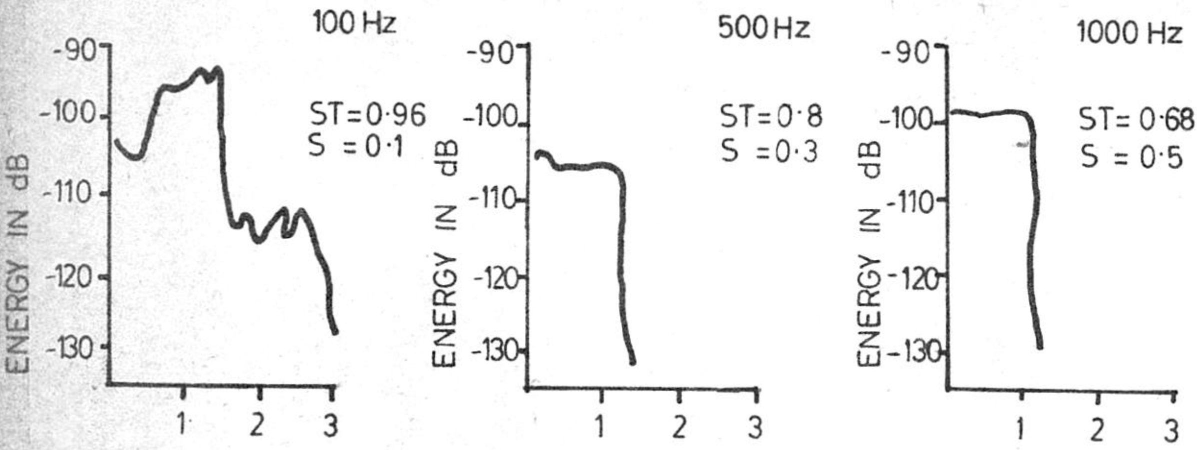

TIME IN UNITS OF 0·246 SECS.

PULSE DURATION 0·25 SECS.

FIG 29(b)

ARRIVAL TIMES FOR THE FIRST FOUR MODES OF PROPAGATION.

RANGE 10^5 FT

LOSSLESS BOTTOM

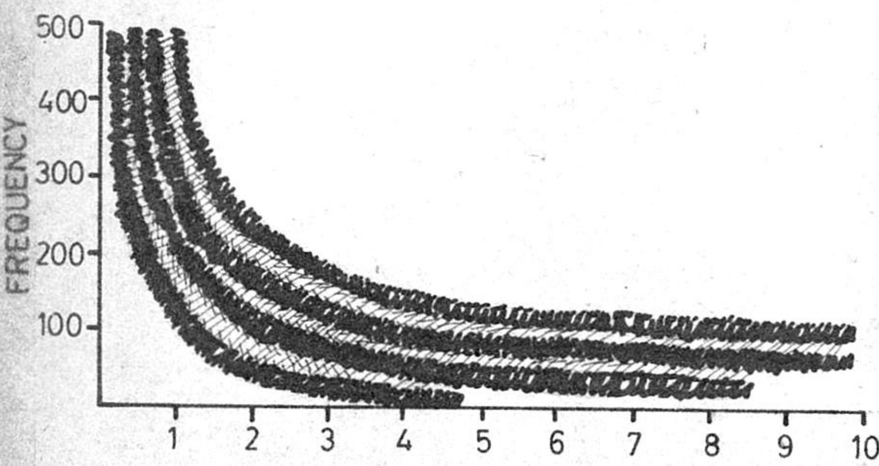

TIME IN UNITS OF 0·246 SECS.

PULSE DURATION 0·05 SECS.

SONAGRAMS OF SIGNALS

FIG: 30